

BUREAU OF ECONOMIC GEOLOGY
The University of Texas at Austin
Austin, Texas 78712

W. L. Fisher, Director

Report of Investigations No. 80

*Depositional Systems, San Angelo Formation
(Permian), North Texas -*

Facies Control of Red-Bed Copper Mineralization

by
Gary E. Smith



1974

QAe3986

BUREAU OF ECONOMIC GEOLOGY
The University of Texas at Austin
Austin, Texas 78712

W. L. Fisher, Director

Report of Investigations No. 80

*Depositional Systems, San Angelo Formation
(Permian), North Texas—
Facies Control of Red-Bed Copper Mineralization*

by
Gary E. Smith



1974
Second Printing, June 1984

TABLE OF CONTENTS

	Page
Abstract	1
Introduction	1
Purpose	1
Location	2
Previous work	2
Regional setting	4
Acknowledgments	4
Stratigraphy	6
Stratigraphic relationships	6
Principal stratigraphic units	7
Choza Formation	7
San Angelo Formation	8
Duncan Sandstone Member	8
Flowerpot Mudstone Member	8
Blaine Formation	10
Depositional systems	10
Choza depositional systems	10
Copper Breaks and Old Glory fluvial-deltaic systems	12
Fluvial-deltaic deposition: A summary	12
Regional patterns and distribution of fluvial-deltaic systems	12
Copper Breaks deltaic system	12
Facies of the Copper Breaks deltaic system	13
Prodelta facies	13
Delta-front facies	16
Distributary mouth bar facies	16
Distributary channel and associated delta-plain facies	16
Old Glory fluvial-deltaic system	17
Facies of the Old Glory fluvial-deltaic system	17
Fluvial-deltaic depositional model	17
Buzzard Peak and Cedar Mountain tidal-flat systems	18
Tidal-flat deposition: A summary	18
Regional patterns and distribution of tidal-flat systems	19
Buzzard Peak sand-rich tidal-flat system	19
Facies of the Buzzard Peak sand-rich tidal-flat system	20
Tidal sandflat facies	20
Tidal channel facies	21
Buzzard Peak sand-rich tidal-flat depositional model	21
Cedar Mountain mud-rich tidal-flat system	23
Facies of the Cedar Mountain mud-rich tidal-flat system	23
Tidal mudflat facies	23
Tidal channel facies	23
Swash-zone facies	26
Algal mat facies	26
Cedar Mountain mud-rich tidal-flat depositional model	26
Blaine sabkha and tidal-flat system	29
Sabkha deposition: A summary	29
Regional distribution of the sabkha and tidal-flat system	29
Facies of the Blaine sabkha and tidal-flat system	29
Sabkha facies	29
Tidal-flat facies	30
Sabkha and tidal-flat depositional model	30

Depositional history	31
Paleontology	35
Copper mineralization in the San Angelo Formation	37
Mineral assemblage	37
Distribution of copper mineralization	38
Paragenesis	39
Origin of copper mineralization	40
Sabkha-diagenetic model	41
Epigenetic models	45
Evaluation of mineralization models	47
Economics of North Texas strata-bound copper deposits	49
History of North Texas copper mining	49
Economic evaluation	50
Summary and conclusions	53
References	54
Appendices	
I Petrographic data.	59
II Significant copper mines and prospects in the San Angelo Formation.	62
III Outcrop copper samples: U. S. Bureau of Mines and this report.	63
IV Trace element analyses.	64
V Summary of U. S. Bureau of Mines drill hole data.	65
VI Synopsis of measured sections.	67
VII Localities.	70
VIII Methods.	72
IX Legends for figures 5 and 6.	74

ILLUSTRATIONS

Figures	
1 Location of study area, North Texas.	3
2 Regional geologic setting, during middle Permian, northern Texas and southwestern Oklahoma.	5
3 Mid-Permian stratigraphic section, northern Texas and southwestern Oklahoma.	6
4 Stratigraphic units and equivalent depositional systems, Choza, San Angelo, and Blaine Formations, North Texas.	8
5 Strike section of the Duncan Sandstone Member and Flowerpot Mudstone Member, San Angelo Formation (middle Permian), North Texas.	9
6 Strike section of the uppermost Choza and San Angelo and the basal Blaine Formations (middle Permian) with inferred depositional environments.	11
7 Depositional model of Old Glory, Copper Breaks, and Buzzard Peak systems.	13
8 Copper Breaks deltaic progradational sequence.	14
9 Net sandstone isolith map, San Angelo Formation.	15
10 Facies relationships in the Buzzard Peak sand-rich tidal-flat system.	20
11 Depositional model of Cedar Mountain mud-rich tidal-flat system.	24
12 Idealized sequence of Cedar Mountain mud-rich tidal-flat and Blaine sabkha and tidal-flat systems.	25
13 Vertical sequence through modern tidal-flat and sabkha deposits, Trucial coast.	28

14	Paleogeography during deposition of the Duncan Sandstone Member, San Angelo Formation.	33
15	Paleogeography during deposition of the upper part of the Flowerpot Member, San Angelo Formation, and the lower part of the Blaine Formation.	34
16	Permian copper prospects, Texas, Oklahoma, and Kansas.	36
17	Distribution of copper minerals, San Angelo Formation, North Texas.	37
18	Sabkha-diagenetic model for copper mineralization.	42
19A	Epigenetic model: fault- or fracture-controlled mineralization.	46
B	Epigenetic model: diffusion-controlled mineralization.	46
20	Price of copper from 1945 to present, and decrease of average grade of ore mined from 1945 to present with a projection to the year 2000.	52

Plates

I	Geologic map—San Angelo Formation, Medicine Mound area.
II	Geologic map—San Angelo Formation, Foard City area.
III	Geologic map—San Angelo Formation, Buzzard Peak area.
IV	Geologic map—San Angelo Formation, Kiowa Peak area.
V	Geologic map—San Angelo Formation, Old Glory area.
VI	Sandstone isolith map of the San Angelo Formation.
VII	A - Pyrite with relict wood structure and “clear” rim.
	B - Pyrite with relict wood structure.
	C - Chalcocite replacing pyrite with relict wood structure preferentially along cell walls.
	D - Covellite replacing chalcocite.
VIII	A - Solution and mechanical disintegration of quartz.
	B - Precipitation of chalcocite in pore space between oolites in dolomite.
	C - Chalcocite replacing organic matter in the nucleus of an oolite.
	D - Mineralized spore and framboidal spherules in copper-bearing claystone, Creta mine.
IX	A - Mineralized polyframboidal structure in dolomite.
	B - Mineralized framboidal spherules in copper-bearing claystone, Creta mine.

TABLE

1	Number of years required to concentrate a 25-cm column of 1-percent copper over 1 sq cm of surface.	44
---	---	----

DEPOSITIONAL SYSTEMS, SAN ANGELO FORMATION (PERMIAN), NORTH TEXAS—

FACIES CONTROL OF RED-BED COPPER MINERALIZATION

by
Gary E. Smith¹

ABSTRACT

The San Angelo Formation is a mid-Permian sandstone and mudstone sequence about 100 feet thick that crops out in North Texas and dips westward into the Midland Basin; it is composed of two superposed members: the basal Duncan Sandstone Member and the overlying Flowerpot Mudstone Member. Depositional systems within the Duncan Member include the Copper Breaks deltaic system in the north, the Old Glory fluvial-deltaic system in the south, and the intermediate, strike-fed Buzzard Peak sand-rich tidal-flat system. Gradationally above these systems is the Cedar Mountain mud-rich tidal-flat system which is coincident with the Flowerpot Member. Cedar Mountain facies include tidal channel-fill sandstone characterized by flaser bedding, red mudstone of tidal mudflat origin, and algally bound shale and dolomite.

Cedar Mountain facies are overlain conformably by the Blaine Formation which was deposited within alternating sabkha and tidal-flat

environments. Nodular gypsum beds comprise the framework of the Blaine sabkha and tidal-flat system.

Copper mineralization occurs primarily within narrow, lenticular, organic-rich tidal channel-fill sandstone facies and thin, widespread algal mat shale facies. A sabkha-diagenetic model is used to explain the mineralization. Evaporative discharge from a sabkha creates an upward decrease in hydrodynamic potential with the result that primarily terrestrial ground water moves upward through the sabkha. Hydrogen sulfide, formed by bacteria, precipitates copper as ground water passes through chemically favorable facies. Calculations indicate that 100,000 to 200,000 years may be necessary to form an economic deposit; alternate epigenetic models, involving diffusion over long distances, or movement of hydrothermal solutions along faults and fractures, were evaluated. Copper minerals include chalcocite, covellite, and malachite.

INTRODUCTION

The San Angelo Formation is a mid-Permian wedge of terrigenous clastic sediments of diverse composition that crops out in North Texas. Westward, the formation can be traced into the Midland Basin where it intertongues with red mudstone and evaporite beds. Along strike, the San Angelo is characterized by numerous facies changes that reflect complex relationships between diverse depositional environments.

Copper mineralization has been recognized in the Permian rocks of North Texas for over 100 years. Many mining ventures were attempted, but because of poor mining practices, primitive technology, erratic fluctuations in the price of copper, and lack of understanding of the geologic relations

between the mineralization and the host rocks, attempts at exploitation have been unsuccessful.

PURPOSE

The principal purpose of this investigation is to integrate outcrop observations with subsurface data to provide a basis for delineating the regional depositional framework for the San Angelo Formation. In addition, the relationship between mineralization and host rock is considered in order to provide alternative sedimentary-geochemical models to explain the origin of the copper. Interpretation of the San Angelo depositional environments and the nature and role of lithologic facies in controlling copper mineralization is based on sedimentary, stratigraphic, and geochemical parameters.

¹The Anaconda Company, P. O. Box 27007, Tucson, Arizona 85726

Field work was conducted during the summer of 1972 and spring of 1973. A geologic map of the San Angelo Formation was constructed (pls. I-V) from aerial photographic interpretation and extensive field checking; the map base consists of parts of eighteen 7.5-minute and two 15-minute U. S. Geological Survey topographic quadrangle maps. Forty-eight measured sections were augmented by Bureau of Mines drill hole data and unpublished measured sections (William E. Galloway, unpublished report, 1970). A net sandstone map of the San Angelo Formation (pl. VI) was constructed from 473 electric logs; interpretations were complemented by sample logs from the Perrini well log library of Abilene, and well samples at the Well Sample Library, Bureau of Economic Geology, Austin. In addition to outcrop observations, 45 samples were analyzed by the Mineral Studies Laboratory, Bureau of Economic Geology, to provide additional information on copper content as well as on the content of selected trace elements. Polished sections of ore samples and petrographic thin sections of field samples supplied additional information on facies and mineralization.

All data points (measured sections, copper sample localities, representative facies outcrops, thin-section sample localities, and abandoned mines) are plotted on the geologic maps and are referred to in the text by reference to the plate number, followed by location number on the plate (e.g. I-3). Data points are numbered consecutively (beginning with 1) on each map (plates I-V). The location and significance of most data points are described in appendix VI (Measured Sections) and appendix VII (Localities). All data points not listed in appendices VI or VII are sample and/or core hole localities of the U. S. Bureau of Mines (Stroud and others, 1970) and are listed in appendix III (Outcrop Copper Samples) or appendix V (Summary of U. S. Bureau of Mines Drill Hole Data). The locations of copper mines and prospects (appendix II) are noted by plate numbers and alphabetical symbols (eg. IV-C).

LOCATION

The San Angelo outcrop area investigated includes approximately 700 square miles in North Texas (fig. 1) between the southern boundary of Stonewall County and Medicine Mounds in Hardeman County, a distance of 84 miles. The area

was chosen to include all known San Angelo copper occurrences in Texas. Subsurface study extended 20 miles southward beyond the limits of the surface investigation.

The San Angelo Formation crops out in the Osage Plains of the Central Lowlands province. Local drainage is into the Red River and the Brazos River. The climate is semiarid with an average rainfall of 23 inches (Cronin and others, 1963; Baker and others, 1963). Well-developed fluvial terraces of Quaternary and Holocene age occur throughout the area (Stricklin, 1961). Significant portions of the San Angelo outcrop are covered by relict, pediment-like surfaces. Well-developed badlands are adjacent to most of the rivers and intermittent streams; it is in these highly dissected areas that the San Angelo Formation is exposed. Resistant layers of dolomite and gypsum in the overlying Blaine Formation form bluffs to the west of the San Angelo outcrop belt. These bluffs trend generally north-south. The underlying Choza Formation crops out east of the San Angelo outcrop in a series of dissected badlands and broad plains.

PREVIOUS WORK

The term "San Angelo Beds" was proposed by Lerch in 1891. The type locality is about 5 miles south of San Angelo, Texas, where it is composed of a basal conglomeratic sandstone, overlain by finer grained sandstone and mudstone. Lerch believed that the beds were Jurassic or Triassic in age because of their similarity to established Triassic units in Colorado and Wyoming. W. F. Cummins (1890) considered these same beds to be of Permian age and proposed that the basal sandstone of the San Angelo defines the base of his Double Mountain Group. W. E. Wrather (1917) named the beds the "Blowout Mountain Sandstone" from an exposure in Taylor County. Beede and Bentley (1918) noted that the formation was thickest (up to 400 feet) in Coke County and that it thinned both southward and northward.

In 1922, the San Angelo Formation was traced northward into Oklahoma where it was determined to be equivalent to the Duncan Sandstone (Beede and Christner, 1926); Beede and Christner described the San Angelo Formation of Foard County. Roth (1945) later changed the name of the Double Mountain Group to Pease

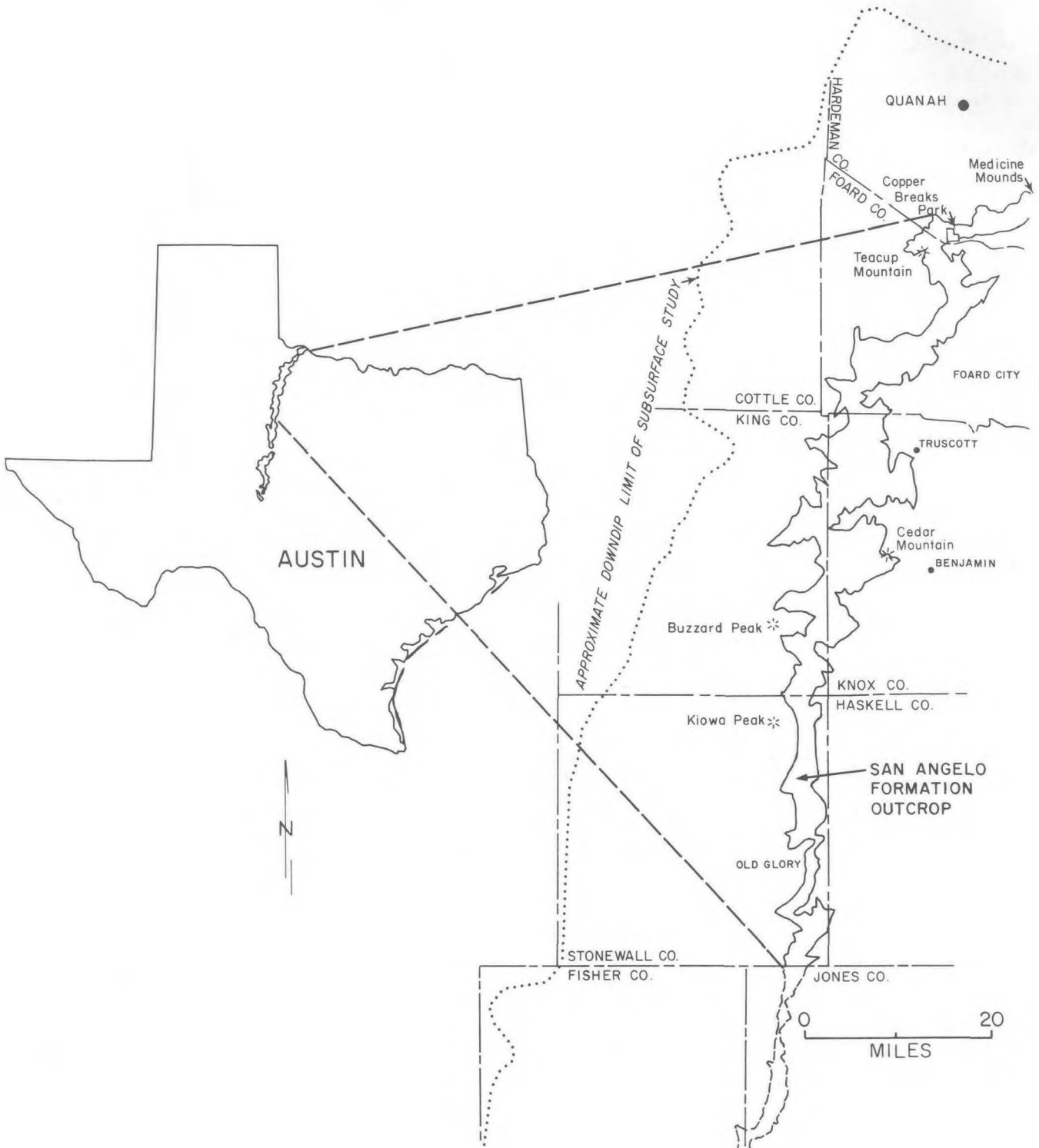


Fig. 1. Location of study area, North Texas.

River Group, named from exposures along the Pease River in King County.

Extensive study of the outcropping San Angelo Formation by Olson and Beerbower (1953) and Olson (1962) was part of an investigation of the vertebrate fauna. Olson delineated two major depocenters in the region covered by this report; Olson's basic depositional framework is substantiated by this investigation.

The U. S. Bureau of Mines (Stroud and others, 1970) investigated copper deposits in the San Angelo with emphasis on distribution and production potential. A preliminary study by the Bureau of Economic Geology (Galloway, 1970) emphasizes the general relationship of copper and lithofacies.

REGIONAL SETTING

The San Angelo Formation was deposited as a progradational unit that built westward across a restricted shelf which formed the eastern margin of the Midland Basin (fig. 2). In this report, shelf is defined as a geomorphic feature bounded by a shoreline and the pronounced break in slope at the continental or basinal margin. During Late Pennsylvanian, the Eastern Shelf formed a specific paleogeographic feature on the eastern flank of the deep Midland Basin (Galloway and Brown, 1972). By early Guadalupian time, the Eastern Shelf was shallow and lacked a distinct basinward depositional shelf edge (Oriol and others, 1967). Restricted shelf refers to a specific depositional environment characterized by hypersaline conditions with a limited biota. These conditions were probably caused by a restriction at the entrance to the Midland Basin and excessive evaporation of shallow water on the shelf (Hills, 1942).

East of the San Angelo shoreline was a wide coastal plain bordered on the east by the Ouachita foldbelt (Flawn and others, 1961). This complex of Paleozoic rocks had been extensively eroded, but was probably still shedding some sediments westward. North of the study area in the

Texas panhandle and southwestern Oklahoma, parts of the Amarillo-Wichita-Arbuckle Mountain system were still exposed. The Wichita Mountains may have been buried or greatly subdued by this time (Ham and Johnson, 1964); the Arbuckle Mountains were probably supplying some sediments to the northern San Angelo coastal plain. The presence of the Arbuckle-derived Chickasha Formation in Oklahoma (Green, 1937) and an average S45°W paleocurrent direction in the northern San Angelo outcrop of Texas supports an Arbuckle source during San Angelo deposition.

The Electra Arch is an elongate, east-west positive structural axis that traverses the southern half of Foard County. The Hardeman Basin is a negative structural element between the Wichita Mountains and the study area. Both structural elements exerted some effect upon San Angelo deposition. The San Angelo dips westward at about 15 feet per mile; in southern Stonewall County the dip increases to about 30 feet per mile.

ACKNOWLEDGMENTS

The manuscript was originally prepared in partial fulfillment of Master's degree requirements at The University of Texas at Austin. L. F. Brown, Jr., Bureau of Economic Geology, The University of Texas at Austin, suggested the study and provided assistance and guidance. A. J. Scott, F. E. Ingerson, and V. R. Baker, Department of Geological Sciences, The University of Texas at Austin, served on my thesis committee and provided constructive criticisms and recommendations. D. G. Bebout, Bureau of Economic Geology, read and criticized the final manuscript. Richard Bloomer, Abilene, Texas, provided access to the Perrini well log library. The Bureau of Economic Geology and Louisiana Land and Exploration Company provided partial financial support for the project. Gerald Bartz and Jeffery Reid evaluated ideas concerning copper mineralization. The project would not have been possible without access to the large ranches in the region. Special thanks go to my wife, Suzanne, for encouragement, perseverance, and aid during the project.

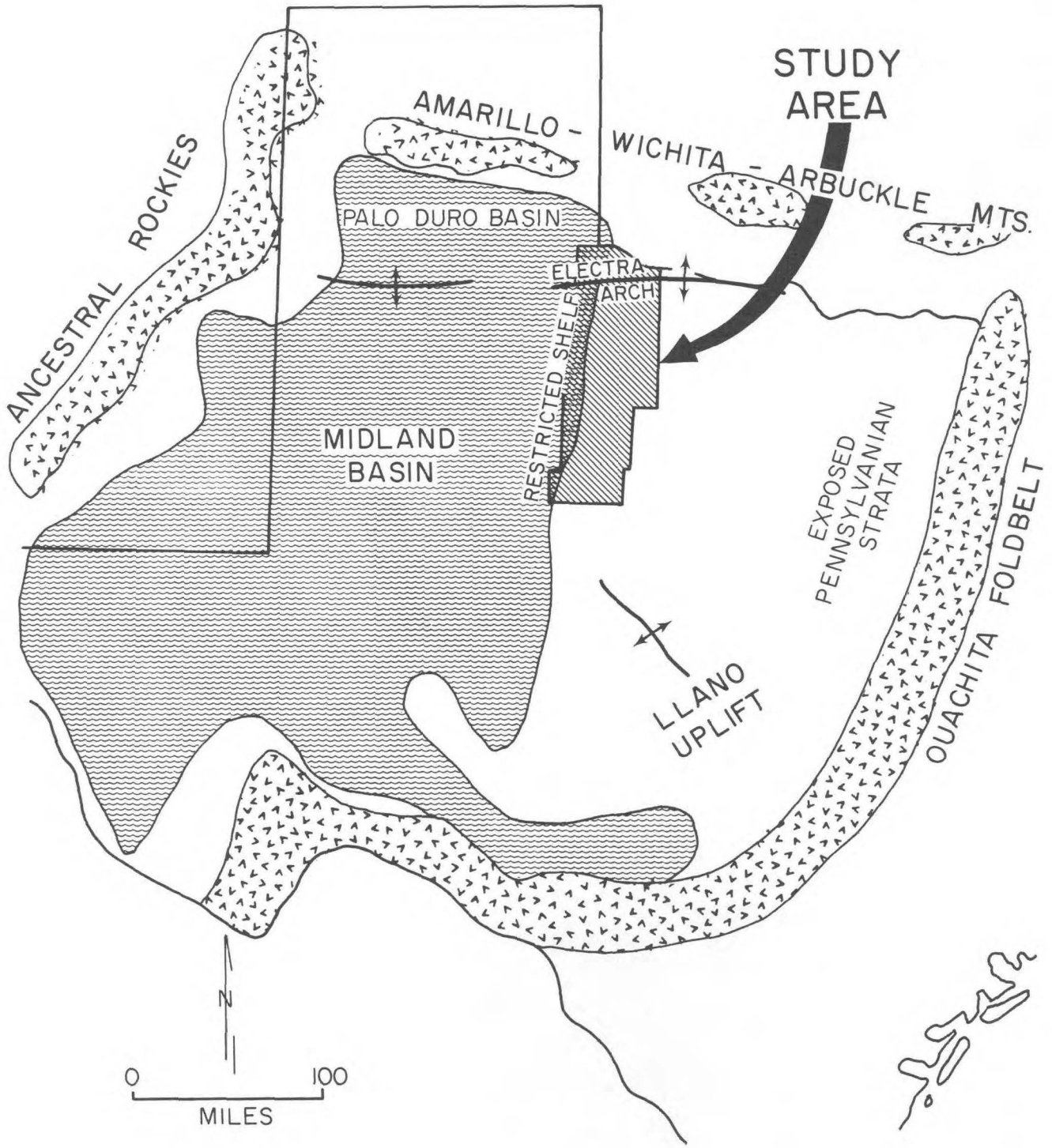


Fig. 2. Regional geologic setting, during middle Permian, northern Texas and southwestern Oklahoma.

STRATIGRAPHY

The San Angelo Formation of this report consists of complexly intertonguing mudstone and sandstone facies that extend vertically from the first massive, horizontal to ripple cross-laminated or channel-fill sandstone lying conformably or unconformably on the Choza Formation (I-2) upward to the first regionally widespread, approximately 1-foot-thick gypsum bed defined in this report as the base of the Blaine Formation (IV-6). As thus defined, the San Angelo Formation includes approximately equal amounts of sandstone and mudstone.

major part of the upper Leonardian Clear Fork Group (Beede and Waite, 1918). Conformable with the Choza at most localities is the overlying San Angelo Formation which is the basal formation of the Pease River Group. At some localities (I-1), channeling during deposition of the San Angelo Formation resulted in local unconformities; sandstone-filled channels disappear into the subsurface where continuous deposition occurred. Along the outcrop in nonchannel areas, conformable, texturally coarsening-upward sequences of terrigenous clastic sediment are common (I-2, III-22).

STRATIGRAPHIC RELATIONSHIPS

Formations in the area comprise portions of two lithologically defined groups (fig. 3). Red mudstone of the Choza Formation composes the

The San Angelo Formation grades upward and downdip into the overlying Blaine Formation. This gradational relationship can be observed along outcrop and can be documented by electric log interpretation. Gypsum and dolomite beds of the

SERIES	GROUP	NORTH TEXAS		SOUTHWEST OKLAHOMA	
		FORMATIONS AND MEMBERS		GROUP	FORMATIONS
GUADALUPIAN	PEASE RIVER	DOG CREEK SHALE		EL RENO	DOG CREEK SHALE
		BLAINE FORMATION			BLAINE FORMATION
		SAN ANGELO FORMATION	FLOWERPOT MEMBER		FLOWERPOT SHALE
			DUNCAN MEMBER		DUNCAN SANDSTONE
LEONARDIAN	CLEAR FORK	CHOZA FORMATION		HENNESSEY SHALE	
		VALE FORMATION			
		ARROYO FORMATION			

Fig. 3. Mid-Permian stratigraphic section, northern Texas and southwestern Oklahoma.

Blaine become thicker and more abundant upwards and downdip as San Angelo sandstone and mudstone beds grade into and interfinger with the Blaine Formation.

The Duncan Sandstone in southwestern Oklahoma is stratigraphically equivalent to the principal sandstone facies that compose the lower part of the San Angelo Formation of Texas, as defined in this report (fig. 3). The Duncan, formally named in 1924 (Gould, 1924), has a maximum thickness of 250 feet near the Arbuckle Mountains, but it thins northward and westward as its outcrop trends around the Wichita Mountains to connect in Texas with the basal sandstone beds of the San Angelo Formation. The Flowerpot Shale, which in Oklahoma overlies the Duncan Sandstone and interfingers with it (fig. 3), was originally named for an exposure in Kansas (Cragin, 1896). The Flowerpot Shale of southwestern Oklahoma is equivalent to the principal mudstone facies in the upper part of the San Angelo Formation of this report, although precise upper and basal contacts may differ with Oklahoma usage. Blaine Formation, named by Gould (1905) for exposures in western Oklahoma, is the term applied to the gypsum and mudstone beds above the San Angelo Formation by Beede and Christner (1926). The Blaine Formation of this report closely corresponds with that defined by Lloyd and Thompson (1929); the formation is considerably thicker in North Texas than at the type locality in Oklahoma.

The age of the San Angelo Formation has been the subject of considerable controversy (Adams and others, 1939) because of the absence of definitive index fossils. Age relationships of Permian strata in the West Texas Midland Basin traditionally have been determined principally from fusulinids and ammonoids; both of these groups are absent in the San Angelo Formation. The Blaine Formation contains ammonoids of the genus *Perrinites* which indicates a Leonardian age for at least the basal part of the Pease River Group (Miller and Furnish, 1940); *Perrinites* ranges through the Clear Fork Group and the Dog Creek Shale (fig. 3). Clifton (1946) reports *Perrinites* in the lower Word Formation of Guadalupian age in the Glass Mountains of Texas.

Olson (1962), who favors a Guadalupian age for the San Angelo Formation, based his interpretation on a distinct vertebrate faunal break that occurs in the middle of the Choza Formation. The San Angelo fauna contains a few elements

characteristic of the earlier Leonard, but the fauna is generally "progressive" since it contains new elements rather than simply minor modifications of predecessors.

PRINCIPAL STRATIGRAPHIC UNITS

The terminology used in this report is rock stratigraphic. The San Angelo Formation has been divided into two informal members: (1) the basal Duncan Sandstone Member, and (2) the upper Flowerpot Mudstone Member (fig. 4). Because of the relatively narrow outcrop of the Duncan and Flowerpot Members, as well as their intergradational contact, the San Angelo Formation was not subdivided on the geologic map (pls. I-V). The basal Choza-San Angelo and the upper San Angelo-Blaine contacts are relatively sharp and were readily mappable at most scales.

Four stratigraphic units are considered in this report: (1) Choza Formation, (2) Duncan and (3) Flowerpot Members, San Angelo Formation, and (4) Blaine Formation (fig. 5). These units are complex associations of rock types that are objectively described, but each unit represents deposits that originated within one or more distinctive depositional systems (fig. 4); genetic interpretation of these depositional systems is considered elsewhere in this report. Only the upper 30 feet of the Choza Formation and the lower 50 to 100 feet of the Blaine were examined.

CHOZA FORMATION

The uppermost 30 feet of the Choza Formation consists of interbedded layers of mudstone, siltstone, and very fine-grained sandstone, which commonly alternate between light gray and reddish brown to create a banded appearance on outcrop. Blocky to massive mudstone is the most common rock type. A few siltstone- or sandstone-filled channels were observed in the Choza; small (less than 0.5 inch in diameter), light-gray spots resulting from reduction by organic matter are common throughout the formation. Horizontal and cross-cutting seams of selenite are also common, and gypsum nodules and dolomitic mudstone beds were observed.

In southern Stonewall County, the Merkle Dolomite Member, which occurs at the top of the Choza, is about 2 feet thick and is characterized by

STRATIGRAPHIC UNITS		DEPOSITIONAL SYSTEMS
BLAINE FORMATION		SABKA AND MUD-RICH TIDAL FLAT
SAN ANGELO FORMATION	FLOWERPOT MUDSTONE MEMBER	CEDAR MOUNTAIN MUD-RICH TIDAL FLAT
	DUNCAN SANDSTONE MEMBER	(SOUTH) BUZZARD (NORTH) OLD GLORY PEAK COPPER FLUVIAL- SAND- BREAKS DELTAIC RICH DELTAIC TIDAL FLAT
CHOZA FORMATION		SABKHA, MUD-RICH TIDAL FLAT, AND SUBTIDAL

Fig. 4. Stratigraphic units and equivalent depositional systems, Choza, San Angelo, and Blaine Formations, North Texas.

oscillatory ripple marks on its bedding surfaces. In the vicinity of Old Glory, the dolomite bed has been eroded because of downcutting by channel-fill facies of the Duncan Sandstone Member of the San Angelo Formation.

SAN ANGELO FORMATION Duncan Sandstone Member

The Duncan Member of Texas is a sequence of interbedded sandstone, siltstone, and mudstone beds from 45 to 68 feet thick that comprises approximately the basal half of the San Angelo Formation. Sandstones are very fine- to fine-grained quartzarenites and sublitharenites (Folk, 1968), which are commonly white, pinkish gray, or moderately reddish brown (Goddard, 1948); upon weathering, many light-colored sandstones become moderately reddish brown. In southern Stonewall County, sandstone of the Duncan Member is slightly conglomeratic and is moderately orange-pink because of a higher percentage of metamorphic and sedimentary rock fragments within the unit. Typically, the sandstone is poorly

cemented by calcite, silica, or gypsum, and bedding types include large-scale trough crossbedding, horizontal bedding, small-scale ripple laminations, and flaser bedding. Mud-chip layers, contorted bedding, and burrows also occur in the member.

Sandstone varieties, grain size, bedding types, and other features are primarily a function of the environments in which the Duncan Member was deposited. These environments and associated depositional processes are discussed elsewhere in this report.

Mudstones of the Duncan Member, which typically are moderately reddish brown, are composed principally of illitic clay with scattered grains of quartz sand and silt.

Flowerpot Mudstone Member

The Flowerpot Member composes the upper half of the San Angelo Formation and ranges from 27 to 63 feet thick; it is gradational with the underlying Duncan Member. The contact between

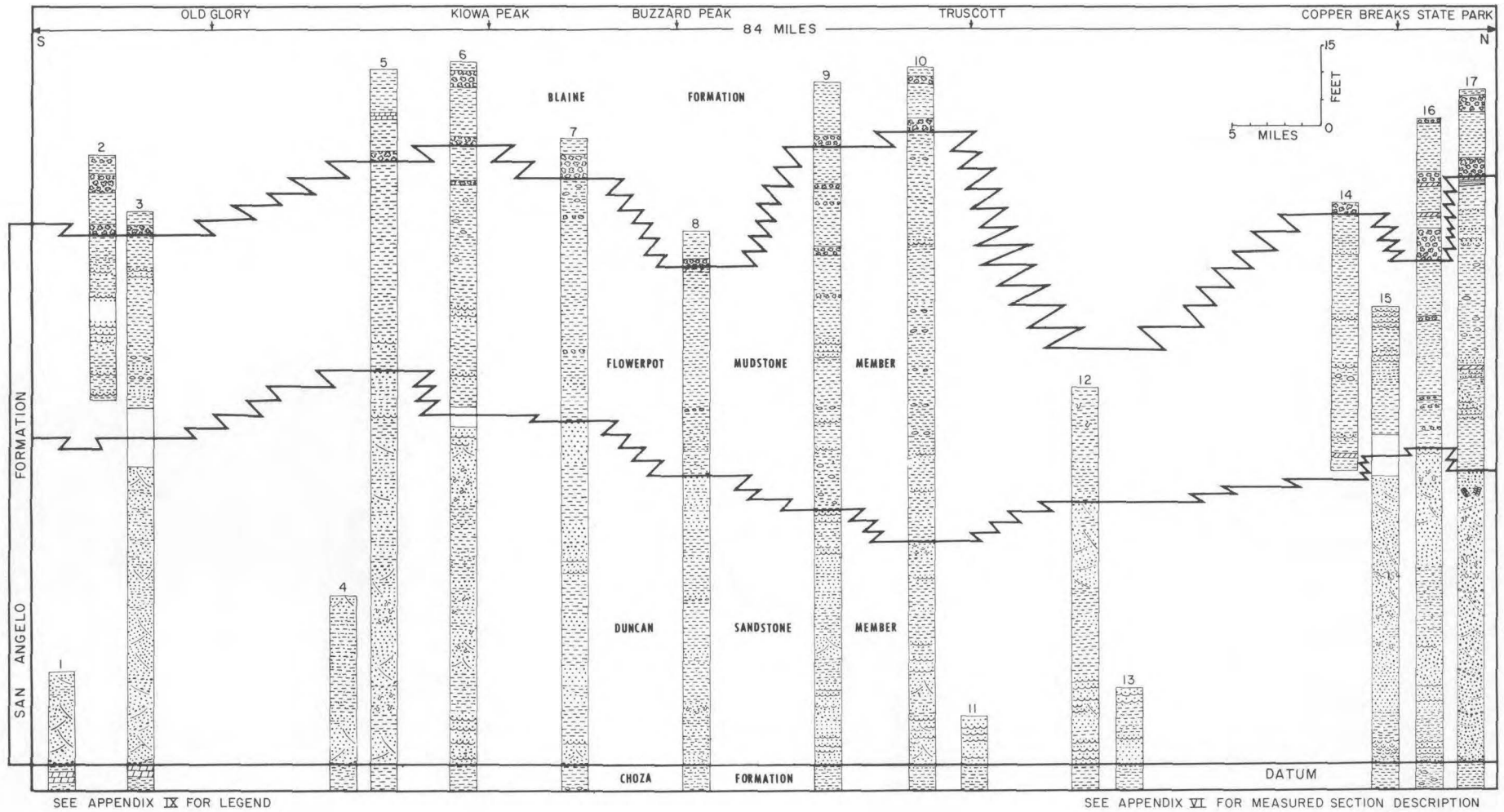


Fig. 5. Strike section of the Duncan Sandstone Member and Flowerpot Mudstone Member, San Angelo Formation (middle Permian), North Texas. (Explanation given in appendix IX.)

the members is characterized at some localities in outcrop by a distinct topographic break in slope caused by the readily erodable Flowerpot Mudstone. Gypsum nodules in the mudstone beds of the Flowerpot Member help distinguish it from mudstone present in the underlying Duncan Member. In measured sections, the uppermost prominent small-scale ripple or trough cross-stratified sandstone of the Duncan Member is defined as the base of the Flowerpot Member.

The Flowerpot Member is composed primarily of moderately reddish-brown and light-gray mudstone and siltstone with a subordinate amount of light-gray sandstone. The mudstone beds of the Flowerpot are primarily illitic with some sand- and silt-size quartz grains scattered throughout. Individual mudstone beds display poor lateral continuity because of localized channeling and other facies changes. Discoidal gypsum nodules commonly weather from the Flowerpot Mudstone. The upper portion of the Flowerpot contains thin beds of light-gray dolomicrite, barite nodules, and thin calcareous shale beds. Sandstone beds within the Flowerpot Member are either thin, ripple cross-laminated units or lenticular channel-fill deposits. Typical bedding types in the sandstones are small-scale ripple cross-stratification, very low-angle trough crossbeds, and flaser bedding.

DEPOSITIONAL SYSTEMS

The San Angelo Formation (fig. 6) is a sequence comprised of the following depositional systems: (1) Old Glory fluvial-deltaic system, (2) Copper Breaks deltaic system, (3) Buzzard Peak sand-rich tidal-flat system, and (4) Cedar Mountain mud-rich tidal-flat system. The upper 30 feet of the underlying Choza Formation examined in this report is interpreted to represent a depositional system composed of subtidal shelf, mud-rich tidal-flat, and sabkha facies that existed in the area prior to initiation of San Angelo deposition. The lower 50 to 100 feet of the overlying Blaine Formation is likewise interpreted to represent a system of sabkha and mud-rich tidal-flat facies in the area covered by this report. These depositional systems are comprised of complex facies associations deposited within sedimentary environments that changed both spatially and temporally. Each facies displays distinctive rock types and sedimentary characteristics which are a function of depositional processes that were active in late Leonardian and

Channel-fill sandstones are composed of well-cemented, light-gray quartzarenites. The top of the Flowerpot Member is defined as the base of the first extensive, approximately 1-foot-thick, gypsum bed of the overlying Blaine Formation.

BLAINE FORMATION

The lower 50 to 100 feet of the Blaine was investigated in this study; it consists of interbedded gypsum, mudstone, and claystone with minor amounts of dolomite and sandstone. At a distance, the color of the outcropping Blaine appears distinctively lighter than that of the Flowerpot. Gypsum layers in the Blaine average 2.0 feet thick, and when slabbed, they commonly reveal an intergrowth of $\frac{1}{4}$ - to $1\frac{1}{2}$ -inch-diameter gypsum nodules within a red or gray clay matrix. Some gypsum beds appear laminated or crenulated. X-ray diffraction studies of outcrop samples indicate that no anhydrite is present in the gypsum beds. Mudstone and claystone are alternately red and gray and are laterally continuous locally. Dolomite beds range from less than an inch to a foot thick and are composed of laminations or clasts of dolomicrite. Channel-fill sandstone bodies are rare within the formation.

early Guadalupian depositional environments of North Texas.

CHOZA DEPOSITIONAL SYSTEMS

The red- and gray-banded mudstone beds of the Choza Formation are part of a mud-rich tidal-flat system. Mud cracks (I-1) and silt- and sand-filled tidal channels (III-12) indicate an intertidal mudflat origin for much of the Choza Formation. Thin dolomites exhibiting oscillatory ripples and *Xenocanthus* shark teeth (Olson, 1956) found lower in the Choza support a subtidal origin for part of the Choza; the presence of gypsum nodules (I-2) and salt hopper casts points to a sabkha origin for some beds in the formation. During deposition of the Choza Formation, a coastal plain of low topographic relief allowed a complex intertonguing of these three principal environments.

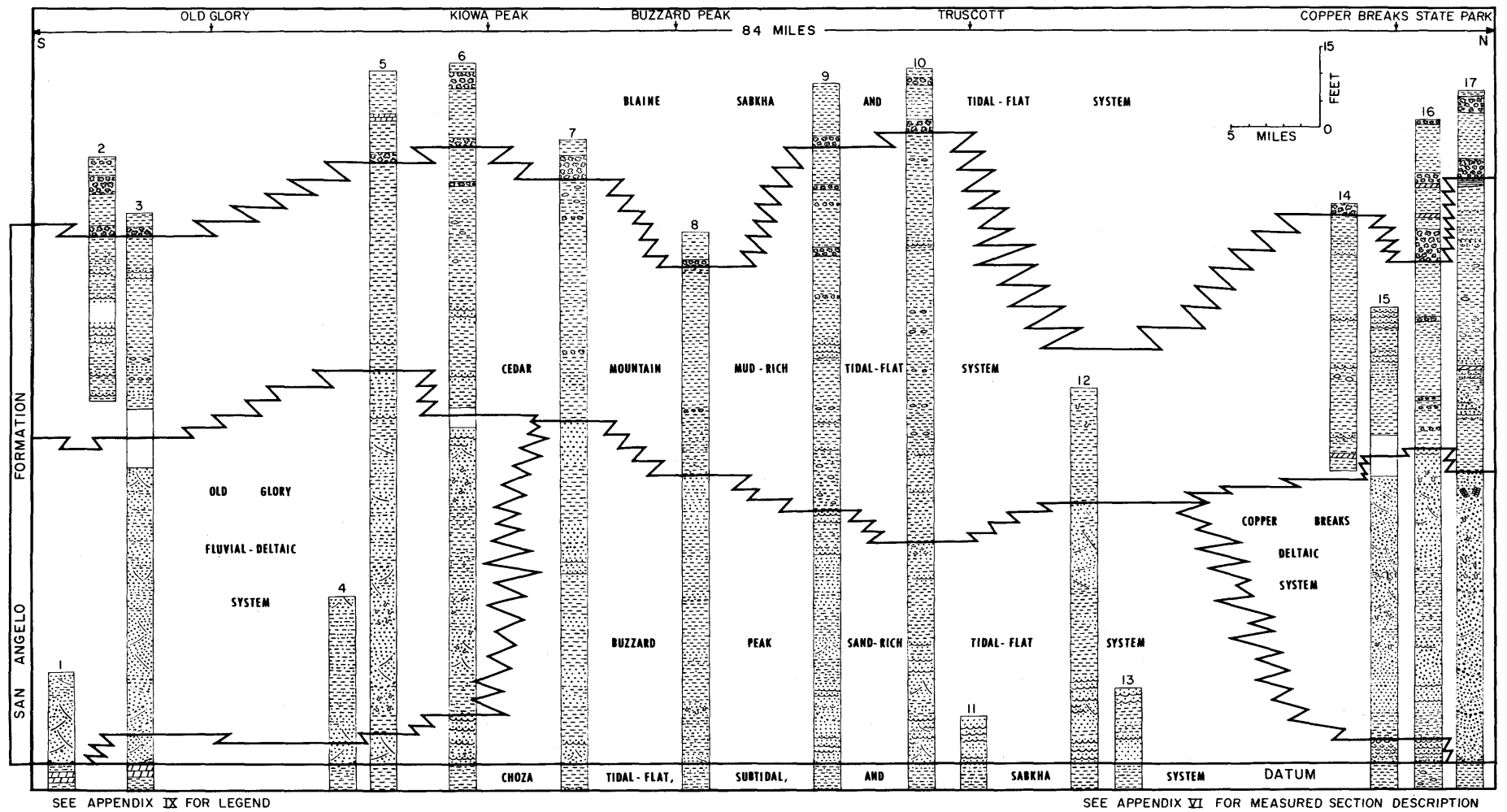


Fig. 6. Strike section of the uppermost Choza and San Angelo and the basal Blaine Formations (middle Permian) with inferred depositional environments. (Explanation given in appendix IX.)

Near the end of Choza deposition, sporadic influx of sand from nearby fluvial-deltaic systems supplied strike-fed sediment that led to the Buzzard Peak sand-rich tidal-flat system that initiated deposition of the San Angelo Formation. The Buzzard Peak sand-rich tidal-flat system is well developed in the central part of the study area and it is present as a thin veneer beneath the Copper Breaks and Old Glory fluvial-deltaic systems (fig. 6). The Buzzard Peak depositional system of the San Angelo Formation is discussed elsewhere in this report.

COPPER BREAKS AND OLD GLORY FLUVIAL-DELTAIC SYSTEMS FLUVIAL-DELTAIC DEPOSITION: A SUMMARY

Fluvial-deltaic facies develop when terrigenous clastic sediments are deposited in an open body of water by a fluvial channel. Many factors control deltaic growth. These include: (1) volume and caliber of river sediment load, (2) depth of water at the delta front, (3) relative river and reservoir water densities, (4) nature of subaqueous substrate, (5) structural nature of depositional basin, and (6) kind and degree of marine energy (Fisk and others, 1954; Fisher and others, 1969).

The delta plain is a complex of interrelated distributary channel, natural levee, interdistributary marsh and bay, and crevasse splay sediments. Distributary channel-fill sand deposits form the framework of this facies complex and mud and silt facies of the delta plain serve to fill in interdistributary areas. The bulk of the delta-plain deposits are fine-grained silts and clays (Frazier, 1967). The sands and silts of delta-front and distributary mouth bar facies form basinward of the delta-plain complex and represent areas of extensive deposition and, in some cases, reworking of sediments being transported through the fluvial-deltaic network. Prodelta mud deposits are gradational upward and landward with the delta-front facies; these muds and silts form distally on the marine shelf as a result of deposition of suspended load introduced by the fluvial system.

Continuous fluvial-deltaic sedimentation results in progradation of fluvial-deltaic facies. Progradation leads to development of a vertical sequence composed (upward) of lowermost prodelta facies overlain by delta-front and distributary mouth bar facies, and capped by facies of the delta-plain complex (Scruton, 1960; Coleman and Gagliano, 1964).

Fluvial-deltaic facies of the Duncan Sandstone Member are interpreted to have been deposited by high-constructive lobate deltas (Fisher and others, 1969) based on analysis of subsurface sand trends and outcrop examination of the deltaic facies.

REGIONAL PATTERNS AND DISTRIBUTION OF FLUVIAL-DELTAIC SYSTEMS

A deltaic system in the northern and a fluvial-deltaic system in the southern part of the area represent principal progradational routes of deltas within the Duncan Sandstone Member. The outcrop intersects the deltaic system at Copper Breaks Park and the fluvial-deltaic system near Old Glory. Only deltaic facies occur at Copper Breaks Park, but alluvial plain - fluvial channel deposits (V-10, V-11) occur at outcrop in the Old Glory area. Sand- and silt-size clastics deposited by distributary streams were transported laterally along the shoreline to supply the intermediate, strike-fed, sand-rich tidal-flat system in the Buzzard Peak region. The northern (Copper Breaks) delta system and southern (Old Glory) fluvial-deltaic system intertongue with the intermediate Buzzard Peak tidal-flat system 5 miles south of Teacup Mountain (pl. I) and near Kiowa Peak (pl. IV), respectively. Sediment dispersal and inferred depositional environments have been proposed for the Old Glory fluvial-deltaic, Copper Breaks deltaic, and Buzzard Peak tidal-flat systems (fig. 7).

COPPER BREAKS DELTAIC SYSTEM

The Copper Breaks deltaic system crops out from Medicine Mounds southwestward through Copper Breaks Park and into the Teacup Mountain area where the deltaic sediments disappear into the subsurface (pl. I). Superposed sand-filled distributary channels crop out in the drainage of Cottonwood Creek near Medicine Mounds (I-4). These channel deposits eroded Copper Breaks prodelta and delta-front facies, the thin veneer of underlying Buzzard Peak sand-rich tidal-flat facies, and locally the channels cut into the underlying Choza Formation (I-1). At Copper Breaks Park, a complete vertical progradational section of deltaic facies is well exposed (I-2; fig. 8). In the Teacup Mountain area, the distal delta-front sandstone facies crops out (I-50); delta-front sandstones are

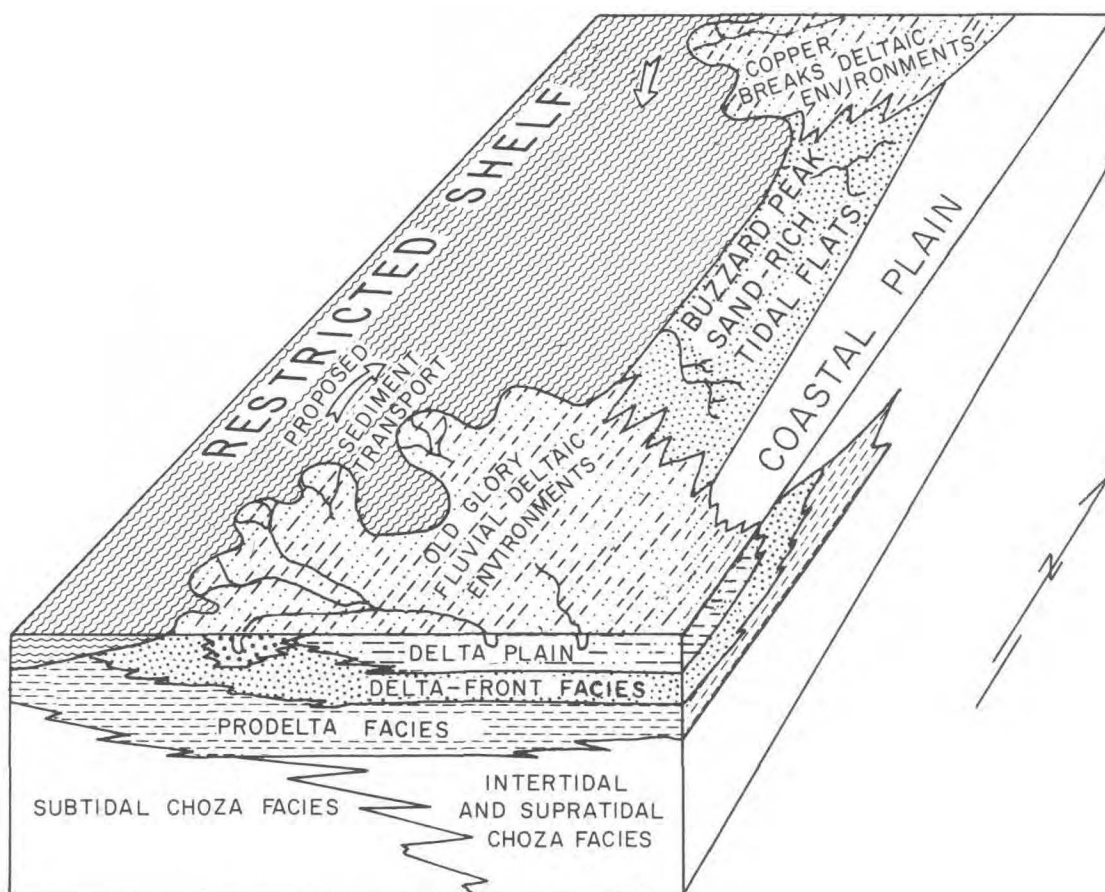


Fig. 7. Depositional model of Old Glory, Copper Breaks, and Buzzard Peak systems. These systems compose the Duncan Sandstone Member.

massive and contain possible authigenic gypsum nodules. Eighty-nine crossbedding measurements and 16 channel orientation measurements taken in the Copper Breaks deltaic system (fig. 9) indicate a general southwest to west sediment transport. A net sandstone map constructed from electric logs indicates that sandstone facies of the Copper Breaks delta system extend only 5 miles into the subsurface (fig. 9). The Copper Breaks delta lobe apparently prograded west-southwest across Choza-restricted subtidal and shelf sediments.

Facies of the Copper Breaks Deltaic System

The Copper Breaks deltaic system displays in outcrop a spectrum of facies from upslope upper delta plain to downslope deltaic. Deltaic facies, in addition, fit well into a tract from delta-plain

through delta-front to distal prodelta facies. Because of the progradational nature of the high-constructive Copper Breaks system, deltaic facies are superposed in a classic vertical sequence (fig. 8).

Prodelta facies.—Prodelta facies occupy a thin zone about 6 feet thick beneath delta-front and distributary mouth bar facies; prodelta mudstone facies rest conformably on the sand-rich tidal-flat facies of the Buzzard Peak system (I-2, I-3; fig. 8). The thin prodelta facies is composed of (appendix I) moderately reddish-brown mudstone and sandy mudstone, which exhibit lateral continuity, thin to medium bedding, and absence of burrowing. In the Medicine Mounds area, the prodelta facies is extensively eroded by distributary channels. The prodelta facies can be distinguished from mudstone of the underlying thin

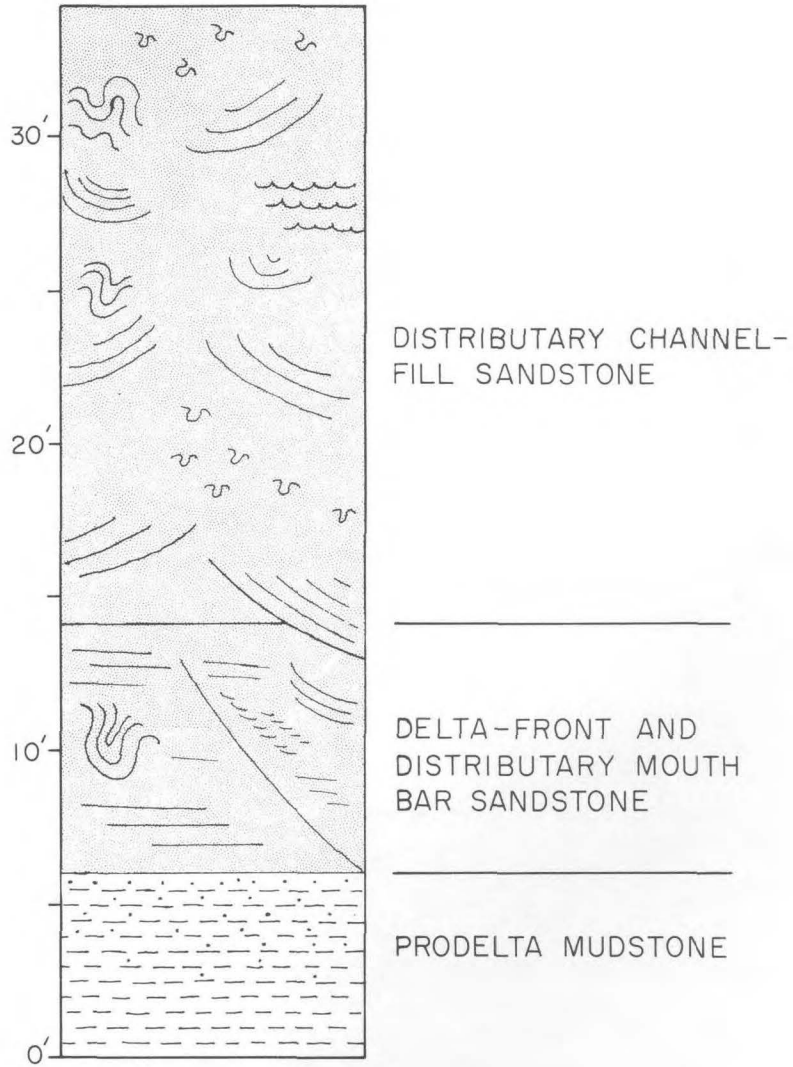


Fig. 8. Copper Breaks deltaic progradational sequence. Based on measured section I-2, Copper Breaks State Park. Base of diagram represents the base of the prodelta facies.

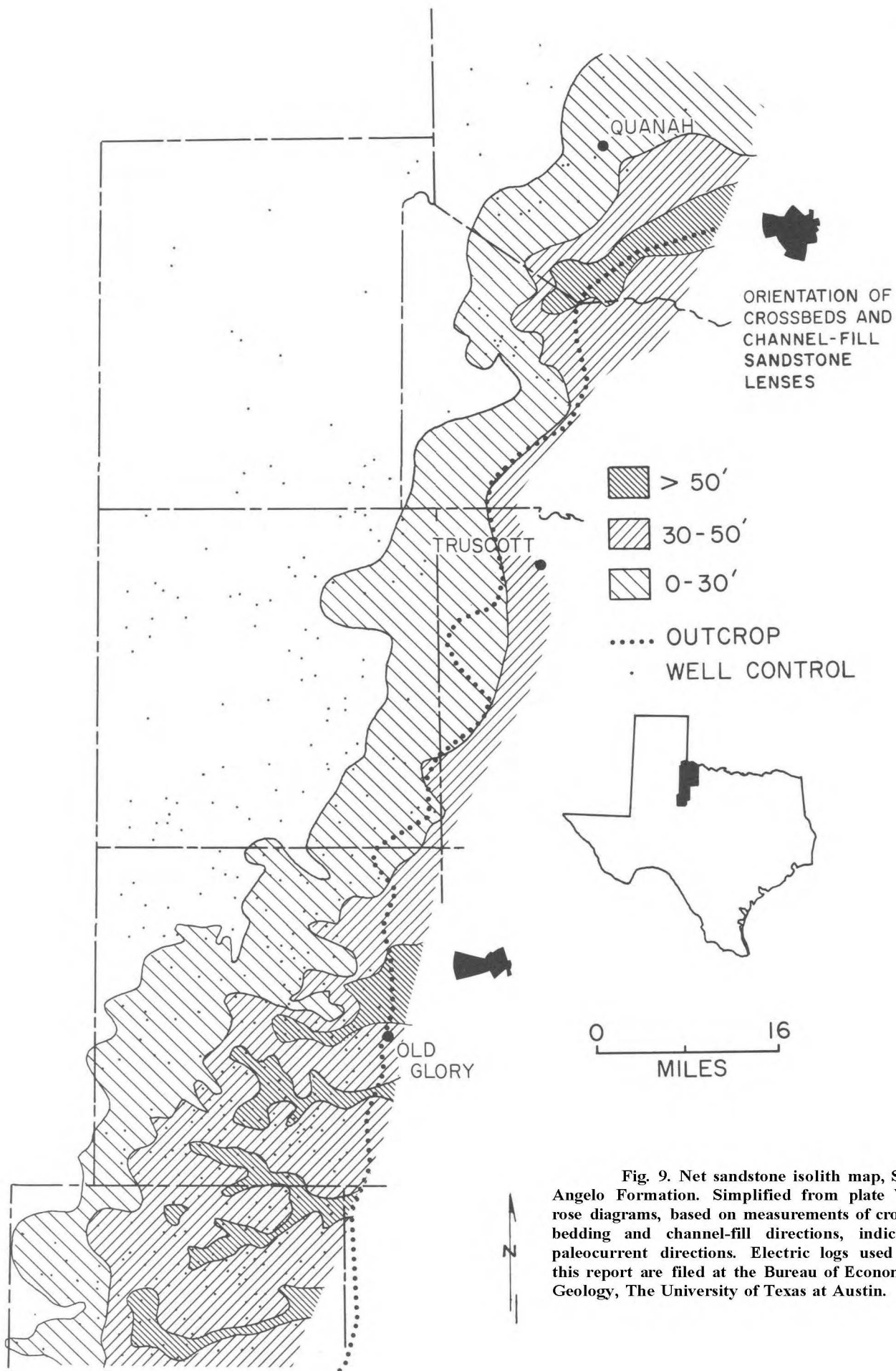


Fig. 9. Net sandstone isolith map, San Angelo Formation. Simplified from plate VI; rose diagrams, based on measurements of cross-bedding and channel-fill directions, indicate paleocurrent directions. Electric logs used in this report are filed at the Bureau of Economic Geology, The University of Texas at Austin.

vener of Buzzard Peak tidal-flat facies and the Choza Formation because the prodelta facies are well bedded and lack gypsum nodules and selenite seams.

Delta-front facies.—Sandstone of the delta-front facies conformably overlies mudstone of the prodelta facies (fig. 8). The delta-front sandstone facies is about 10 feet thick and forms a sheetlike body containing abundant horizontal bedding. A characteristic feature of the delta-front sandstone is the presence of thin clay laminae separating thicker, horizontal sand laminae. On such a shallow, restricted shelf, wind-generated as well as astronomic tides may have periodically reworked the delta-front sands; clay laminae may represent deposition during periods of very low physical energy. Delta-front sandstone facies are (appendix I) composed of white, fine-grained, moderately to well-sorted quartzarenite and sublitharenite. Weathered delta-front sandstone facies are light reddish brown. No evidence of burrowing was observed in the delta-front facies; rapid deposition, coupled with saline to hypersaline conditions on the shelf probably prevented burrowing.

The delta-front facies is composed of closely spaced distributary mouth bar deposits and laterally reworked delta-front sheet sands. Delta-front facies are best preserved in the Copper Breaks Park area (I-2, I-20, I-15); they were removed by channel erosion in many other areas.

Distributary mouth bar facies.—Along the outcrop (I-2), delta-front facies can be traced laterally into clean, fine-grained, well-sorted sandstone which represents deposition at the mouth of distributary channels. Color, composition, and stratification types are very similar in both delta-front and distributary mouth bar facies; the principal difference is an absence of clay laminae and minor amounts of medium-scale trough crossbeds and climbing ripple cross-stratification in the distributary mouth bar facies. Contorted bedding was also observed in distributary mouth bar facies (I-20), indicating that subjacent prodelta muds were soft and that overloading and subsidence had occurred.

Distributary channel and associated delta-plain facies.—Distributary channel-fill sandstone facies (fig. 8) in the northern part of the outcrop belt near Copper Breaks Park and Medicine Mounds are composed of (appendix I) moderately

reddish-brown, fine-grained, well- to moderately well-sorted sublitharenite and quartzarenite. Medium- to large-scale trough crossbeds are the principal bedding type; minor amounts of horizontal bedding, small-scale ripple cross-stratification, and climbing ripple crossbeds are also present. No definite vertical succession of bedding types was noted, although horizontal bedding was most common at the top of some distributary channel deposits. The closely spaced nature of distributary channel-fill sandstone deposits along with poor exposures make it difficult to determine precisely the maximum or average thickness and width of channel-fill deposits. Distributary channel-fill sandstone units up to 30 feet thick and 200 feet wide were observed (I-5, I-10). A well-exposed channel-fill deposit in Copper Breaks Park (I-3) is 11 feet thick and 122 feet wide. Channel deposits have erosional bases, and they normally display evidence of reoccupation and partial erosion by later streams (I-4). Contorted, flow-roll sandstone structures, which are common throughout the distributary channel-fill facies (I-2), were probably caused by soft-sediment deformation of channel-fill deposits. In some cases, sandstone bedding planes continue undisturbed through the roll structure; in these cases the roll structure may be the result of cementation phenomena that took place during lithification. Distributary channel-fill sandstone facies grade laterally and upward into poorly developed, moderately reddish-brown siltstone, mudstone, and thin sandstone units that constitute other delta-plain facies, such as interdistributary bay, crevasse splay, and levee deposits.

Burrows are common in Copper Breaks distributary channel sandstone; the nature of the burrowing organism was apparently controlled by the salinity of the environment. *Ophiomorpha*-like walled burrows are present in the upper part (upstream facies) of the Copper Breaks deltaic distributary facies near Medicine Mounds (I-11). These burrows are large (1 to 2 inches thick and as much as 1 foot long), and they occur in friable sandstone poorly cemented by calcite and dolomite. Stratigraphically lower (downstream facies) in the distributary channel sandstone of the Copper Breaks system, the large *Ophiomorpha*-like walled burrows give way to a smaller (less than half an inch thick and a few inches long) type of burrows (I-14). The small burrows are associated with gypsum cement and gypsum nodules. Apparently, the large burrowing organisms were able to

thrive only in the less saline water higher in the inactive distributary channels. Lower in the delta system, where the water in distributaries was hypersaline, only burrowing organisms that were tolerant of high salinity were able to exist. Carbonaceous material is rare in all of the deltaic facies, probably because of oxidation of woody material during and shortly after deposition.

OLD GLORY FLUVIAL-DELTAIC SYSTEM

The Old Glory fluvial-deltaic system crops out from about 3.5 miles south of the northern border of Stonewall County southward into Fisher County (fig. 9). Subsurface mapping southward to the latitude of central Fisher County failed to delineate a southern limit to the fluvial-deltaic system. The Old Glory system prograded basinward approximately 30 miles west of the present outcrop to terminate in western Stonewall and Fisher Counties (fig. 9). Four areas of east-west trending, high net sand values have been recognized (fig. 9) and are interpreted to represent individual fluvial-deltaic lobes. Each lobe is composed of delta-front and distributary channel-fill deposits, as well as superimposed upper delta-plain and alluvial plain - fluvial channel deposits. Exposures of these facies occur near localities IV-5, V-4. Fluvial-deltaic sandstone north of the Old Glory system is composed of fine-grained sublitharenite; south of Old Glory, the fluvial-deltaic sandstone becomes slightly conglomeratic with pebbles of metamorphic quartz, metamorphic rock fragments, and sedimentary rock fragments. This southward change in composition is indicative of a closer source area, different source rocks, and/or a steeper paleostream gradient. The appearance of pebbles in the Old Glory system corresponds with a local increase in dip of the strata, possibly supporting a hypothesis that a steeper paleo-gradient aided in bringing coarser material into the coastal area. Thirty-two crossbedding measurements taken on outcrops of the fluvial-deltaic facies north of the Salt Fork of the Brazos River (fig. 9) strongly indicate a westward direction of sediment transport.

Facies of the Old Glory Fluvial-Deltaic System

Compositionally and texturally, the southern outcrop area of distributary channel and delta-plain facies (fig. 6) is similar to the Copper

Breaks deltaic complex. Interdistributary mudstone and siltstone and thin crevasse splay sandstone beds (IV-7, IV-41, V-11) are well developed in outcropping delta-plain deposits of the Old Glory system. Mud-chip conglomerates are also common in the Old Glory distributary channel and delta-plain facies (V-5).

Net sandstone trends in the Old Glory fluvial-deltaic system (pl. VI) exhibit elongate to lobate patterns. Sandstone isolith lines (0 to 30 feet) delineate a sheetlike geometry indicative of reworked distributary mouth bar sands associated with a shoal-water (lobate) delta (Fisk, 1955).

South of Old Glory (pl. V, fig. 9) composition, texture, and scale of sedimentary structures exhibited by outcropping distributary channel-fill sandstone deposits change; sandstone beds (appendix I) are slightly conglomeratic, with siliceous and calcareous cement, and commonly are moderately orange-pink (V-10, V-6). Sandstone samples exhibit compositions that grade from sublitharenite to almost litharenite. Rock fragments are commonly siltstone, phyllite, and schist; quartz pebbles are commonly of a metamorphic quartz variety. Large-scale trough crossbeds from 5 to 15 feet are common. Changes in the nature of the fluvial-deltaic channel-fill sandstone deposits south of Old Glory indicate that deposition of these coarser clastics probably took place in channels higher on the upper delta plain and lower alluvial plain. Large-scale sedimentary structures may have formed in response to structural or tectonic steepening of the depositional slope.

FLUVIAL-DELTAIC DEPOSITIONAL MODEL

The Copper Breaks and Old Glory fluvial-deltaic systems (fig. 7) are interpreted to be high-constructive lobate deltas (Fisher and others, 1969). Net sand distribution (pl. VI, fig. 9) in the individual fluvial-deltaic lobes of the Old Glory system exhibits a lobate pattern, and a vertical sequence of prodelta, delta-front, and delta-plain facies (fig. 8) suggests high-constructive deltaic processes. Although the preserved Copper Breaks and Old Glory systems cover a relatively large area (greater than 630 and 1,560 square miles, respectively), they are relatively thin sequences (figs. 8 and 9) when compared to many modern and ancient delta systems.

The restricted shelf during San Angelo deposition was shallow and salinity was higher than normal marine salinity. Marine energy was characterized by low wave and current conditions except during storms. The thin Copper Breaks and Old Glory fluvial-deltaic deposits suggest that the depositional basin was stable, that water was shallow, and that the subaqueous substrate was relatively competent with only minor compaction caused by sediment loading. The absence of thick prodelta muds and a relatively high proportion of sandstone in the fluvial-deltaic and tidal-flat systems suggest that the sand to mud ratio of the sediment carried through the fluvial-deltaic systems was relatively high, with a significant proportion of the sand being distributed laterally by tidal energy and longshore drift to supply the Buzzard Peak tidal flats. The Buzzard Peak tidal-flat facies, composed of approximately 50 percent sandstone and 50 percent mudstone, received a large proportion of the mud supplied by the fluvial-deltaic systems. Part of the mud fraction of the sediment load was deposited as a thin prodelta facies; a small amount of the mud may have been carried further out onto the shelf by the lens of lighter fluvial-deltaic water that overrode the denser, highly saline marine water as a result of hypopycnal flow conditions (Bates, 1953).

Depositional processes and facies of the Guadalupe River delta (Donaldson and others, 1970) are analogous in some respects to the depositional factors that are inferred for the Copper Breaks and Old Glory fluvial-deltaic systems. The modern Guadalupe River delta is a compound elongate-lobate, high-constructive delta that is prograding into less than 7 feet of water in San Antonio Bay, Texas. The prodelta facies of the Guadalupe delta averages about 2 feet thick, compared with 6 feet of prodelta facies in the Copper Breaks deltaic system (I-2). A sheetlike delta-front facies about 3 feet thick in the Guadalupe delta has formed in response to a coalescence of closely spaced distributary mouth bar deposits caused by rapid progradation into shallow water. The delta-front sandstone facies exposed in Copper Breaks State Park (I-2, I-19) is 10 feet thick and probably represents deposition in shallow water with some coalescence of distributary mouth bar deposits. Distributary channel-fill deposits of the Guadalupe River delta are up to 16 feet thick and have eroded into the underlying bay facies. Individual distributary channel-fill deposits of the Copper Breaks deltaic

system are 10 to 20 feet thick and have eroded into the underlying Choza Formation (I-1). The Guadalupe delta sequence is from 9 to 16 feet thick, compared with the Copper Breaks and Old Glory fluvial-deltaic systems which are about 55 feet thick (fig. 6).

Some factors associated with deposition of the Copper Breaks and Old Glory fluvial-deltaic systems were different from those that are influencing the geometry and composition of the Guadalupe River delta. The Guadalupe delta has a relatively low sand to mud ratio with well-developed, mud-rich interdistributary deposits and silty delta-front sediments. This contrasts with the San Angelo fluvial-deltaic systems which exhibit a lower proportion of mudstone or siltstone (fig. 6). Wind-induced tidal currents are more important than astronomic tides in San Antonio Bay, but neither significantly affect Guadalupe delta deposition. Permian wind and astronomic tides are inferred to have been strong enough to cause winnowing of deltaic silt- and clay-size particles and to induce lateral redistribution of sand during deposition of the Copper Breaks and Old Glory systems; tidal currents were insufficient to form tide-dominated fluvial-deltaic systems. Evidence for tidal currents include tidal channel facies, mud laminae, flaser bedding, and bimodal crossbedding in the Buzzard Peak and Cedar Mountain tidal-flat systems.

The Copper Breaks and Old Glory fluvial-deltaic systems prograded across submerged tidal-flat facies and onto the shallow restricted shelf. Continued progradation and bifurcation of distributary channels led to development of high-constructive lobate delta lobes. Sand and mud were distributed laterally to supply the contemporaneous Buzzard Peak sand-rich tidal-flat system; a small proportion of the mud formed the thin prodelta facies. Superposition of distributary channels (I-46, I-4, IV-5) and a maximum 68 feet of fluvial-deltaic facies (Old Glory system) suggest that sediment loading, compaction of underlying sediments, and basin subsidence allowed some stacking of fluvial-deltaic facies.

BUZZARD PEAK AND CEDAR MOUNTAIN TIDAL-FLAT SYSTEMS

TIDAL-FLAT DEPOSITION: A SUMMARY

Tidal-flat facies result from deposition in the intertidal zone between mean low-tide and

mean high-tide levels. Tidal-flat deposition occurs in response to complex factors directly related to coastal energy and sediment supply (Beall, 1968). Factors include (1) wave energy, (2) width of the inner shelf, (3) tidal range, and (4) orientation of the intertidal zone with respect to the prevailing wavefront. Sediment supply factors include (1) ratio of sand to mud supplied to the tidal-flat system, (2) quantity of each sediment type, (3) proximity of sediment source, and (4) salinity of the inner-shelf water.

Tidal flats that develop under conditions of relatively low sediment influx and weak to moderate tidal energy tend to be dominated by tidal processes that result in a winnowing of tidal-flat sediments and separation of sand-size grains from clay-size particles. The result of this process is the formation of relatively isolated lenses of sand analogous to the cheniers along the southwestern Louisiana coast (Gould and McFarlan, 1959). Tidal-flat facies formed in coastal zones dominated by high tide and low sediment load (Evans, 1965) exhibit a fining-upward textural profile (van Straaten, 1954); mud accumulates high on the tidal flats because of settling lag, scour lag, organic baffling, and ebb currents that are weaker than flood currents (van Straaten and Kuenen, 1957; Kellerhals and Murray, 1969). In contrast, tidal-flat facies formed along coasts with significant sediment supply exhibit a complex of interrelated facies because of a shifting balance between quantity, rate, and type of sediment supplied to the environment (Curry, 1964).

Facies developed in a tidal-flat environment exhibit a sheetlike geometry elongate parallel with the coastline. In a dip-oriented cross section, tidal-flat facies are wedge-shaped (Reineck, 1972) and their width perpendicular to the coastline is determined by tidal range, rate of sediment supply, and topographic slope of the coastal zone. The thickness of tidal-flat facies is dependent on the rate of compaction and subsidence of previously deposited sediments, as well as structural subsidence of the margin of the basin. Tidal channels, exhibiting a lenticular shape in transverse cross section and a meandering pattern in plan view, drain the tidal flats. Materials composing a tidal flat may be mud, silt, sand, or biogenic (algal mats, foraminiferal tests, shell hash) sediments, depending on the supply of each of these components to the tidal environment.

Tidal-flat systems in the San Angelo Formation were formed by seaward accretion and aggradation of terrigenous sediments attendant with compaction and subsidence of previously deposited sediments; the early tidal flats (Buzzard Peak system) were sand-rich; later tidal flats (Cedar Mountain system) became mud-rich.

REGIONAL PATTERNS AND DISTRIBUTION OF TIDAL-FLAT SYSTEMS

The Buzzard Peak sand-rich tidal-flat system (figs. 6 and 7) occurs in outcrop from near Kiowa Peak (pl. IV) where it interfingers with the Old Glory fluvial-deltaic system, northward to a location about 5 miles south of Teacup Mountain (pls. I, II) where it intertongues with the Copper Breaks deltaic system. Buzzard Peak facies are also present as a thin veneer beneath the San Angelo fluvial-deltaic systems.

Initiation of fluvial-deltaic sedimentation supplied sediment for a thin veneer of Buzzard Peak tidal-flat and subtidal facies that were prograded over by the Old Glory and Copper Breaks systems (fig. 6). Continued deltaic progradation, longshore transport of sand-rich terrigenous sediments, and winnowing during low sediment input led to contemporaneous accretion of the well-developed Buzzard Peak sand-rich tidal-flat system between the fluvial-deltaic systems (fig. 7).

Gradational above the Buzzard Peak system is the Cedar Mountain mud-rich tidal-flat system (fig. 6) which extends over the Old Glory, Buzzard Peak, and Copper Breaks systems in the area of this report. Mud accretion that formed the Cedar Mountain system occurred as a result of longshore transport of mud-rich sediments from a fluvial-deltaic complex centered possibly in Coke County about 80 miles south of the southernmost limit of study in this report.

BUZZARD PEAK SAND-RICH TIDAL-FLAT SYSTEM

Buzzard Peak tidal-flat facies are composed of layers of sandstone interbedded with sandy mudstone (fig. 10). The Buzzard Peak system averages about 52 feet thick and is composed of approximately 50 percent sandstone. Sandstone extends 4 miles downdip into the subsurface where it pinches out into mudstone (pl. VI, (fig. 9). West

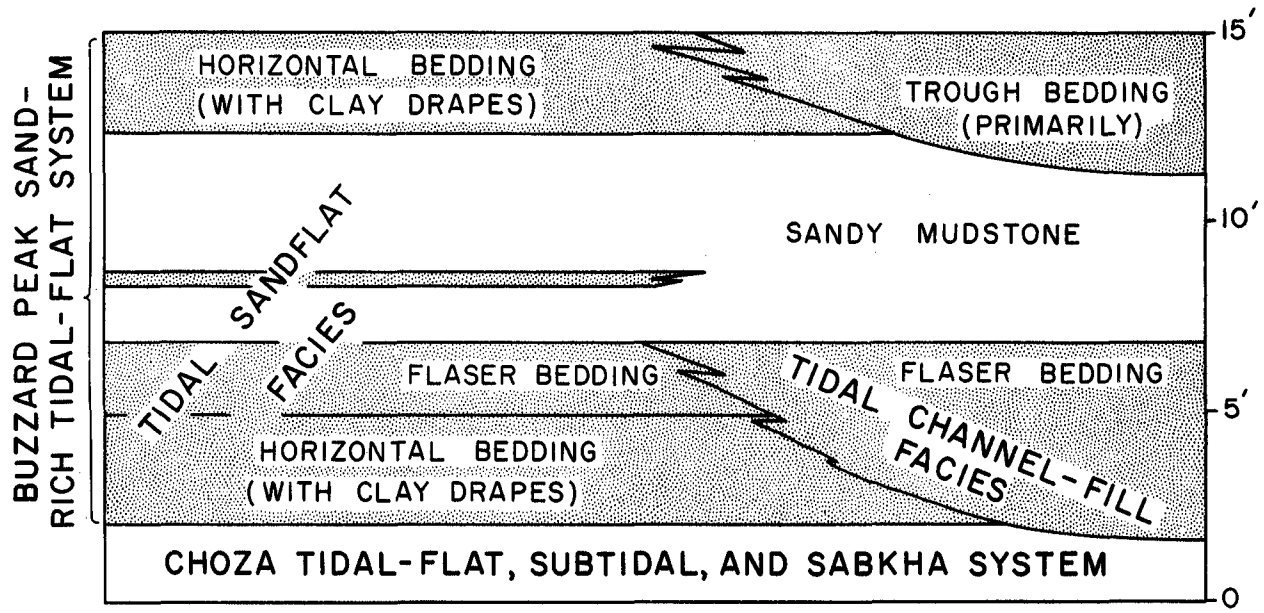


Fig. 10. Facies relationships in the Buzzard Peak sand-rich tidal-flat system. Left side of figure based on measured section II-11.

of Truscott (fig. 9), a lobe-like net sandstone pattern less than 10 feet thick extends 8 miles downdip beyond the outcrop. Net sandstone contour patterns in the San Angelo Formation suggest a strike-fed origin for the Buzzard Peak system (fig. 9).

The Buzzard Peak system is inferred to have originated in response to longshore transport of sand and mud with intermittent periods of tidal winnowing; the system apparently prograded by seaward accretion across Choza subtidal and submerged tidal-flat sediments. Compaction of previously deposited sediments, possible structural subsidence, and repeated accretion allowed tidal-flat sandstone and mudstone beds to accumulate to a thickness that cannot be accounted for by a single progradational sequence. Sandy mudstone beds interbedded with the sandstone beds probably represent periods during which deltaic sedimentation was supplying a heavy load of sediment to the intermediate tidal flats. Maximum sediment supply resulted in rapid progradation of the tidal flats with little opportunity for winnowing to develop sandstone lenses. The sandstone beds, therefore, probably represent periods during which sediment input from the deltaic systems was low and tidal

currents and low wave energy extensively reworked tidal-flat sediments. Reworking and winnowing concentrated sand deposits; the winnowed mud fraction probably was transported into embayments within the Buzzard Peak system where marginal mud-rich tidal flats were nourished. A dry climate inferred for the area during mid-Permian suggests that normal discharge through the Old Glory and Copper Breaks systems was low; main pulses of sediment influx may have occurred seasonally or during storms.

Facies of the Buzzard Peak Sand-Rich Tidal-Flat System

Tidal sandflat facies.—Sandflat facies form the framework of the Buzzard Peak system and are separated by beds of sandy mudstone. Individual tidal-flat sandstone beds are 3 to 10 feet thick, thicken and thin along outcrop, and are locally continuous; sandstone beds pinch out laterally and are replaced by beds at slightly different stratigraphic levels. Sandstone beds in the basal 10 to 20 feet of the Buzzard Peak system exhibit maximum regional lateral continuity. Tidal-flat sandstone beds are composed of very fine- to fine-grained, well-sorted, white to tan quartzarenite that is

weakly cemented with silica. Weathered tidal-flat sandstone beds are light reddish brown.

Sandstone beds exhibit horizontal laminations, ripple cross-stratification, and flaser bedding (fig. 10) that are laterally and vertically intergradational (II-11). Some horizontal-laminated sandstone beds exhibit current lineations (III-22), and clay drapes less than a quarter of a millimeter thick commonly separate thinly to thickly laminated sandstone layers (III-11, III-20). Clay drapes (Reineck, 1967) may originate in a tidal-flat environment during the period of slack water when tides are changing; sand layers originate during periods of current activity. Clay drapes may also be caused by wind tides (Fisk, 1959) that push thin sheets of turbid water over the tidal flats. The clay is deposited from suspension as thin parallel laminae when the wind-induced current slackens.

Burrows are present in some of the sand-flat sandstone beds of the Buzzard Peak system. They are smooth sided and one-fourth to three-eighths inch in diameter (III-14). Moderately reddish-brown sandy mudstone interbedded with the sandstone is 2 to 8 feet thick; some gray sandy mudstone may also be present. Some sandstone beds have been mottled by burrowing activity (III-6). Some mudstone within the sandy tidal-flat facies may represent facies deposited in an upper tidal-flat or marsh environment, but interbedded sandstone and mudstone is probably related to sediment supply and tidal winnowing of mud, rather than a vertical stacking of progradational facies.

Tidal channel facies.—Lenticular tidal channel-fill deposits, composed of gray, very fine- to fine-grained, well-sorted quartzarenite, are present throughout the Buzzard Peak system (III-14, IV-1). Tidal channel facies at the base of the Buzzard Peak system (I-2, IV-8) grade laterally into muddier sediments. Tidal channel-fill deposits are 1.5 to 7 feet thick, 75 to 160 feet wide and are characterized by flaser bedding, horizontal bedding, and low-angle trough crossbedding. The principal stratification is flaser bedding, a form of small-scale ripple cross-stratification, with the troughs between ripple crests filled with silt and clay; this ripple type occurs in modern sediments deposited by tidal currents (Reineck, 1967). During flood tides, sand and clay are carried as part of the traction and suspended load within tidal channels. During this period of channel transport,

some sand is deposited by ripple bed forms. As current slackens before the beginning of ebb tide, some suspended clay is deposited between ripple crests. In most cases, the returning ebb tide flow will wash out these finer grained sediments, but some flasers are later covered by sand ripples and thus preserved. Both small-scale ripple cross-stratification and flaser bedding are related to low flow-regime bed forms (Harms and Fahnestock, 1965).

Basal tidal channel-fill deposits are thoroughly cemented by gypsum (I-2, III-7). Above the basal channel-fill, tidal channel-fill deposits are composed of very fine- to fine-grained, white to buff quartzarenite that is poorly cemented by calcite and silica. Channel-fill sandstone lenses grade laterally into sandstone beds of the sandflat facies (III-14, III-5). These channel-fill deposits are comprised of medium- to large-scale trough cross-stratification with less common flaser bedding, horizontal bedding, and low-angle trough crossbedding. Flaser and horizontal bedding are most common in the upper part of the tidal channel-fill sequence. Trough crossbedding may represent scouring related to channels formed during periodic storms or possibly deposition in deeper major tidal channels that received runoff from smaller, shallower tidal channels and runnel systems on the sand-rich tidal flats.

Buzzard Peak Sand-Rich Tidal-Flat Depositional Model

The Buzzard Peak system (figs. 6 and 7) is interpreted to have been deposited by regression or seaward accretion and vertical aggradation of sand-rich deposits supplied by longshore transport from the adjacent fluvial-deltaic systems. Sandstone isoliths (pl. VI) aligned parallel with the inferred coastline suggest a strike-fed coastal tidal-flat origin for the system which is 35 miles long and bounded on the south and north by the Old Glory and Copper Breaks fluvial-deltaic systems, respectively. The system averages 52 feet thick, suggesting significant vertical accretion or aggradation caused by contemporaneous compaction and subsidence of the tidal-flat deposits. Individual sandstone and mudstone beds exhibit sheetlike geometry over local areas; lenticular tidal channel-fill facies of the Buzzard Peak system are present at the base of the fluvial-deltaic systems and throughout the sand-flat facies.

The restricted shelf over which the Buzzard Peak tidal flats prograded was shallow and it is inferred that tidal energy was low, dominated perhaps equally by astronomic and wind-tidal processes. A subdued coastal topography allowed a broad tidal flat to form even though tidal range was low.

Depositional conditions that formed Costa de Nayarit littoral sands on the west coast of mainland Mexico (Curry and Moore, 1964) and the chenier plain of southwestern Louisiana (Gould and McFarlan, 1959) are somewhat analogous to the model proposed for the Buzzard Peak system. In addition, sedimentary processes operative on northwestern Australian (Russell and McIntire, 1966), Jade Bay (Reineck, 1967), and Wadden Sea (van Straaten, 1961) tidal flats are similar to processes inferred for the Buzzard Peak sand-rich tidal flats.

During the past few thousand years, emergence and lateral accretion of submerged longshore bars formed at the plunge point of breakers has resulted in depositional regression of a sheetlike body of littoral sand along Costa de Nayarit (Curry and Moore, 1964). Emergence of longshore bars is dependent on a sufficient amount of sand supplied both by longshore transport from a cusped delta that is being destroyed by wave action, and by winnowing of sand from previously deposited shoreline sediments. Along the chenier plain of southwestern Louisiana (Gould and McFarlan, 1959), chenier ridges develop primarily as accretionary ridges along segments of shoreline that have remained relatively stable long enough to permit winnowing and construction of a subaerial ridge of sand. Cheniers are ridges of sand and shell (Hoyt, 1969) 150 to 1,500 feet wide, commonly less than 15 feet thick, and several tens of miles long. Size of the sand ridge depends on the amount of reworking, the amount of sand introduced from nearby areas undergoing erosion, and the amount of sand in the sediment being reworked. Individual chenier ridges generally have an erosional contact with underlying mudflat and marsh sediments; however, there can be considerable interfingering of sand and mud facies resulting in gradational contacts (Hoyt, 1969). During periods of low sediment influx from the Mississippi River, chenier development, mudflat accumulation, and coastal erosion can occur simultaneously along different segments of the coast. During periods of abundant sediment influx from the Mississippi River, condi-

tions of relative stability give way to rapid coastal progradation of mudflats (Gould and McFarlan, 1959).

Dynamic conditions of simultaneous chenier ridge development, erosion, and mudflat accretion, perhaps alternating with conditions of more pervasive mudflat accumulation, such as along the chenier plain of southwestern Louisiana, is inferred to have formed the Buzzard Peak sand-rich tidal-flat system. Sandstone beds of the tidal sandflat facies are commonly 3 to 10 feet thick and laterally pinch out into mudstone. Width of Buzzard Peak sandstone beds is unknown although the beds may be considerably wider than the individual chenier ridges of southwestern Louisiana; cheniers may be more analogous to Costa de Nayarit sands (Curry and Moore, 1964) that form a sheetlike body of sand by accretion of individual ridges. Compound ridges are also present along the chenier plain (Gould and McFarlan, 1959) but they are relatively narrow. Low tidal energy inferred to have been active during deposition of the Buzzard Peak system may have developed poorly defined sand ridges, therefore, creating a tidal-flat depositional environment somewhat different from the chenier plain or Costa de Nayarit. In any case, physical processes that formed the modern cheniers and strandplains are inferred to have resembled processes that formed the Buzzard Peak system.

The most common bed form on the sand-rich tidal flats of northwestern Australia (Russell and McIntire, 1966) is small-scale ripples formed when a shallow, relatively low-energy tidal bore moves across the tidal flats. Small-scale ripple cross-stratification is also common in the Buzzard Peak system (III-11). Current lineations form on Australian tidal flats during ebb tide as thin sheets of water drain off the tidal flat; similar features are preserved in the Buzzard Peak sandflat facies (III-22). Drainage of Australian tidal flats is accomplished mainly by runnel systems; lenticular zones of small-scale ripple bedding enclosed in sandstone beds of the Buzzard Peak system (III-11) may represent preservation of runnels. Flaser bedding is common on mixed sand and mud tidal flats of Jade Bay along the northern coast of Germany (Reineck, 1967), and in the Buzzard Peak system sandflat and tidal channel-fill facies (IV-12, II-4). In the Wadden Sea along the Dutch coast (van Straaten, 1961), tidal channels rapidly shift across the tidal flats and are filled by lateral accretion

with finely laminated sediment, but on the low tidal flat, the channel deposits exhibit both large- and small-scale cut and fill structures. Analogous tidal channel-fill deposits are present in the sand-flat facies of the Buzzard Peak system (III-4).

Introduction of fluvial-deltaic sediment to San Angelo coastal areas initiated deposition of the Buzzard Peak sand-rich tidal-flat system. Progradation of the Old Glory and Copper Breaks fluvial-deltaic systems with consequent longshore transport of sand and mud from these systems supplied sediment to the regressive Buzzard Peak system (figs. 6, 7). Winnowing during periods of low sediment input developed lenses of sand on tidal sandflats. Contemporaneous compaction and subsidence of the tidal flats allowed a relatively thick sequence of tidal-flat deposits to accumulate by vertical accretion or aggradation.

CEDAR MOUNTAIN MUD-RICH TIDAL-FLAT SYSTEM

The Cedar Mountain mud-rich tidal-flat system is gradational with the subjacent Buzzard Peak system (fig. 6) and is composed principally of moderately reddish-brown and light-gray mudstone, siltstone, and sandy siltstone; the system is essentially coincident with the Flowerpot Mudstone Member (fig. 5). Very fine-grained, light-gray sandstone forms from 2 to 20 percent of the Cedar Mountain system, but averages only 8 percent of the total system. Small amounts of shale, gypsum, selenite, barite, dolomitic mudstone, and dolomite also occur in the Cedar Mountain system. The Cedar Mountain system averages 46 feet thick, but is only 28 feet thick over the Electra Arch (fig. 6); the system is 77 feet thick 2 miles south of Truscott (fig. 6). Thickening may have occurred in the vicinity of small undefined subdeltas. Thicker Cedar Mountain tidal deposits are delineated by a slight bulge in the 0 to 10-foot sandstone isolith (pl. VI).

Cedar Mountain deposition began as Old Glory and Copper Breaks fluvial-deltaic deposition slowly ended, probably because of avulsion or stream capture on the coastal plain. Fluvial-deltaic sediments compacted slowly, and deltaic sands subsided into underlying muds. Loss of fluvial-deltaic sediment sources in the area resulted in diminished sand supply to adjacent tidal flats. Mud of the Cedar Mountain system was probably transported from sources far to the south. The

slow change from sand- to mud-dominated tidal-flat systems resulted in progradation or seaward accretion of mud-rich Cedar Mountain tidal flats (fig. 11). The mud-rich tidal flats were drained by a network of relatively shallow, meandering tidal channels. In local areas where sedimentation rates were low, wave and tidal energy created thin ripple-bedded sandstones in the swash zone; swash-zone sandstone beds are thin destructional units in an otherwise progradational sequence.

Facies of the Cedar Mountain Mud-Rich Tidal-Flat System

Tidal mudflat facies.—Mudflat facies (figs. 11 and 12) constitute the principal deposits within the Cedar Mountain system. Mudstone units are blocky to massive, locally continuous, primarily moderately reddish brown, and rarely sandy or silty. Gray, sandy mudstone beds a few inches to 2 feet thick alternate vertically with and grade laterally into red mudstone. Discoidal-shaped gypsum nodules up to 7 inches in diameter are common throughout the Cedar Mountain system and in some places (III-1) form zones of nodules; barite and dolomite nodules are also present (III-16, II-3).

Coarsening-upward horizontal and ripple cross-stratified, moderately reddish-brown sandstone and siltstone beds from about 4 inches to 3 feet thick are interbedded with red mudstone (I-46). These sandstone beds, which grade laterally into sandy, moderately reddish-brown mudstone, probably result from sporadic influxes of sand along with the mudstone. Mottling, possibly caused by burrowing organisms, occurs at a few localities (II-1).

Tidal channel facies.—Tidal channel-fill deposits (figs. 11, 12) are present throughout the Buzzard Peak and Cedar Mountain tidal-flat systems but are more common and better exposed in the Cedar Mountain system. Cedar Mountain tidal channel-fill deposits exhibit a facies tract that is divided in this report into lower, middle, and upper tidal channel-fill segments (fig. 11) in reference to relative position on the tidal flat.

Lower tidal channel-fill deposits are a complex mixture of poorly cemented, very fine-grained, gray, muddy sandstone, siltstone, and sandy mudstone. The deposits are 6 to 8 feet thick and occupy channels eroded into red mudstone. At

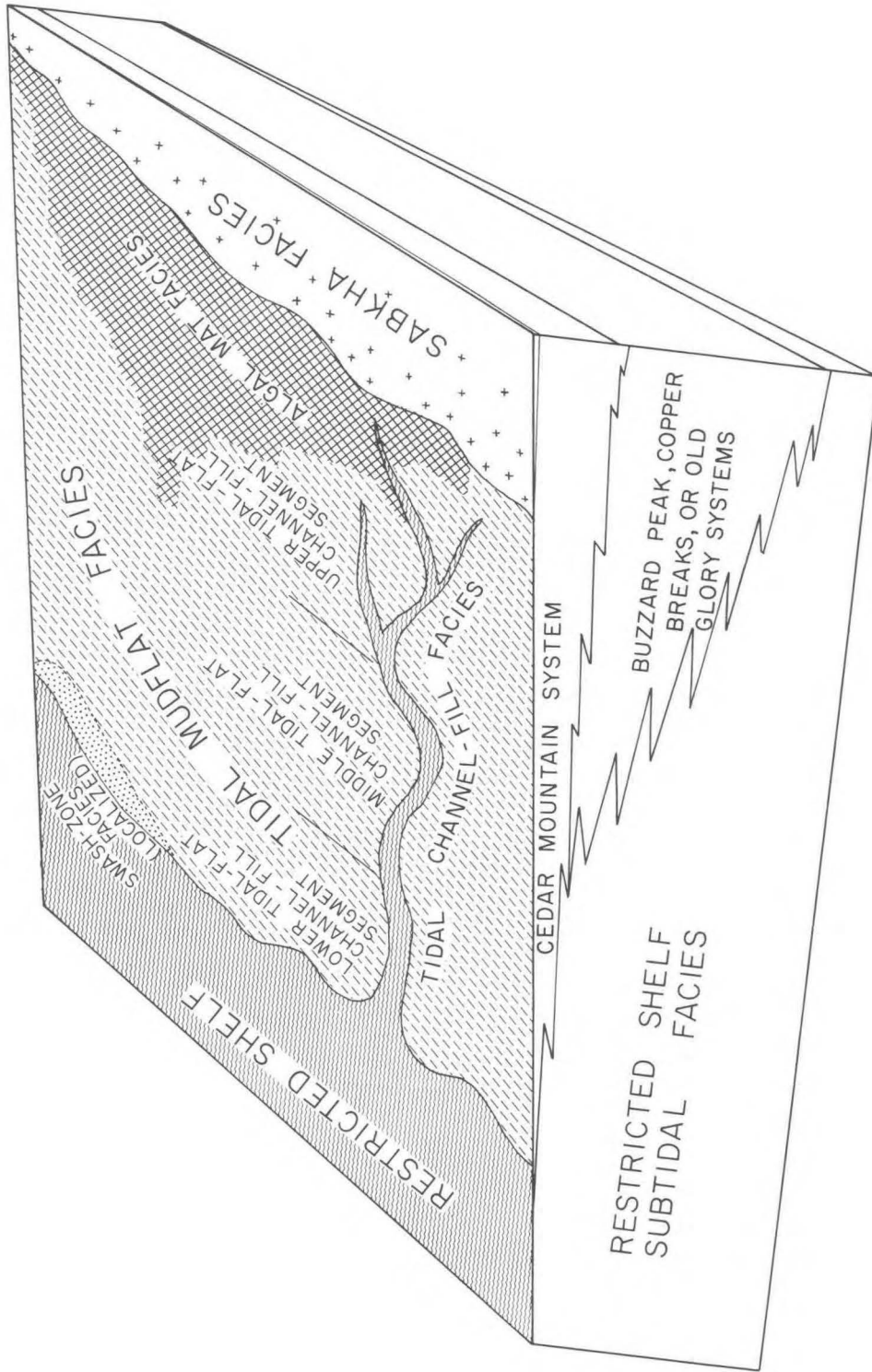


Fig. 11. Depositional model of Cedar Mountain mud-rich tidal-flat system. This system is coincident with the Flowerpot Mudstone Member.

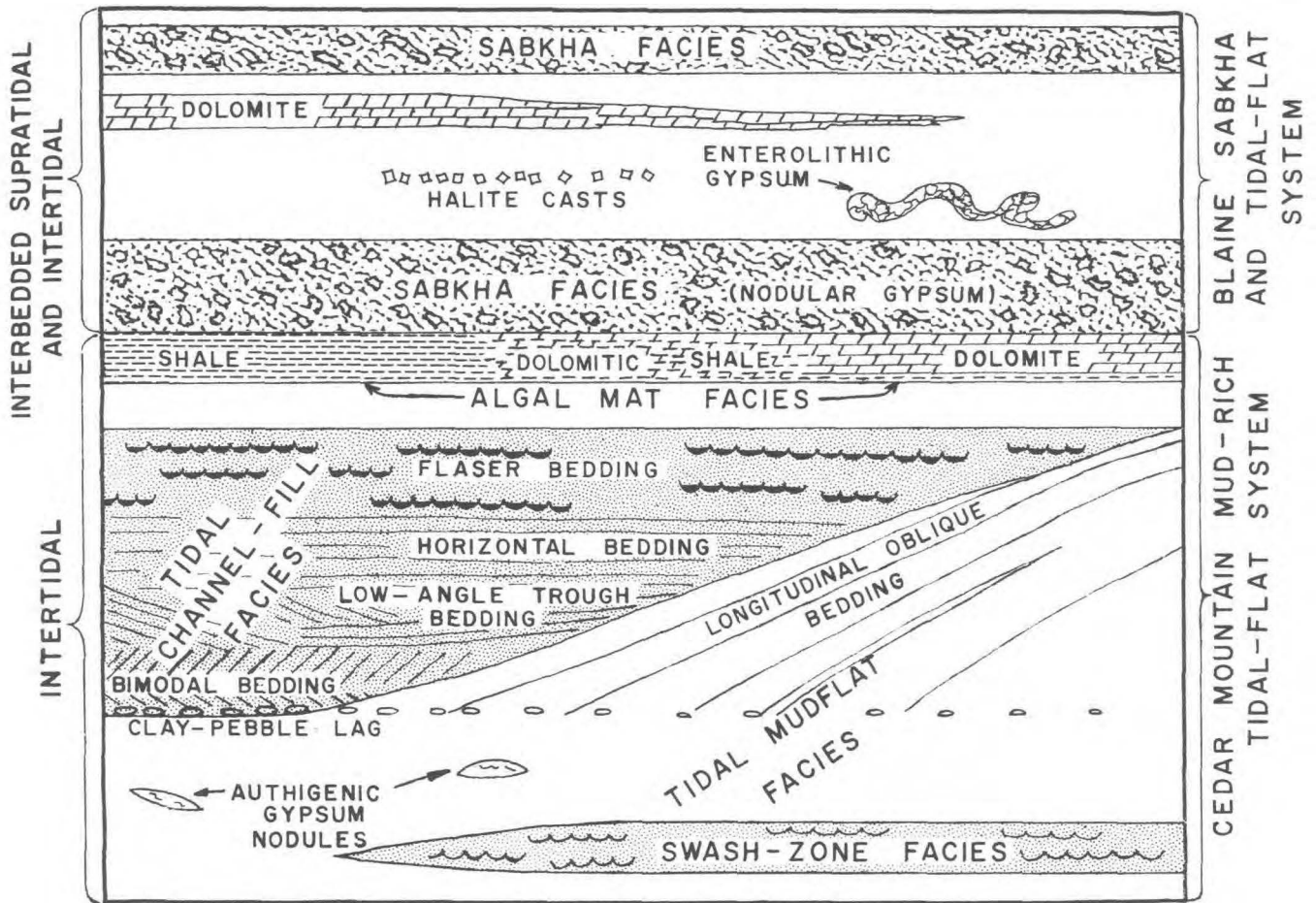


Fig. 12. Idealized sequence of Cedar Mountain mud-rich tidal-flat and Blaine sabkha and tidal-flat systems.

two localities (III-F, IV-9), mining activities have exposed the lower tidal channel-fill facies. Organic matter often replaced by copper minerals is common in lower tidal channel-fill deposits (IV-9); finely divided carbonaceous material, discontinuous half-inch-thick vitreous coal layers, and small to large woody plant fragments with a charcoal texture are common.

Middle tidal channel-fill deposits are lenticular-shaped channel-fill sandstone bodies that average 4 feet thick and 100 feet wide. They are composed of very fine-grained, hard, gypsum-cemented quartzarenite. Characteristic bedding types include large-scale trough cross-stratification, horizontal bedding, flaser bedding, and wide, low-angle trough cross-stratification. The middle tidal channel-fill deposits at localities III-F and IV-9

form a cap over lower tidal channel-fill deposits suggesting that progradation or accretion of tidal flats created a vertical stacking of tidal channel-fill facies.

Upper tidal channel-fill deposits are lenticular, gray, gypsum-cemented quartzarenite bodies from 1 to 3 feet thick and 30 feet wide (III-15, III-6). An idealized vertical sequence of bedding types (fig. 12) in the upper channel-fill facies includes bimodal foreset beds and low-angle trough beds at the base, followed upward by horizontally stratified beds, and capped by flaser beds. Bimodal foreset beds are rare, perhaps because of low or unequal velocity of ebb- and flood-tidal currents. Bimodal bedding is a form of cross-stratification (Harms and Fahnestock, 1965) caused by tidal currents that flow up the tidal channel during

flood tide and back to the sea during ebb tide. If either the flood or ebb tide velocity is greater, more of the higher velocity crossbedding will be preserved. Flaser bedding, which is a type of ripple cross-stratification, is the most common bedding type and suggests relatively weak current energy in the tidal channels (Harms and Fahnestock, 1965).

Modern erosion of tidal-flat mudstone surrounding upper tidal channel-fill sandstone (III-13, III-15) has locally exhumed the channel-fill bodies which exhibit a meandering pattern. Longitudinal-oblique bedding (Reineck, 1967) composed of reddish-brown and gray mudstone is marginal to upper tidal channel-fill deposits and dips towards the axis of the channel fill (V-4; fig. 12). Mud-ripple lag is commonly present at the base of tidal channel-fill sequences (III-15).

Swash-zone facies.—Sandstone beds of the swash-zone facies are commonly 2 to 6 inches thick, tabular, light-gray, ripple cross-stratified, well-sorted, very fine quartzarenite (near I-45, IV-3). They have relatively sharp basal contacts with underlying red mudstone and locally pinch out laterally into red or gray mudstone. The relatively sharp basal contact, uniform gray color, good sorting, and small-scale ripple cross-stratification suggest that this facies formed in a shallow subaqueous environment under the influence of wave or tidal energy. During periods of low sediment supply, wave and tidal energy may have winnowed out mud and concentrated sand in localized areas on tidal flats of the Cedar Mountain system.

Algal mat facies.—Dolomite, dolomitic shale, and well-laminated gray shale in the Cedar Mountain system (fig. 12) are inferred to have formed in association with algal mat zones on the mud-rich tidal flats (fig. 11). Dolomite, dolomitic shale, and well-laminated shale are believed to grade laterally into each other over a distance of 11 miles (V-4, V-14, V-18). South of Old Glory (V-4), gray, well-laminated shale grades vertically into dolomitic shale in a 6-inch interval.

Dolomite beds are commonly 0.5 to 2 inches thick and are composed of light-gray dolomitic. Individual samples exhibit mud cracks (V-3, I-6), mud-clast aggregates (near IV-C), crenulations (I-8), and in thin section, discontinuous brown laminae and oolites (I-6). Crenulations and brown laminae are indicative of an algal mat origin.

Cavities, 0.5 to 4 mm in diameter (V-18) and creating a birdseye texture, are present in some dolomite samples. Some cavities are euhedral and may be molds of small gypsum crystals; others may be methane or hydrogen sulfide gas cavities caused by decomposition of algae prior to lithification of the dolomite.

Gray dolomitic shale beds and well-laminated gray shale beds are 3 to 10 inches thick and exhibit 0.5-cm-thick graded laminae, rhythmic 1.5- and 0.5-mm laminae of dolomitic shale and laminated gray shale (V-4), and syneresis cracks (V-14). Thin dolomite beds occur throughout the Cedar Mountain system, but the calcareous shale beds and well-laminated gray shale beds are found only at the top of the system (fig. 12). At localities I-8 and V-19, algal mat facies immediately underlie the first nodular gypsum of the Blaine sabkha and tidal-flat system. At locality IV-3, gray (algal mat) shale is present about 2 feet below the base of the Blaine system.

Cedar Mountain Mud-Rich Tidal-Flat Depositional Model

The Cedar Mountain system (figs. 6 and 11) is interpreted to have been deposited on tidal flats during regression and vertical aggradation; mud-rich sediment was supplied by longshore drift from fluvial-deltaic systems centered possibly 80 miles south of the area of this report. The Cedar Mountain system extends the length of the study area and is gradational with the underlying Old Glory and Copper Breaks systems and intermediate Buzzard Peak system (fig. 6). Stratigraphically, the Cedar Mountain system is coincident with the Flowerpot Mudstone Member of the San Angelo Formation. The system averages 46 feet thick and is overlain conformably by Blaine sabkha and mud-rich tidal-flat facies.

The shelf over which the Cedar Mountain tidal flats prograded was shallow and deposition is inferred to have been influenced by astronomic and wind-tidal currents and shallow-water wave energy. A subdued, featureless coast, sparse plant growth, tidal range of a few feet, and ample longshore sediment influx allowed broad, nearly level mudflats to develop.

Depositional processes active along southwestern Louisiana coastal mudflats, on Texas Laguna Madre wind-tidal flats, and on intertidal

algal flats along the Trucial coast of the Persian Gulf provide a composite modern analog of the Cedar Mountain tidal-flat system. Mudflats are forming today along the southwestern Louisiana coast (Morgan and others, 1953) because of mud supplied from the Atchafalaya River; in an analogous manner, mudstones were deposited on Cedar Mountain tidal flats. Coastal Louisiana mudflats are dominated by weak wave energy (except during hurricanes), a tidal range of 1.5 to 3 feet, and a rapid growth of marsh vegetation that effectively stabilizes the mud against further tidal and wave effects. Low coastal topography, shallow water on the shelf, and a relative lack of vegetation probably characterized the Permian coastline during deposition of the Cedar Mountain system. A tidal range slightly higher than along the Louisiana coast and persistent onshore winds may have enhanced Cedar Mountain system tidal-flat conditions.

Laguna Madre, Texas, is characterized by low-energy, subtidal, intertidal (tidal-flat), and supratidal environments sheltered landward of Padre Island (Fisk, 1959). Tidal-flat sediments include clay, sandy clay, and sand, with minor amounts of gypsum and salt. Deposition on the tidal flats is by wind and wind-tidal processes; precipitation of evaporites and biochemical action of bacteria and algal mats are other significant processes. Transport of sediment across the Laguna Madre flats by wind tides is analogous to the processes that are inferred to have been active on the Cedar Mountain tidal flats.

Tidal channels with mud-pebble channel lags, longitudinal-oblique bedding, and primarily low flow-regime bedding types typify many modern tidal flats (van Straaten, 1961; Reineck, 1967); similar channels existed on the Cedar Mountain system flats. Longitudinal-oblique bedding deposits similar to those present in modern Jade Bay tidal flats (Reineck and Singh, 1967) occur in the Cedar Mountain system tidal flats (V-4); oblique bedding is genetically similar to point bar deposits in a fluvial system.

On modern mud-rich tidal flats, blue-green algal mats are common (Fisk, 1959; Davies, 1970; Russell and McIntire, 1966; Kendall and Skipwith, 1969). The thin graded beds from Shark Bay, Australia, that are described by Davies (1970) are similar to those found in the dolomitic shale at the top of the Cedar Mountain system. Graded beds of

fining-upward laminae are deposited on top of algal mats by pulses of sediment-rich water. Algae grow up through the sediment and continue to flourish. Fine-grained dolomite and dolomitic shale in the Cedar Mountain system may have been caused by sulfate-reducing or ammonifying bacteria producing aragonite during decomposition of the algal mats (Purdy, 1963). Aragonite may also have formed by either direct evaporation or respiration of the living algae (Dalrymple, 1965); later diagenesis altered the aragonite to dolomite. Cedar Mountain system algal mats were characterized by a smooth surface with minor stromatolitic structures. Smooth algal mats are described by Davies (1970), who attributes them to frequent submergence of the algal mats by thin sheets of water.

Gypsum nodules in the Cedar Mountain system resemble nodules in modern tidal-flat sediments that develop in response to interstitial diagenetic precipitation (Butler, 1969; Kendall and Skipwith, 1969; Fisk, 1959). Formation of the gypsum is related to high evaporation and low rainfall. On the Trucial coast (Kendall and Skipwith, 1969), the gypsum nodules are forming in tidal-flat facies under supratidal sabkha facies which have prograded seaward over the intertidal tidal flats (fig. 13). Butler (1969) reports finding small gypsum crystals at the base of carbonate-bearing algal mats along the Trucial coast. Formation and later dissolution of gypsum crystals in the algal mat facies of the Cedar Mountain system may partly account for the birdseye texture present in the dolomite at the top of the Cedar Mountain system (V-18). Oolitic dolomite at the top of the Cedar Mountain system contains oolites with organic and quartz-grain centers; blebs of organic matter are interpreted to be flocculent organics and fragments of algal mats. Kendall and Skipwith (1969) found oolites on the Trucial coast that contain organic mucilage, blue-green algae, and quartz-grain nuclei.

Near Old Glory (V-14), an 18-inch-thick zone of gray, poorly laminated shale is overlain by a 4-inch-thick zone of well-laminated gray shale. The basal nodular gypsum bed of the Blaine sabkha and tidal-flat system is immediately above the well-laminated shale (although removed by dissolution at V-14, the gypsum is preserved at V-19). This vertical sequence of poorly laminated shale, well-laminated shale, and gypsum is analogous to the algal peat (poorly laminated), algal mat (well laminated), and gypsum mush sequence (fig. 13)

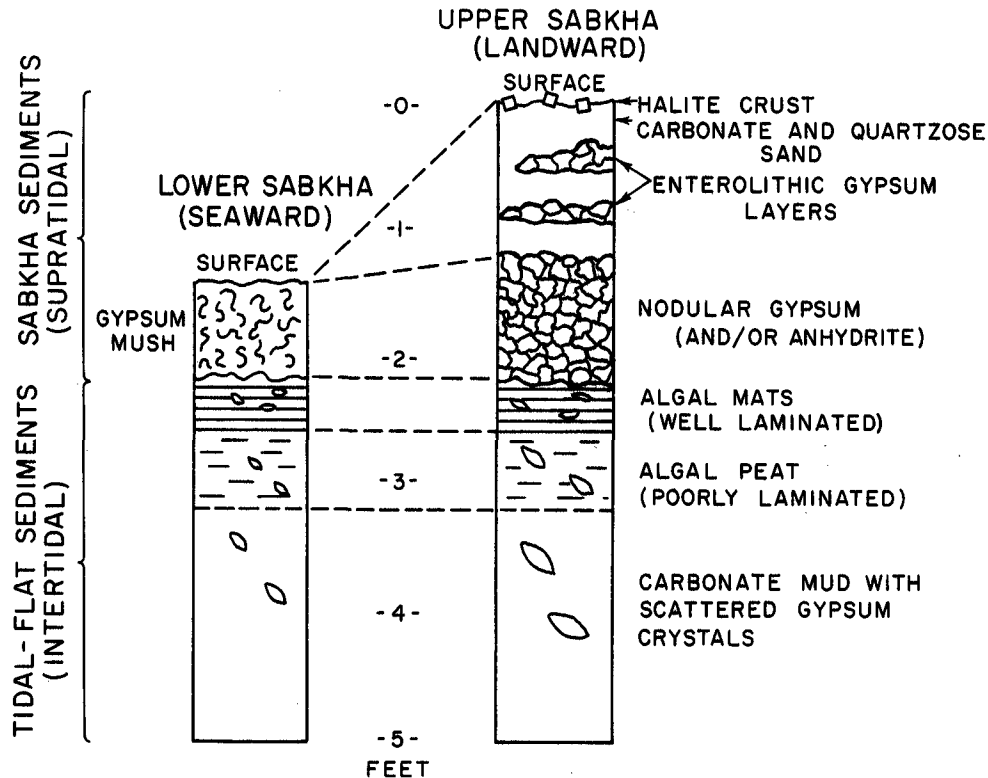


Fig. 13. Vertical sequence through modern tidal-flat and sabkha deposits, Trucial coast. Modified from Kendall and Skipwith (1969), and Butler (1969).

recognized by Kendall and Skipwith (1969) on the Trucial coast; the sequence represents a vertical facies tract from approximately middle tidal flat to lower sabkha. This evidence indicates that algal mats of the Cedar Mountain system may have formed in middle to upper intertidal zones of the mud-rich tidal flats.

Development of the Cedar Mountain mud-rich tidal-flat system began with abandonment of the Old Glory and Copper Breaks fluvial-deltaic systems which led to a diminished supply of sandy sediment available to the Buzzard Peak tidal flats. Longshore transport of sand-rich sediment was gradually replaced by mud-rich sediment transported by longshore drift from a postulated fluvial-deltaic system south of the area of this report.

With contemporaneous compaction and subsidence of the fluvial-deltaic deposits, mud-rich tidal flats spread over the former fluvial-deltaic systems and ultimately covered the entire area of this report (fig. 6). The tidal flats prograded seaward; subsidence and compaction during regression of the tidal flats led to significant vertical aggradation of up to 50 feet of tidal-flat deposits in the Cedar Mountain system. Tidal channels, which can be divided into lower, middle, and upper segments (fig. 11), served to drain the flats. Thin, tabular sandstone beds (swash-zone facies) were developed in localized areas because of reduced mud input and a relative increase in wave and tidal action which winnowed the mud-rich deposits to form residual, ripple cross-stratified sandstone. Algal mat facies spread over broad interchannel areas of the tidal flats (figs. 11 and 12).

BLAINE SABKHA AND TIDAL-FLAT SYSTEM SABKHA DEPOSITION: A SUMMARY

Along many coastlines with very low relief, wind- or tide-generated currents may periodically flood vast coastal areas to elevations several feet above the reach of normal daily tides. Such broad tidal flats are called supratidal flats, and modern examples provide insight into the depositional nature of the Blaine Formation in the area of this report.

Salt-encrusted supratidal surfaces that are only occasionally inundated are known in Arab countries as sabkhas (Kinsman, 1969). Local climate dictates whether a supratidal surface will be a marsh environment, as along the western Louisiana coast (Morgan and others, 1953), or a sabkha environment, as along the Persian Gulf Trucial coast (Kinsman, 1969). The climate on the Trucial coast is hot and arid, and the net rate of evaporation is high (Butler, 1969). As a result, interstitial emplacement of evaporite minerals within the shallow sabkha sediments is common. Trucial sabkhas form a linear coastal zone that has a gradual slope of 1:1,000 and that averages about 2 feet thick and 5 to 6 miles wide. Interstitial precipitation of evaporites and vertical accretion of windblown and tidally introduced sand and calcareous mud prograde the zone seaward across intertidal tidal flats (Kinsman, 1969; Butler, 1969). Butler (1969) divides the Trucial coast sabkha environment into five zones based on periodicity of flooding, diagenetic minerals, and nature of host sediments. The sabkha zone nearest to the intertidal flat is flooded monthly or more, whereas the outermost-floor recharge zone is flooded every 4 to 5 years (Butler, 1969). The seaward edge of the sabkha facies is a gypsum mush zone up to 12 inches thick; landward, the gypsum mush develops a nodular appearance (fig. 13) and may be replaced by anhydrite (Butler, 1969). Above the nodular gypsum zone (Kendall and Skipwith, 1969) is a layer of calcareous mud and sand.

The Blaine Formation (fig. 5) in the area of this report is interpreted to be a complex sequence of repetitive sabkha facies and tidal-flat facies (fig. 6). Blaine sabkha and tidal-flat deposits developed as the initial thin sabkha facies prograded westward over the underlying Cedar Mountain tidal flats. Later, with compaction and slight subsidence, tidal flats inundated the sabkha, resulting in deposition of a thin veneer of tidal-flat facies.

Continuous sabkha progradation and tidal-flat inundation led to development of a thick sequence of interstratified sabkha and tidal-flat facies. The lower 50 to 100 feet of the Blaine Formation in the area of this report is inferred to have been deposited in alternating sabkha and tidal-flat environments.

REGIONAL DISTRIBUTION OF THE SABKHA AND TIDAL-FLAT SYSTEM

The Blaine sabkha and tidal-flat system conformably overlies the Cedar Mountain system (fig. 6) and crops out throughout the area of this report. The sabkha facies is composed of laterally continuous nodular gypsum beds (fig. 12). Tidal-flat facies are pale reddish-brown and gray mudstone and claystone beds, with minor amounts of dolomite and sandstone. Some of the dolomite beds and fine-grained clastics were probably deposited in a sabkha environment, but differentiation between a tidal-flat or sabkha environment of deposition for individual thin beds was not attempted in this study.

FACIES OF THE BLAINE SABKHA AND TIDAL-FLAT SYSTEM

Sabkha facies.—Laterally continuous nodular gypsum beds of the sabkha facies are from 8 inches to 6 feet thick, with a median thickness of 1½ feet; they form the framework elements of the Blaine system (fig. 6). Individual nodular gypsum beds thicken and thin along outcrop and pinch out regionally to be replaced at slightly different stratigraphic levels. Nodular gypsum beds have a muddy appearance and, in general, appear to lack bedding (V-16). On cut surfaces, the beds exhibit gypsum nodules that have coalesced to differing degrees; red or gray clay matrix constitutes from 5 to 40 percent of the gypsum beds. Individual nodules are ¼ inch to 1½ inches in diameter and exhibit some flattening in the horizontal plane. These nodules exhibit a fine-grained, alabaster texture at their centers; the outside rims of the nodules have been altered to clear selenite. Gypsum beds may exhibit sequences of enterolithic layers as much as 4 feet thick, similar to small crenulations and tight folds of pygmatic quartz veins (V-16). In a lenticular-shaped gypsum bed (III-A), the top of the bed exhibited polygonal desiccation cracks.

Tidal-flat facies.—Pale reddish-brown and gray mudstone and claystone and gray dolomite that form the bulk of the tidal-flat facies are continuous in local areas (V-6). Minor amounts of sandstone occur as isolated flaser-bedded tidal channel-fill deposits (III-A). Laminated and intraclastic dolomicrite beds are thin to medium bedded and up to a foot thick (near III-10). Salt hopper casts and molds averaging half an inch in diameter (II-6) are present on dolomite beds in the Blaine system.

SABKHA AND TIDAL-FLAT DEPOSITIONAL MODEL

Modern supratidal sabkha environments provide the basis for a depositional model for the Blaine sabkha and tidal-flat system. Blaine deposits are at least 50 to 100 feet thick and probably represent couplets of facies deposited in alternating sabkha and tidal-flat environments. Individual beds of nodular gypsum, red and gray mudstone and claystone, and dolomite locally exhibit thinning and thickening. Gypsum and dolomite strata cannot be traced and correlated regionally because of pinch-out and erosion.

Sabkha facies were deposited in a hot and dry climate characterized by a high rate of evaporation and low annual rainfall. The arid coastal zone had a low, featureless slope that permitted vast areas to be sporadically covered by water because of unusual wind tides, storm tides, or abnormally high astronomic tides.

Depositional and diagenetic processes associated with the formation of sabkhas along the Trucial coast and western Qatar in the Persian Gulf provide modern analogs to explain processes that formed the Blaine sabkha and tidal-flat system.

In 3,000 years, shoreline regression along the Trucial coast has formed a sabkha zone locally 5 to 6 miles wide (Evans and others, 1969). On the western Qatar coast, algal bound sediment of the intertidal zone passes landward into a barren sabkha. The sabkha is largely featureless when viewed from the ground, but from an aerial view slightly different color patterns are observable, reflecting the extent of recent floods (Illing and others, 1965). Sediments of the Trucial coast sabkha are detrital quartz sand, calcareous mud, and evaporite minerals (Kendall and Skipwith, 1969). Evaporite minerals forming in and on the

sabkha are gypsum, anhydrite, halite, celestite, and dolomite (Kinsman, 1969). The gypsum and anhydrite are the result of precipitation and crystal growth within the sediment and are, thus, the result of diagenesis rather than primary sedimentation. Displacement of the surrounding sediment is the most common mechanism involved in the diagenetic process on sabkhas (Lucia, 1972).

Halite in the form of hopper-shaped crystals forms a patchy crust over much of the Trucial coast sabkha (Kendall and Skipwith, 1969); analogous layers of halite casts were found (II-6) in the Blaine facies. A layer of gypsum mush, which is up to 12 inches thick, marks the seaward boundary of the Trucial coast sabkha surface (fig. 13); landward, this layer is progressively replaced by a bed of nodular anhydrite up to 12 inches thick separated by thin films of carbonate sediment and quartz sand (Butler, 1969). Nodular gypsum layers commonly 1 foot thick (mode of 54 measurements) occur in the Blaine sabkha and tidal-flat system (V-16). Hydration by meteoric water has altered the original anhydrite of the Blaine to the gypsum now exposed at outcrop. Beds of gypsum up to 8 feet thick containing enterolithic bedding are forming on the landward margin of the Trucial coast sabkha (Butler, 1969); relatively thick gypsum beds with enterolithic bedding in the Blaine system (V-16) may have a similar origin. Fay (1964) interprets gypsum beds in the Blaine Formation of Oklahoma as having been deposited by evaporation and direct precipitation from a large body of hypersaline water. Dolomite in the Blaine system (V-16, near III-10) may have formed because of processes active in both the tidal-flat and sabkha environment. Interstitial precipitation of aragonite in both modern tidal-flat and sabkha deposits is followed by diagenetic alteration to micritic dolomite mud in the Qatar coast sabkha (Illing and others, 1965). Additionally, Illing and others found gypsum crystals up to 5 inches across growing in these dolomitic muds. This association is analogous to the occurrences of gypsum nodules in dolomite present in the Blaine system (near V-15). Direct precipitation of gypsum may occur in shallow, isolated ponds on modern sabkha surfaces (Lucia, 1972), and with complete desiccation, mud-cracked gypsum may form. Similar mud-cracked gypsum occurs in the Blaine system (III-A).

Persian Gulf sabkhas are analogous to the Blaine sabkha and tidal-flat system except for the

occurrence of terrigenous (silicic) mudstone and claystone in the undifferentiated supratidal and intertidal facies of the Blaine system. On the Persian Gulf sabkhas, the underlying intertidal sediment is primarily carbonate mud with biogenic debris, and the veneer of sabkha sediment is primarily quartzose sand. Relatively large amounts of terrigenous mud were strike-fed from clastic sources south of the area of this report into the intertidal system during offlap of the Blaine sabkha sediments; in addition, hypersaline conditions on the restricted Blaine shelf precluded extensive marine faunas.

DEPOSITIONAL HISTORY

Mid-Permian depositional conditions in North Texas (fig. 1) consisted of a broad, low, almost featureless coastal zone characterized by a hot and arid climate. West of this coastal zone was the broad, restricted, shallow shelf of the Midland Basin, which served to dampen incoming waves; to the east was a broad, alluvial plain of low relief. Bordering the alluvial plain on the east were the subdued mountains of the Ouachita foldbelt; to the northeast and southeast, respectively, were the Arbuckle Mountains and the Llano Highlands (fig. 2). These mountains and exposed Pennsylvanian and older Paleozoic rocks provided sediment to mid-Permian fluvial systems.

During late Choza time, the area of this report was a low coastal zone in which subtidal, tidal-flat (intertidal), and thin sabkha (supratidal) facies were being deposited. Together, these facies comprise the Choza depositional system (fig. 6). Dampening of waves because of shallow water and the gentle slope of the shelf resulted in development of low-energy tidal-flat systems rather than a high-energy beach and shoreface strandplain system.

Initiation of nearby fluvial-deltaic activity increased the input of sand into the coastal zone causing the development of a thin veneer of offlapping, sand-rich tidal flats of the Buzzard Peak system that marked the beginning of San Angelo deposition in the area of this report (fig. 6). The increase of terrigenous clastics was soon followed by progradation of thin, but areally widespread, high-constructive, lobate deltas of the northern

The Blaine sabkha and tidal-flat system is a sequence of regressive, offlapping, sabkha facies and transgressive tidal-flat facies. Each regressive and transgressive process formed a thin layer of sediments; repetition of these processes caused aggradation of a thick sabkha and tidal-flat sequence. Transgression of tidal-flat facies landward over the sabkha was the result of compaction and subsidence of the subjacent sabkha and tidal-flat facies. This may have occurred when a critical weight of offlapping sabkha sediments had accumulated. The initial progradation of the sabkha facies covered the Cedar Mountain mud-rich tidal-flat system (fig. 11) and brought an end to San Angelo deposition in the area.

Copper Breaks deltaic system and the southern Old Glory fluvial-deltaic system (fig. 6) over deposits of the lowermost part of the Buzzard Peak system which had undergone compaction and subsidence. In Copper Breaks State Park, a vertical sequence (upward) of prodelta, delta-front, and distributary mouth bar, as well as distributary channel-fill facies (fig. 8) represents a progradational facies tract of deltaic sediments (1-2). The Old Glory fluvial-deltaic system is composed of a complex of four principal delta lobes that can be followed about 30 miles westward into the subsurface in Stonewall and Fisher Counties (fig. 9). Outcropping facies of the Old Glory system were deposited high on the delta plain. The presence of gravel and an increase in rock fragments in the fluvial facies south of Old Glory (fig. 9) suggest that a different source area was supplying sediment to the Old Glory system.

Sand and mud were transported laterally by longshore drift from the fluvial-deltaic systems into the intermediate Buzzard Peak tidal system. Tidal processes generated by astronomic and wind-tidal action (fig. 7) resulted in regression of the Buzzard Peak sand-rich tidal-flat system. During relatively short periods of high sediment influx, tidal-flat regression was rapid and sandy mudstones were deposited; during intervening periods of low sediment influx, tidal reworking resulted in the winnowing and removal of clay-size particles and the concentration of sands in layers 3 to 10 feet thick (fig. 10). Compaction and subsidence contemporaneous with progradation created a relatively thick (fig. 6) sequence of facies.

The Copper Breaks deltaic system, Old Glory fluvial-deltaic system, and Buzzard Peak sand-rich tidal-flat system together comprise the Duncan Sandstone Member of the San Angelo Formation (fig. 5); the paleogeography of the Duncan Member is illustrated in figure 14.

Upstream avulsion of rivers supplying sediment to the fluvial-deltaic systems ended deposition by the Old Glory and Copper Breaks systems; the fluvial-deltaic deposits slowly compacted and subsided into underlying muds. Sand supply for the San Angelo depositional systems was drastically reduced when fluvial-deltaic progradation ended, but was replaced eventually by mud-rich sediment transported by longshore drift from a fluvial-deltaic complex active south of the area. The mud influx initiated accretion of mud-rich tidal flats of the Cedar Mountain system (fig. 11) that eventually covered the previously deposited depositional systems. The Cedar Mountain mud-rich tidal-flat system prograded over the restricted shelf deposits; contemporaneous compaction and subsidence created a relatively thick sequence of mud-rich tidal-flat facies. The Cedar Mountain tidal flats were drained by tidal channels

that became progressively smaller up the tidal flat (fig. 11); portions of the middle and upper tidal flats were covered by algal mat facies.

As coastal tidal-flat progradation continued, the inner, landward portion of the Cedar Mountain tidal-flat system was gradually raised above mean high tide and a thin, supratidal sabkha facies began to offlap the intertidal deposits (fig. 11). The end of extensive tidal-flat deposition concluded deposition of the Cedar Mountain system and led to development of the Blaine sabkha and tidal-flat system (fig. 15). The mud-rich Cedar Mountain system essentially is stratigraphically coincident with the Flowerpot Mudstone Member of the San Angelo Formation; termination of Cedar Mountain deposition marked the close of San Angelo deposition in the area.

Continued offlap of the initial Blaine sabkha facies covered the Cedar Mountain system (fig. 6). Each regressive episode of thin sabkha facies was followed by compaction, subsidence of the sabkha deposits, and onlap of thin tidal-flat facies. Continued repetition of these processes created a relatively thick sequence of Blaine sabkha and tidal-flat facies.

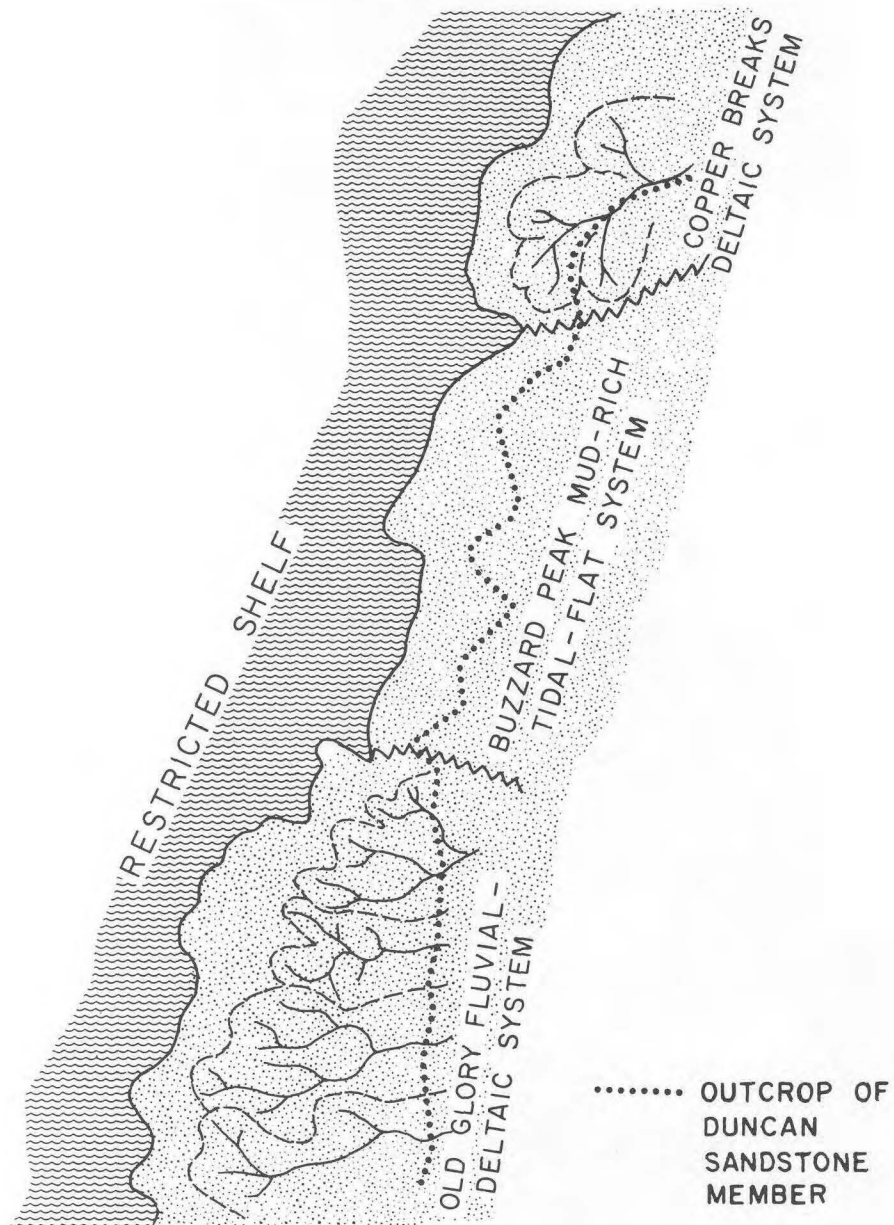


Fig. 14. Paleogeography during deposition of the Duncan Sandstone Member, San Angelo Formation.

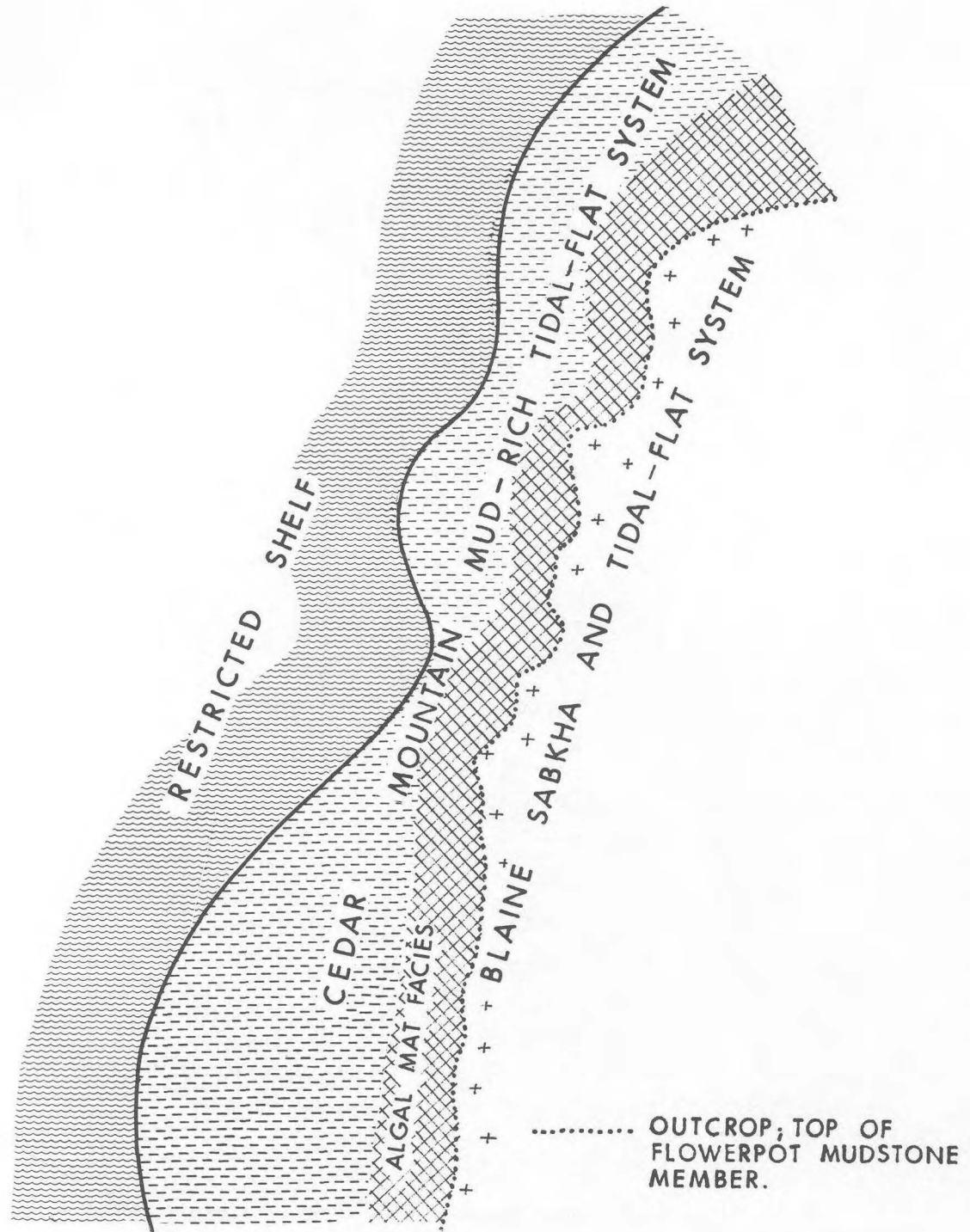


Fig. 15. Paleogeography during deposition of the upper part of the Flowerpot Member, San Angelo Formation, and the lower part of the Blaine Formation.

PALEONTOLOGY

Faunal and floral remains are sparse in the San Angelo Formation because of its terrestrial origin and post-depositional changes. It may also be assumed that the hot, dry climate and the hypersaline conditions of the restricted shelf served to restrict the numbers and diversity of invertebrates.

Vertebrate fossils, although scarce and normally very fragmental, are the only significant fossil remains found in the San Angelo Formation. Vertebrate fossils collected by Olson (1962) make the middle Permian fauna of North Texas one of the most completely known in the world. Olson (1962) divided the post-Choza and pre-Blaine rocks of the area into the San Angelo and Flowerpot Formations. The San Angelo was further subdivided into a lower, middle, and upper part based on lithologic differences. The boundary between the middle and upper San Angelo of Olson is approximately equivalent to the gradational boundary between the Buzzard Peak and Cedar Mountain tidal-flat systems. Olson's upper San Angelo and the basal part of his Flowerpot Formation are approximately equivalent to the Cedar Mountain system as used in this report (fig. 6). Most of the Flowerpot Formation, as defined by Olson, is equivalent to the lower part of the Blaine system of this report.

Twenty genera of vertebrates from the San Angelo and Flowerpot Formations have been described (Olson, 1962). Of these genera, two are fish, one is amphibian, and the rest are reptiles. Most of the reptiles are large herbivores. The scarcity of amphibians may be attributed to high salinity in the waters of the shelf, distributary

channels, interdistributary bays, and tidal channels. Four-fifths of the identifiable specimens were found in Olson's upper San Angelo, with the rest coming from his middle San Angelo and lower Flowerpot (Olson, 1962). Most of the bones were found near Little Croton Creek and Maverick Flat (pl. III). Their burial occurred mainly in the upper part of the sand-rich tidal flats and throughout the mud-rich tidal flats. Olson (1962) found some bones in positions indicating that animals had died on the tidal flats and were buried without any disarticulation taking place; others were apparently torn apart by carnivores and their bones were scattered. Other bones exhibit evidence of some degree of transportation.

A specimen of the ammonoid *Perrinites hilli* and an unidentified nautiloid were collected from dolomicrite composed of rip-up clasts in the bottom 10 feet of the Blaine sabkha and tidal-flat system (III-10). These marine invertebrates may have been transported by a storm onto the supratidal surface. Numerous pieces of wood, some of which appear to be reed-like, were found in tidal channel-fill facies (I-G).

The distribution of burrowing organisms was apparently controlled by the salinity of water in the depositional environments. Large, rough-walled, *Ophiomorpha*-like burrows are present in the upstream part of the Copper Breaks deltaic system distributary channel-fill facies (I-11). In the downstream, stratigraphically lower facies of the Copper Breaks deltaic system (I-14) and in the sand-rich tidal-flat sediments of the Buzzard Peak system (III-14), small, smooth-walled burrows are present.

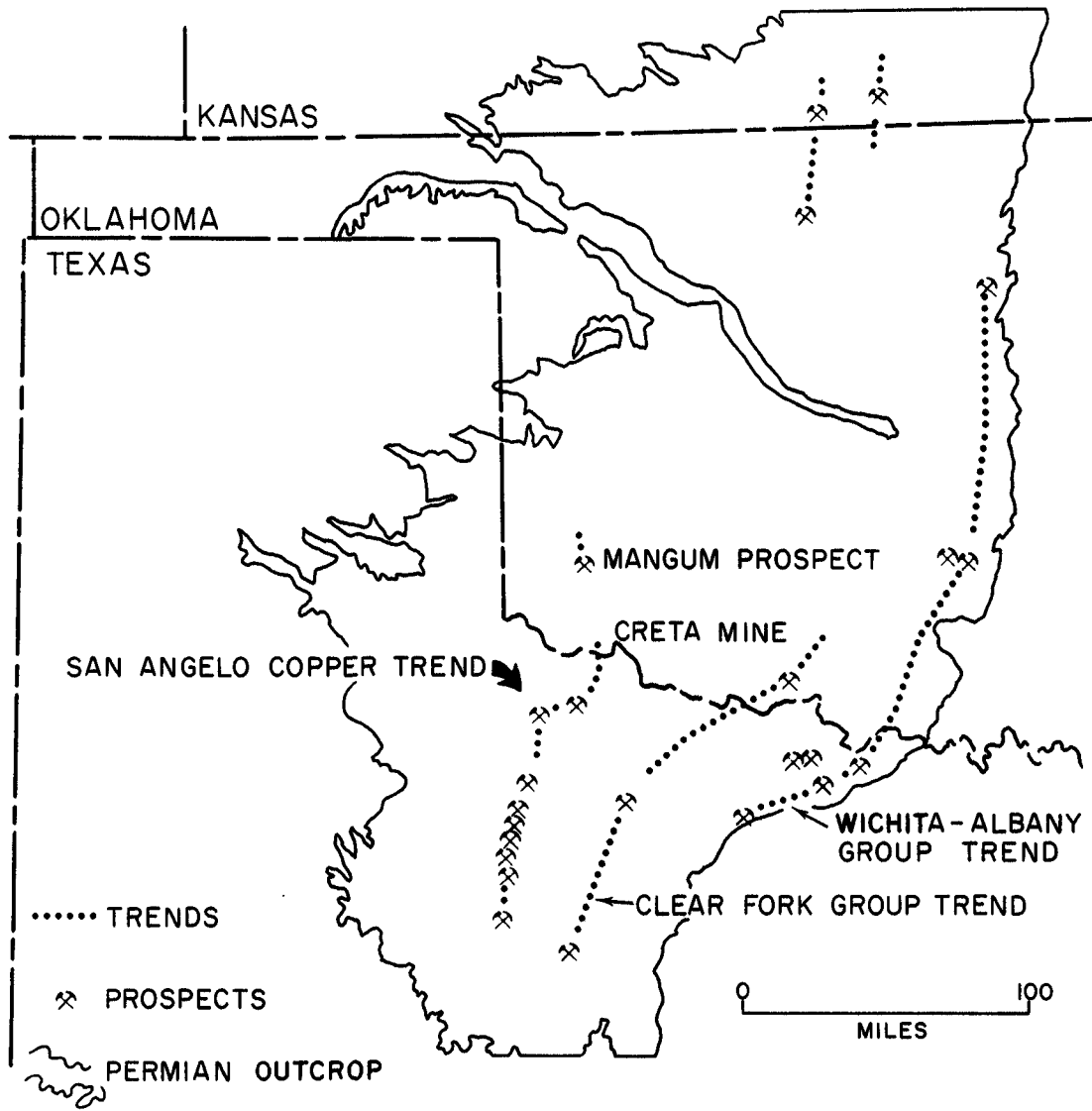


Fig. 16. Permian copper prospects, Texas, Oklahoma, and Kansas.

COPPER MINERALIZATION IN THE SAN ANGELO FORMATION

Copper prospects of the strata-bound type are scattered throughout the Permian outcrop in northern Texas, Oklahoma, and southern Kansas (fig. 16). A 6-inch copper-bearing layer of shale currently is mined from the Flowerpot Shale in southwestern Oklahoma about 25 miles north of the Medicine Mounds area. Permian strata-bound copper prospects occur in three general stratigraphic zones (fig. 16).

In North Texas, copper occurs in the lower parts of the Pease River and Clear Fork Groups (fig. 3) and in the lower part of the Wichita-Albany Group (Brown and Goodson, 1972). Mineralization in the Pease River Group is restricted to the Duncan and Flowerpot Members of the San Angelo Formation and the basal part of the Blaine Formation and the basal part of the Blaine

Formation (fig. 17). Copper occurs principally in localized channel-fill sandstone lenses associated with masses of woody material and in laterally persistent shale beds. It occurs less frequently in thin dolomite beds, at the base of gypsum layers, and as disseminations or coatings associated with thin, ripple-bedded sandstone units.

MINERAL ASSEMBLAGE

Malachite $[\text{Cu}_2(\text{CO}_3)(\text{OH})_2]$, azurite $[\text{Cu}_3(\text{CO}_3)_2(\text{OH})_2]$, covellite $[\text{CuS}]$, and chalcocite $[\text{Cu}_2\text{S}]$ are the only copper minerals found during this study. Malachite is the most common mineral at outcrop, whereas in unweathered samples, chalcocite predominates. Pyrite $[\text{FeS}_2]$ is present in minor quantities as an accessory mineral.

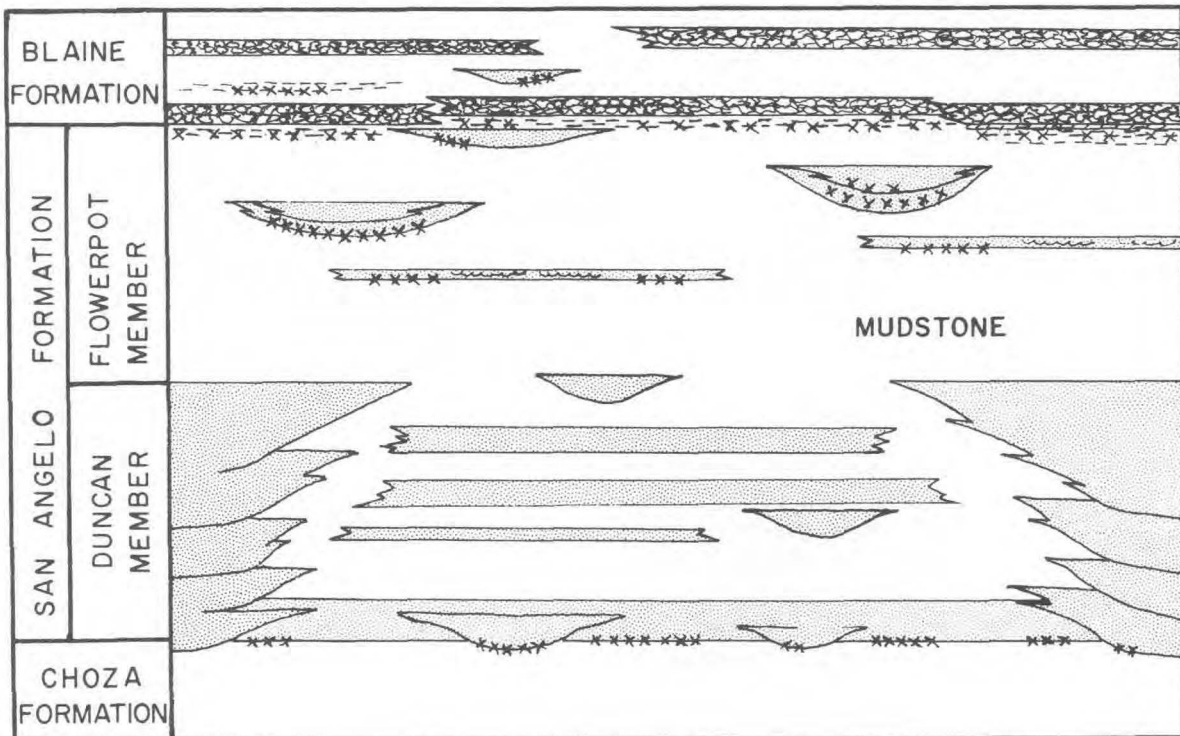


Fig. 17. Distribution of copper minerals, San Angelo Formation. North Texas, x = copper mineral zones.

DISTRIBUTION OF COPPER MINERALIZATION

The lowermost sandstone bed of the Buzzard Peak, Old Glory, and Copper Breaks systems (figs. 6 and 17) is commonly bounded at its base by a zone of light-gray mudstone or sandy mudstone averaging 2 to 12 inches thick. Copper mineralization in the Duncan Sandstone Member of the San Angelo Formation is restricted to this gray layer and the bottom 6 inches of the overlying sandstone (I-20, IV-1, II-5). The highest copper concentration is normally found at the contact between the overlying sandstone and the gray zone. The copper occurs as widely disseminated blebs of sulfide and malachite and as localized interstitial malachite cement. Some possible charcoal and tar-like organic material occurs in the copper-bearing layer (III-7).

The bulk of the copper minerals occurs in the Cedar Mountain mud-rich tidal-flat system of the San Angelo Formation (Flowerpot Member), and in the basal 10 feet of the overlying Blaine sabkha and tidal-flat system of the Blaine Formation (figs. 6 and 17).

Copper occurs in the following four facies of the Cedar Mountain and Blaine systems: (1) swash-zone facies, (2) algal mat facies, (3) sabkha facies, and (4) tidal channel-fill facies (figs. 12 and 17).

Ripple cross-stratified sandstone beds of the swash-zone facies are thin, destructive units that are distributed randomly through the Cedar Mountain system. Copper, in the form of malachite, can be found weathering out of the base of the sandstone beds and as thin coatings on weathered fragments of the sandstone (near III-F, IV-3, I-49). Copper sulfides and organic matter were not observed in the swash-zone facies on outcrop. During formation of the sandstone, organic matter may have accumulated in the swash-zone as flotsam; later post-depositional decay may have removed traces of the organics.

Mineralization in the gray, well-laminated shale, dolomitic shale, and dolomite of the algal mat facies at the top of the Cedar Mountain system and in the basal 10 feet of the Blaine system exhibits the best lateral continuity. The copper-bearing gray shale beds range from 3 to 14 inches thick, and there is commonly a 2 to 3 inch interval of a gray, well-laminated shale near the middle or

upper part of the zone which contains the highest concentration of copper (I-6, IV-3, V-4; see appendix IV for trace element analyses in location V-5). Copper is present in these thin, extensive algal mat shale beds as malachite and chalcocite; these minerals are present as platelets of malachite on shale laminae, as blebs of chalcocite, and as copper nodules. In outcrop only malachite is observable unless the shale is artificially exposed; a magnifying lens is necessary to see the chalcocite. Black specks of what may be bituminous matter are present in the shale (IV-3). No recognizable organic matter was actually noted in the algal mat facies, but their origin as algal bound sediment and their dark color suggest that a significant amount of organic matter was present in these sediments at the time of burial. Dolomitic gray shale beds of the algal mat facies that are commonly found with and laterally continuous to the gray, well-laminated shale beds (V-4, V-14) also contain malachite stains.

Dolomite layers in the algal mat facies at the top of the Cedar Mountain system and in the basal 10 feet of the Blaine system contain chalcocite and infrequent malachite (I-6, V-3, near III-10). These minerals occur as scattered blebs, partial fillings in small vugs, and small fracture fillings. The dolomite is thin bedded and ranges from less than an inch to a foot thick. Thin-section examination (I-8) supports an algal-related origin for much of the dolomite. Thin sections (I-6) also show that copper was preferentially deposited in pore space and as a replacement of organic matter. Vertical fractures in the dolomite (I-6) may be desiccation cracks that formed in carbonate layers soon after deposition.

Copper may also occur in trace amounts at the base of the first nodular gypsum bed of the sabkha facies in the Blaine system, immediately above the algal mat facies of the Cedar Mountain system (figs. 12 and 17); the copper occurs as both malachite and chalcocite. One-sixteenth-inch cubic crystals of chalcocite, possibly pseudomorphic after pyrite, were imbedded at the base of a gypsum bed (V-15) near Old Glory.

The thickest ore, and the ore with the highest copper concentration, occurs in tidal channel-fill facies in the Cedar Mountain mud-rich tidal-flat system (I-G, III-F, IV-9, V-B) and in the basal portion of the Blaine system (III-A). Copper in these channel-fill deposits has been mined

intermittently since 1877. The bulk of the copper comes from lower tidal channel-fill sandy mudstone and muddy sandstone (fig. 11; III-F). Some copper has also been mined from middle tidal channel-fill sandstone (I-G). Based on observations made by Phillips (1917a?), it is apparent that in many of the copper mines, the hard sandstone of the middle tidal channel-fill facies was not mined, even though it contained some copper, because it could provide roof support for the mining of the underlying copper-bearing sandy mudstone and muddy sandstone of the lower tidal channel-fill facies. Phillips (1917b?) notes that mineralized zones in the lower tidal channel-fill facies range from 2 to 11 feet thick, 15 to 45 feet wide, and about 150 feet long; these observations have been substantiated. Copper minerals present in the tidal channel-fill deposits include malachite, azurite, covellite, and chalcocite. At the Farris prospect (IV-D), pyrite nodules are exposed at the entrance to the abandoned shaft. The ore in the tidal channel-fill facies occurs as copper nodules, replacements of wood fragments, disseminated blebs of copper, and interstitial cement. Copper nodules are 1 to 2 inches long, $\frac{1}{2}$ to 1 inch in diameter, and are found in a variety of shapes. Some have exterior textures, suggesting that they grew around a wood nucleus, whereas other nodules have a completely amorphous appearance.

PARAGENESIS

The paragenetic sequence has apparently been a three step process, outlined as follows: (1) pyrite replacing woody material, (2) chalcocite replacing pyrite, and (3) covellite replacing chalcocite, with malachite and azurite also being formed. The precise time relationship between the first two steps depends on the origin of the mineralization, which has not been definitely established. The position that covellite occupies in this sequence is equivocal since the textures noted may have formed under a variety of conditions.

The essential parts of this sequence are shown in polished thin sections of copper nodules (pl. VII, A-D). Pyrite has replaced woody material and preserved the cellular structure of the woody host material (pl. VII, A and B). Contortion of cell geometry, inferred to have been caused by lithostatic pressure, is more extreme in some examples (pl. VII, A) than others (pl. VII, B). Rims of clear, noncellular pyrite have formed around some of the

pyrite blebs that contain an inner portion with the organic cellular structure preserved (pl. VII, A). Chalcocite replaces pyrite (pl. VII, C), and in some instances (pl. VII, C, upper right) ghosts of cells of woody material are preserved by chalcocite. Replacement textures of pyrite by chalcocite (pl. VII, C, lower left) suggest preferential replacement along cell boundaries. Covellite replaces chalcocite (pl. VII, D). This replacement has advanced from the outer margins of the chalcocite and from numerous cracks that are present in the chalcocite bleb (pl. VII, D). Nodules of copper minerals also form by enveloping quartz grains (pl. VIII, A). Some of the quartz grains exhibit evidence of solution and mechanical disintegration during precipitation of the sulfides.

Polished thin sections of mineralized dolomite exhibit preferential replacement of organic matter by chalcocite and crystallization of chalcocite in pore spaces (pl. VIII, B and C). In an oolitic dolomite (pl. VIII, B), a bleb of chalcocite is present in the pore space among four oolites. The black centers in some of the oolites are organic matter. In some cases this organic matter is being replaced by chalcocite (pl. VIII, C).

Thin sections of mineralized gray shale and mudstone from the Creta copper mine of Eagle-Picher Industries in Southwest Oklahoma and from near Medicine Mounds (I-6) contain scattered circular blebs of chalcocite 0.10 to 0.15 mm in diameter (pl. VIII, D) and oblong blebs of chalcocite 0.05 to 0.27 mm in length (pl. IX, A); numerous smaller circular blebs of chalcocite from 4 to 10 microns in diameter are also present (pls. VIII, D; IX, A and B). The size and shape of the 4- to 10-micron blebs suggest that they are framboids of chalcocite pseudomorphic after pyrite; the oblong 0.05- to 0.27-mm chalcocite blebs may be polyframboidal structures. Tiny pyrite cubes and grains clustered together in a spheroidal outline are known as framboidal spherules (Rust, 1935). The size of pyrite framboids is restricted from 3 to 23 microns with an average size of about 6 microns (Lougheed and Mancuso, 1973). Their origin has been attributed to inorganic crystallization of colloidal gels (Rust, 1935), biogenic precipitation caused by the action of sulfate-reducing bacteria on decomposing organics which produces hydrogen sulfide that can combine with iron in solution to form pyrite (Lougheed and Mancuso, 1973), and filling of bacteria cells by pyrite (Love, 1962). The oblong chalcocite structures appear to be com-

posed of numerous small framboids and may be similar to polyframboids described by Love (1971). The 0.10- to 0.15-mm chalcocite spheres (pl. VIII, D) from the copper-bearing shale at the Creta mine are interpreted as mineralized spores. The gray, relatively unmineralized mudstone under the copper-bearing shale at the Creta mine contains orange spheres 0.08 to 0.15 mm in diameter that have been identified as spores (Clair R. Ossian, personal communication, 1973). As strongly mineralized shale is approached, the spores are mineralized from the inside to the outside in a progressive manner until, in the ore zone, only spheres of chalcocite can be observed. In almost all of the exposed copper-bearing shale beds, malachite is present as a recent oxidation product on shale laminae because of solution of copper sulfide in ground water, slight movement of the copper in solution, and reprecipitation of the copper as malachite.

Textural relationships among the ore minerals, as observed in polished thin sections by the writer and as reported by other workers who have studied diagenesis and oxidation processes in modern sediments, allow some comments to be made concerning the time of ore deposition. Replacement of organics by pyrite may be an early diagenetic phenomenon that occurs soon after burial; pyrite is currently forming under reducing conditions at a depth of 40 to 70 cm in tidal-marsh sediments on the west coast of Florida because of anaerobic bacterial processes related to decomposing organic matter (Swanson and others, 1972). In Florida tidal-marsh sediments, Swanson and others found that total sulfur, primarily as iron sulfide, increases with depth and that mobile sulfur (mostly the reduced HS^- ion or gaseous H_2S) decreases with depth; strongest H_2S odor came from samples having the highest organic-matter content. Swanson and others suggest that a distinctive, strong odor of H_2S in samples from any depth in the tidal-marsh sediments may indicate that excess-reduced sulfur is available in the sediment to bind any metals that form insoluble sulfides, provided that the metals are present in the sediment. Part of the reduced sulfur in Florida tidal-marsh sediments goes through a transition from largely dispersed HS^- and H_2S in the upper 10 cm, to a very unstable hydrous iron sulfide phase in the 10- to 25-cm interval, to a relatively stable amorphous iron sulfide in the 25- to 40-cm interval, and finally to a stable crystalline pyrite below 40 cm. The rim of clear pyrite around pyrite

with relict cell structure (pl. VII, A) may indicate that bacterial decomposition of organic matter in the Permian sediments was forming an H_2S or HS^- halo around the organic matter, causing precipitation of iron sulfide to extend beyond the confines of the organic particle.

The age of the chalcocite, which is now the dominant sulfide present, is less definite. Depending on the origin of the mineralization, chalcocite may have formed diagenetically before lithification of the sediment (but later than the pyrite), or after lithification of the enclosing sediments. This question is considered further in the section on the origin of the copper. Covellite may have formed a little later as an early replacement mineral, or during the Holocene as an oxidation product of chalcocite. If covellite formed as an early replacement of chalcocite, its formation may have been caused by a relative decrease in reducing conditions present in the concentrating environment as H_2S and HS^- were consumed in precipitation of copper sulfide. Covellite would then represent slightly higher Eh conditions, but still probably negative.

There is also a possibility that some of the covellite formed at the same time as the chalcocite. A polished section of a copper sulfide nodule (III-15b) contains small isolated masses of covellite within chalcocite, which may indicate segregation of cupric and cuprous ions during formation of the copper sulfides. Some of the covellite exhibits the permanent blue (or blue-remaining) characteristic described by Ramdohr (1969). Ramdohr lists similar occurrences of primary chalcocite and covellite of the "arid alluvial basin" and "sulfur cycle" type from Mansfeld and Frankenberg in Germany and from the Colorado Plateau region of the United States. He admits that the distinction between primary and secondary covellite is difficult to make and that both are probably present. Replacement of organic matter in oolites (pl. VIII, C) by chalcocite indicates that some solid diffusion over at least short distances has occurred. Malachite and azurite probably formed during the Holocene as the result of oxidation of sulfides by surface and ground water followed by reprecipitation in the presence of carbonate anions.

ORIGIN OF COPPER MINERALIZATION

Strata-bound ore deposits have been attributed to numerous modes of origin. Many theories

on the origin of these deposits are outlined by Dunham (1971) and are considered here only when applicable to the San Angelo deposits.

The depositional history of the host rocks, the obvious facies control of the mineralization, the importance of organic matter, a lack of mineral zonation, and the absence of known igneous activity point to one of three origins for these deposits. A sabkha-diagenetic origin that involves evaporative discharge through the sabkha surface is proposed (fig. 18). Alternate epigenetic origins involve vertical movement of an aqueous solution containing copper chloride complexes along basin-rimming growth faults (fig. 19A), or metasomatic intergranular diffusion of copper over relatively long distances (fig. 19B). Copper mineralization appears to be unrelated to any structural influence, and there is no apparent faulting in or near the study area.

SABKHA-DIAGENETIC MODEL

Diagenetic processes associated with the sabkha environment may concentrate copper into economic deposits provided that the following conditions are met: (1) adequate copper in the ground water, (2) high evaporation rate, (3) sufficient amount of reductant, and (4) persistent sabkha and intertidal sedimentation.

In the sabkha-diagenetic model (fig. 18), evaporative discharge at the sabkha surface induced by evaporation may create an upward decrease in hydrodynamic potential with the result that ground water of primarily terrestrial origin would be induced to flow upwards through the sabkha. Hydrogen sulfide that formed as a metabolic by-product of sulfate-reducing bacteria in decomposing algal mats and in decomposing organic matter in tidal channels and ripple-bedded sands should be capable of stripping out the copper by causing it to precipitate as copper sulfide. Hydrogen sulfide associated with decomposing organic matter at the base of the Duncan Member would likewise precipitate some copper. It has been demonstrated (Baas Becking and Moore, 1961) that digenite (Cu_9S_5), which is very similar to chalcocite (Cu_2S), can be produced by bacteria in a medium of lactate and cuprous oxide. Lactate is one of the two main organic compounds utilized by sulfate-reducing bacteria in natural environments (Trudinger and others, 1972). In such a

model, the lack of copper in the bulk of the Duncan Member could be explained by oxidation of organic matter during and shortly after deposition. Later, small-scale diffusion and diagenesis could further concentrate available copper. Pyrite, which forms by early diagenesis prior to any significant concentration of copper, is partially replaced by copper sulfide during concentration of the copper. The copper content of the ground water, which is elaborated later, need only be of approximately average value. A condition of depositional equilibrium allowing sabkha processes to exist in the same area for a relatively long period of time would allow the diagenetic copper-concentrating process to continue long enough for a potentially economic concentration of copper to accumulate. Renfro (1974) has proposed that a sabkha-related diagenetic theory can be used to explain mineralization in the Roan in Africa and possibly such deposits as the Kupferschiefer in Europe and Creta in southwestern Oklahoma.

Evaporation rates in the Persian Gulf area are as much as 50.4 inches (128 cm) per year and rainfall averages only 1.5 inches (3.8 cm) per year (Butler, 1969). Hsü and Siegenthaler (1969) show that this high rate of evaporation causes a vertical hydraulic gradient to form in the sabkha. In response to the upward decrease in hydrodynamic potential caused by the interstitial-water loss, evaporative pumping, or discharge, takes place. Saline lagoon water and terrestrial water are "pumped" laterally, and then vertically, to be discharged at the sabkha surface. The relative amount of terrestrial ground water and saline lagoon water that is evaporated depends on the dynamic equilibrium that exists between the two. The writer proposes that most of the water evaporated in the model was terrestrial in origin (fig. 18). This hydrodynamic process would occur if the slope of the water table in the coastal zone created a hydraulic head sufficient to push the salt-water wedge of the Midland Basin away from the area immediately under the sabkha. Along the arid Trucial coast today, terrestrial ground water has been found in the "high supratidal zone" of the sabkha (Butler, 1969). This suggests that a hydraulic head sufficient to force a salt-water wedge away from the area under the sabkha facies may be able to form in an arid region, provided that there is a sufficiently elevated aquifer recharge area to create the hydraulic head. During concentration of the San Angelo copper deposits, subdued highlands in the Ouachita foldbelt may have

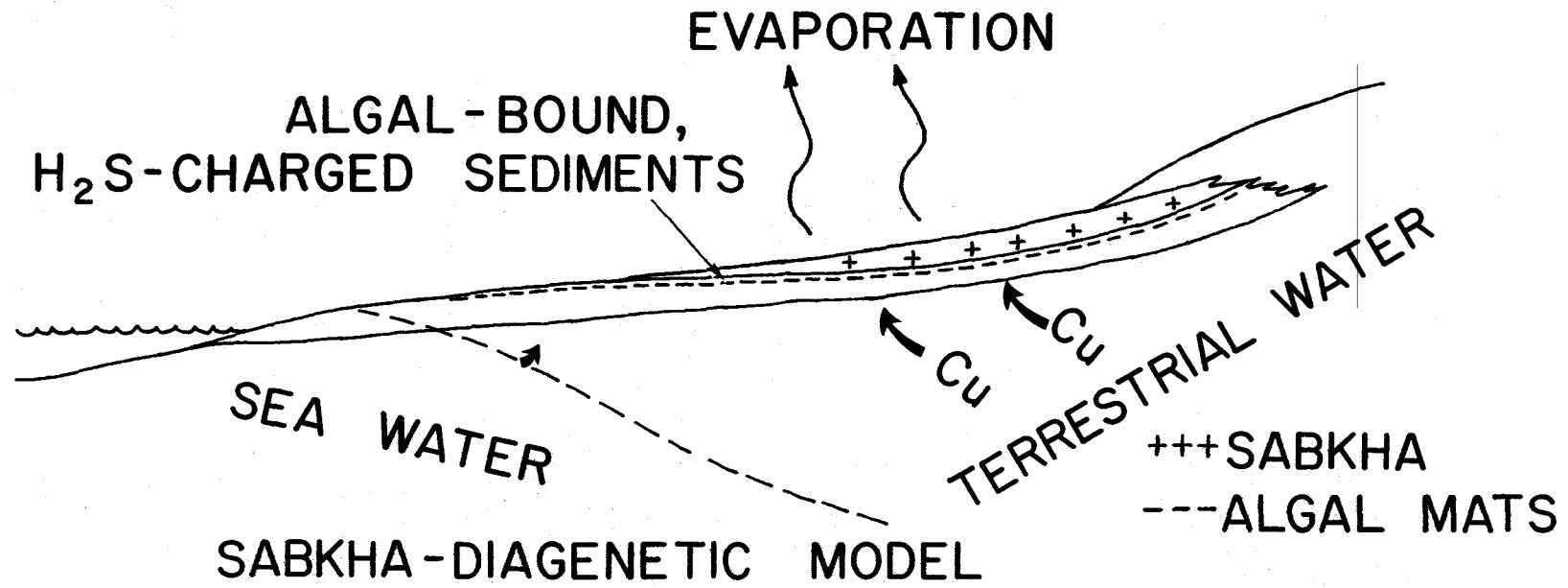


Fig. 18. Sabkha-diagenetic model for copper mineralization. Modified from Renfro (1974).

provided the elevation necessary to produce a sufficient hydraulic head. Hsü and Siegenthaler stress that this process is governed by evaporation and not permeability and would not take place in a humid climate where ground-water movement is induced by a large gravity head. Hydrogen sulfide gas, sulfate ions, gypsum, and anhydrite are common features found in sabkha and intertidal sediments of the Trucial coast (Butler, 1970). Anaerobic, sulfate-reducing bacteria utilize organic material present in algal mats to provide energy to reduce sulfate, which is in the form of sulfate ions. The reduction is a metabolic process in which oxygen is provided by sulfate breakdown with H_2S or HS^- formed as a by-product. Presence of these gases and a lack of oxygen result in a low pH and a negative redox potential (Eh) in the sediments.

With hydrogen sulfide acting as a reductant, and evaporative discharge serving as a driving force, the stage may be set for the accumulation of copper. Copper is contained in the ground water as dissolved copper in ionic form, copper adsorbed on clay-size particles, and colloidal and soluble organo-copper complexes which are pumped through the sabkha. As water goes through the zone of H_2S and HS^- , copper is extracted and precipitated as chalcocite or perhaps covellite. Breakdown of the various organic complexes and desorption of the copper may be facilitated by the strongly ionic (Na^+ and Cl^-) conditions under the sabkha facies, and the low Eh and slightly acidic pH in the organic-rich facies (Butler, 1969). Desorption or release of copper may partly occur by substitution of Na^+ for Cu^+ (Rickard, 1970; Kharkar and others, 1968). Studies by Temple and LeRoux (1964) show that metal toxicity would limit the continued action of sulfate-reducing bacteria only if the rate of introduction of metals to the environment exceeds the rate of H_2S production. It is proposed by the writer that, in the sabkha-diagenetic model, copper was passing through organic-rich zones at a relatively average concentration and that production of H_2S was keeping pace with the introduction of copper. The gypsum layer above the algal mat zone may have acted as a partial seal to upward dispersal of H_2S . The presence of some copper mineralization in the gypsum indicates that some H_2S did seep into the base of the gypsum layer. The gypsum layer of the sabkha would also serve as a seal to oxygen, thus preventing oxidation of the algal mats. The pH values in the intertidal-sabkha environment are zoned (Butler, 1969). Interstitial algal flat waters

have a pH of 7.5; landward across the sabkha and vertically downward through the sabkha sediments, the pH decreases to the 6.0 to 6.8 range. This decrease in pH is due to bacterial decomposition of organics (i.e. algal mats) that are being prograded over by sabkha deposits.

Information on the Eh values is essentially lacking; values in the -270 millivolts or lower range (Swanson and others, 1972; Butler, 1970) should be expected. Around pieces of decaying organics, the Eh may be lower than -270 millivolts. A consideration of the stability fields of chalcocite and covellite (Garrels and Christ, 1965), along with the Eh and pH conditions present in sabkha sediments, indicates that copper sulfides could form in the algal mat zone under the sabkha-facies gypsum (figs. 12 and 13). A theoretical study by Trudinger and others (1972) supports the hypothesis that biogenic processes may take part in forming strata-bound copper deposits. Lockwood (1972) reports that chalcocite from Creta exhibits a spread in the relative ratio of sulfur isotopes (S^{34}/S^{32}) that suggests a biogenic origin for the sulfide anion.

The amount of copper present in the ground water and the length of time in which the concentrating process is active are critical factors in the sabkha-diagenetic theory. Hem (1959) reports that sea water contains 0.003 ppm copper. The mean copper content of fresh-water streams is 0.010 ppm (Livingston, 1963). The fresh-water figure is undoubtedly too low since most analyses do not consider copper that has been complexed by naturally occurring chelators such as humic acids, copper in metallo-organic compounds, or copper in suspension adsorbed on inorganic and organic detrital particles. Vol'fson and Arkhangel'skaya (1971) report that streams in the Azov-Black Sea and Caspian Sea basins carry 0.06 ppm and 0.038 ppm of copper, respectively; much of the copper is carried in suspension. From data by Kharkar and others (1968), it can be seen that adsorption of cobalt by particles in streams causes a fourfold increase (average) in total cobalt content. Collins (1973) suggests that similar figures may be obtained from a study of copper because of their similarities in behavior. Rashid and Leonard (1973) have demonstrated the importance of organic compounds (e.g. humic and amino acids) in dissolving insoluble metallic salts and in keeping them in solution by preventing their precipitation under conditions that would other-

wise lead to immobilization. Humic acids have a base-exchange capacity and tend to sequester or complex metal ions (Martin and others, 1971).

Baker (1973), in a laboratory study using humic acid extracted from a podzolic soil in Tasmania, has shown that "metal humates" are readily dissolved and mobilized in the presence of humic acids. Unfortunately, very few quantitative data are available on copper adsorbed on particles or as organo-copper complexes in ground water. White and others (1963) report as much as 0.12 ppm copper in ground water from a shale and siltstone terrane. Most values of copper in ground water from all terraces composed of unmineralized rocks are apparently under 0.010 ppm (based on study of charts in White and others, 1963). No mention is made by White of copper present as part of soluble or colloidal organic compounds, or adsorbed on particles that may travel in ground water.

The length of time during which a sabkha environment can exist naturally depends on the stability of depositional conditions. On the Trucial coast, an average of 2.5 feet of upper intertidal (algal mat) and sabkha sediments have accumulated in about 3,500 years (Evans and others, 1969). Depositional processes in the Trucial coast sabkha are such that the sabkha is slowly prograding across intertidal algal flats and into a lagoon connected to the Persian Gulf. Under alternate conditions suggested for the Blaine sabkha and tidal-flat system, a sabkha could prograde over an intertidal flat, subsidence could then occur creating a wide intertidal algal flat over the sabkha, and finally a new sabkha could again prograde over the intertidal zone. This process could be repeated many times. The same mechanism is proposed elsewhere in this report to explain the deposition of the Blaine Formation in North Texas. Bossellini and Hardie (1973) and Bebout and Maiklem (1973) propose a similar process for thick, ancient sabkha sediments in Italy and Canada. At location V-16, 110 feet of the Blaine appears to be sabkha-intertidal in origin. At a deposition rate of 2.5 feet per 3,500 years, it would take 154,000 years of sabkha deposition to accumulate 110 feet of the Texas Blaine Formation.

Calculations (table 1) were made to determine the feasibility of concentrating economic copper deposits by the diagenetic process just described. From figures supplied by Hsü and

Table 1. Number of years required to concentrate a 25-cm column of 1-percent copper over 1 square cm of surface¹ (Calculations given in appendix VIII)

Sabkha evaporation rates (cm per year)	Copper ppm in ground water ⁴	Number of years required
100 ²	.06	100,000
100	.01	600,000
100	.003	2,000,000
50 ³	.06	200,000
50	.01	1,200,000
50	.003	4,000,000

1 — 1% copper and 25-cm (10-inch) thickness are personal estimates of average thickness and tenor of copper-bearing shale in the study area chosen partly for ease of calculation.

2 — From Hsü and Siegenthaler (1969), evaporation from standing surface of water.

3 — From Hsü and Siegenthaler (1969), evaporative loss of interstitial water for sediments of 40-percent porosity.

4 — previously given in text.

Siegenthaler (1969) and using the 154,000 years estimated to deposit the Blaine sabkha and tidal-flat deposits, it can be seen that the sabkha-diagenetic theory may be valid provided that there are approximately 0.06 parts per million (or slightly less) copper in the ground water, that the rate of evaporation from the sabkha is between 50 and 100 cm per year, and that ground water is almost totally terrestrial in origin. Evaporation-rate data from Schlanger (1965) indicates that an evaporation rate of 120 cm per year may be more accurate for the upper limit of the evaporation rate.

An important aspect of the sabkha-diagenetic theory of copper concentration is the necessity for having most of the ground water pulled through the lowermost sabkha even when sabkha-intertidal sediments are at least 110 feet thick. This requirement may be acceptable for the following reasons. Sabkha sediments form as a wedge of low-permeability sediments with a slight seaward tilt that have prograded over intertidal sediments (Evans and others, 1969; figs. 4 and 5). In general, the sediments seaward of the sabkha have a low permeability, whereas sediments under and landward of the sabkha have a relatively high permeability; this generalization holds true for the San Angelo Formation even though there is a

higher mud content in the San Angelo than in Trucial coast sediments. Therefore, ground-water flow lines tend to come in under the sabkha (fig. 18), and for reasons previously stated, from the landward side. The presence of some copper in dolomite and gypsum layers above the main copper zone at the top of the Cedar Mountain system indicates that some copper either passed through the bottom gypsum layer or came in above the bottom layer.

EPIGENETIC MODELS

Epigenetic mineral deposits are those deposits that have formed later than the enclosing host rocks (Bateman, 1951). Theories of ore genesis have been proposed that involve either hydrothermal solutions from a magmatic source (Davidson, 1962), or lateral or upward secretion of metal-bearing solutions from basinal deposits (Noble, 1963; Dozy, 1970; Davidson, 1965). In the latter three theories, the sediments may not be completely lithified although compaction would have already occurred. Davidson (1962) proposes that hydrothermal solutions are disseminated in lithified country rock during the early part of an orogenic event; then, during a later stage in the orogeny, they are forced into chemically receptive host rocks or sediments.

The discovery of mineralized brines in the Red Sea (Degens and Ross, 1969) and in Salton Sea sediments (White, 1968) has recently focused attention on the importance of saline solutions as a transporting medium for a variety of elements (Tarling, 1973). The importance of chloride complexes in the transportation and deposition of ore-forming metals has been pointed out by Helgeson (1964), and the formation of complex ions has been shown to increase the solubility of some metals by several orders of magnitude (Barton, 1959).

Transport of copper in chloride complexes (e.g. $\text{Cu}(\text{H}_2\text{O})_{n-3}\text{Cl}_3^-$, or simply CuCl_3^-) vertically along faults or fractures and then laterally along permeable horizons with precipitation taking place in favorable chemical zones is proposed by the writer as an alternate, epigenetic origin for the copper deposits in the San Angelo Formation (fig. 19A). Faulting or fracturing may have occurred in or near the area of this report in response to sedimentary loading in the Midland

Basin or as a result of separation of the North American and South American plates during the late Paleozoic and early Mesozoic (see Walper and Rowett, 1972). Apparent alignment of copper deposits along the Midland Basin and other basins in Oklahoma and southern Kansas (figs. 2 and 16) may possibly result from growth faulting along the margin of these basins. Copper in the form of chloride complexes may have traveled vertically along faults or fractures and spread out laterally along porous sandstone beds. Deposition could have occurred when the mineralizing solutions came in contact with hydrogen sulfide in organic-rich zones such as tidal channel-fill facies and algal mat facies. Reduction of solubility as a result of lower temperature may have had some influence on concentrating the copper, although the effect is probably minimal (Barton, 1959). The copper could have been derived from the leaching of deeply buried copper-rich detrital minerals (i.e. biotite, and possibly hornblende and augite), connate water in older Paleozoic rocks, and possibly some copper ions from deep-seated, unidentified magmatic sources. A high geothermal gradient along the eastern side of the Midland Basin, perhaps related to the separation of lithospheric plates (Walper and Rowett, 1972), may have provided additional heat for leaching copper and increasing its solubility. Tarling (1973) discusses the application of plate tectonic concepts to ore genesis and stressed the importance of high heat flow connected with plate movements and organic-rich zones as places for deposition of metals.

A second epigenetic theory involving thermal diffusion and metasomatic processes (fig. 19B) was investigated in order to obviate the necessity of a fluid moving upward along a fault or fracture. Garrels and others (1949) stress the possible importance, theoretically, of diffusion in transferring significant quantities of materials over relatively long distances. Ramberg (1952) proposes that a high geothermal gradient may cause intergranular diffusion of atomic, ionic, or molecular-size particles over relatively long distances, giving rise to a low-temperature metasomatic type of ore deposit. Microporosity may be developed in lithified and perhaps semilithified, deeply buried rocks as a result of intragranular microfissuration (Dandurand and others, 1972). This porosity would be intermittently formed and destroyed as a result of uneven lithostatic stresses. The multitude of healed fractures noted in quartz grains (Sipple,

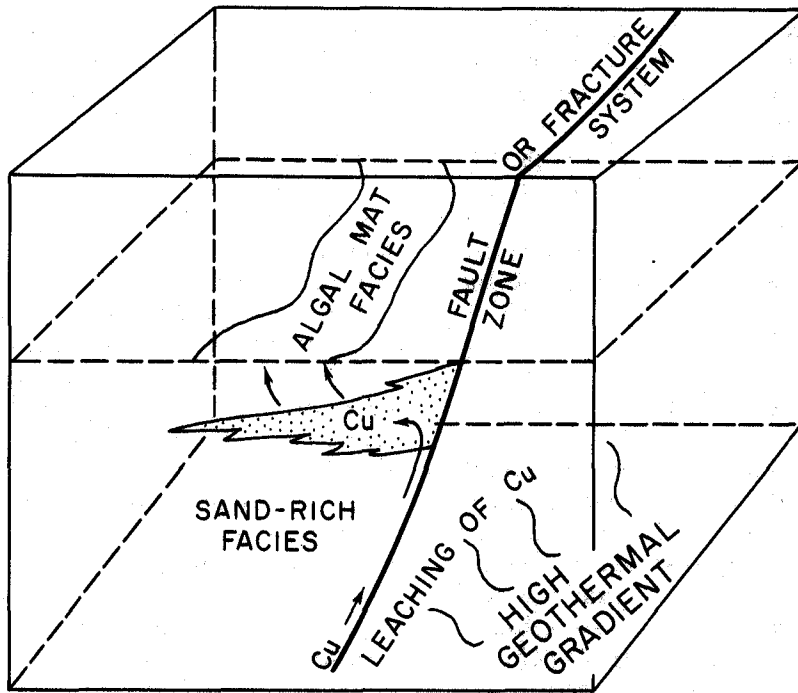


Fig. 19A. Epigenetic model: fault- or fracture-controlled mineralization.

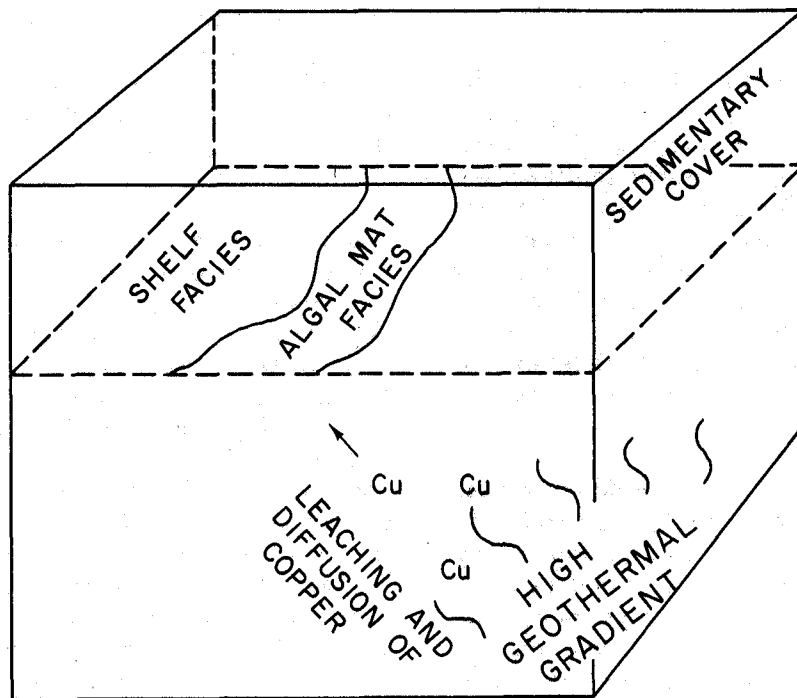


Fig. 19B. Epigenetic model: diffusion-controlled mineralization.

1968) may be partly caused by these processes. During the microfissuration process, fluids are released and the solubility of many minerals is increased (Dandurand and others, 1972).

Copper may be able to move out of its position in the lattice of minerals bearing trace amounts of copper, and move into an intergranular position, or if microfractures in the grains develop, into an intragranular position. In this intergranular or intragranular position, the copper ion may go into solution as perhaps a chloride complex and be physically transported a short distance by fluid movement, or the ion itself may diffuse a short distance through the solution and, perhaps, along grain boundaries. Given a sufficient period of time, a general upward movement of copper in the direction of the inferred concentration gradient coupled with an integration of this process over a large area may lead to the concentration of an economic copper deposit, provided that an HS^- or H_2S -bearing strata is reached and the microfissuration process ceases. A delicate balance among these three factors may be necessary, thus providing indirect evidence for an apparent lack of copper mineralization in rocks older than the Permian. An abnormally high geothermal gradient might increase the rate and efficiency of this diffusion process. As in the previous epigenetic theory involving mass movement of aqueous solutions along fault or fracture zones, the source for the copper could be deeply buried copper-rich detrital minerals, connate water, or an as yet unidentified magmatic source. The emplacement of ore bodies by either epigenetic theory could take place after deposition of the host rocks and after an unspecified thickness of sediments has been deposited over the host rocks.

EVALUATION OF MINERALIZATION MODELS

Three theoretical models, a sabkha-diagenetic model and two, alternate, epigenetic models, are proposed in this report for the origin of the strata-bound copper deposits in the San Angelo Formation. In the sabkha-diagenetic model (fig. 18), it has been proposed that evaporative discharge through the Blaine sabkha and tidal-flat system drew through the previously deposited San Angelo Formation primarily terrestrial ground water carrying an essentially average concentration of copper as ions, in soluble or colloidal organic compounds, and adsorbed on particles that could

travel in ground water. As the ground water passed through organic-rich facies, such as the algal mat facies and the middle and lower parts of the tidal channel-fill facies of the Cedar Mountain tidal-flat system, the copper was reduced and precipitated as chalcocite by either H_2S or HS^- which are available in these facies because of chemical reactions connected with the metabolism of sulfate-reducing bacteria. Economic copper concentrations are the result of a continuation of this process through a number of sabkha and tidal-flat depositional cycles.

In the alternate, epigenetic models, it has been postulated that either (1) transport of copper in a chloride complex along faults or fractures (fig. 19A), or (2) intergranular and intragranular diffusion and short-distance fluid transport of copper, integrated over a large volume and a relatively long distance (fig. 19B), may have led to a concentration of copper in chemically favorable zones. Chemical and physical processes associated with both of these epigenetic models may have been aided by tectonic stresses and a high heat flow caused by separation of the North American and South American plates during late Paleozoic and early Mesozoic (see Walper and Rowett, 1972).

Both the sabkha-diagenetic model and the epigenetic models for the origin of copper deposits in the San Angelo Formation stress the importance of H_2S and HS^- that are produced in organic-rich zones by sulfate-reducing bacteria. These models differ, though, in the emphasis that is placed on facies control and time of copper deposition. The sabkha-diagenetic model is closely linked spatially and temporally to specific facies. Without the relatively rapid progradation of sabkha facies over the Cedar Mountain algal mat facies and continued deposition of sabkha and tidal-flat cycles (thus forming the Blaine system), the mechanism of evaporative discharge, which regulated the concentration of copper in the sabkha-diagenetic theory, would not have been able to operate. In the epigenetic models, only an HS^- or H_2S -rich facies is required. For movement of copper chloride complexes laterally from a fault or fracture, the H_2S should be in or adjacent to a permeable facies such as sandstone. Diffusion of copper through a few feet or a few tens of feet could transport the copper from a permeable sandstone facies through relatively impermeable mudstone strata to a chemically favorable facies (Garrels and others, 1949), such as the algal mat facies.

The evaporative discharge process involves diagenetic concentration of copper in the host facies during deposition of the overlying Blaine sabkha and tidal-flat system and may occur in a short interval of geologic time, perhaps 100,000 to 200,000 years. The epigenetic process involving movement of fluids along faults or fractures could occur in a very short period of time shortly after deposition or sometime during or perhaps after lithification of the host facies. A time limit may be imposed by the length of time during which the sulfate-reducing bacteria can remain active (which is partially dependent on the amount of organic matter present) or the length of time during which H₂S can remain in or near the host facies. The epigenetic process principally involving diffusion would entail very slow movement of copper and presence of H₂S for a much longer time.

The writer favors the sabkha-diagenetic model rather than the epigenetic models for the origin of the San Angelo copper deposits. Facies control of the copper deposits observed on outcrop fits well with the vertical succession of facies and the inferred paleogeographic history in the area of this report. Lack of copper mineralization in underlying coal deposits and other organic-rich facies of Pennsylvanian age and an absence of igneous or metamorphic activity in the region of this report suggest that perhaps a diagenetic process such as outlined in the sabkha-diagenetic model was active in concentrating the copper.

An epigenetic model involving movement of copper chloride complexes in solution along faults or fractures cannot be ruled out, but until evidence of faulting or fracturing is detected in or near the area of this report, facies control as described in the sabkha-diagenetic model seems to be the more plausible of these two theoretical models for concentrating San Angelo copper deposits. Movement of solutions along fault or fracture zones would appear to be a suitable explanation for the fact that there are roughly three copper zones in the Permian of North Texas (fig. 16), but dense drilling for oil, especially near the zones east of the San Angelo Formation, has failed to detect faults or anomalous fracture patterns. It is remotely possible that the movement occurring along any faults or fractures was solely of an opening and closing nature, which would make it extremely hard, if not impossible, to detect the existence of these former zones.

Calculations were made (see appendix VIII) using the diffusion equation (Weast, 1971) to see the time it would take to concentrate a 10-inch layer of 1-percent copper. By using 4,500 feet, which is the approximate depth to the basement (Flawn, 1956), as the length distance through which diffusion occurred and an initial concentration of 100 ppm copper, it was determined that concentration of copper by diffusion would take 2.4 million years. The diffusion coefficient was for the diffusion of CuCl₂ in an aqueous solution (Bruins, 1929); the length of time derived by using this diffusion coefficient value may be substantially too low for the following reasons. According to Manheim (1970), diffusion in unconsolidated sediments generally occurs at rates ranging from one-half to one-twentieth of those occurring in free solution. Part of this slower rate of net ion flux is caused by reactions between diffusing ions and the enclosing sediments. The 100-ppm initial concentration may also be too high since, in the Salton Sea geothermal area, the concentration of copper in pore waters is only 8 ppm (White, 1968). It would appear from these calculations that diffusion may not be a satisfactory theory for explaining the copper mineralization in the San Angelo Formation, although diffusion may be useful in explaining concentration phenomena that may require movement of copper over distances of only a few inches or feet (e.g. nodules of copper minerals).

The copper deposits at Creta and near Mangum (fig. 16) in southwestern Oklahoma, although not part of this study, were generally examined since they are located at approximately the same stratigraphic level as the copper-bearing shales in Texas. The cap gypsum bed on top of the copper shale at Creta exhibits, on cut surfaces, a nodular texture suggesting a sabkha origin. Nodules in the slabs are more tightly packed, more highly distorted, and have less matrix present than gypsum beds from Texas. The high boron content (X2) of the copper-bearing shale, as compared to other shale in the Creta area, may point to a lagoonal origin for the shale as Ham and Johnson (1964) propose, or the high concentration may result from bathing of upper tidal-flat algal mats by waters of the restricted shelf during supratidal flooding. A depositional system analysis of these Oklahoma rocks is recommended.

ECONOMICS OF NORTH TEXAS STRATA-BOUND COPPER DEPOSITS

Economic evaluation of copper deposits in North Texas should be preceded by: (1) an examination of early copper mining ventures in North Texas and the reasons that they were failures, (2) an examination of modern copper mines that are being operated under geologic conditions similar to those that would be encountered in North Texas, (3) a thorough understanding of the facies control of the North Texas copper deposits, (4) an understanding of modern exploration and mining techniques, and (5) an appreciation of the United States and international copper industry pricing and marketing patterns.

HISTORY OF NORTH TEXAS COPPER MINING

The presence of copper in North Texas was first noted by Captain R. B. Marcy in 1852 during exploration of the Red River drainage basin for the U. S. Army (Marcy, 1854). In his report he stated, "... in the course of the march to-day we met with numerous detached pieces of copper ore, mixed with volcanic scoria." This misinterpretation of what was probably water-worn caliche with secondary coatings of copper carbonate misled some of the early prospectors into looking for vein deposits.

In 1864 some copper was mined in Archer County and sent to Austin for analysis and smelting. The copper was used to make percussion caps for use by the Confederate Army (Cummins, 1891).

In 1877 an expedition to the copper deposits of the San Angelo Formation was led by retired General George B. McClellan. This mining venture was financed by a group who invested a million dollars to establish the Grant Belt Copper Company (Scales, 1959). Their efforts included drilling a 1,000-foot hole in the hopes of intersecting a larger plutonic deposit (Schmitz, 1897).

Additional mining activities in North Texas were initiated by Goldberg Mining Company in 1880 (Stroud and others, 1970), the Foard County Mining Company in 1916 (Phillips, 1917b?), and other small companies.

In 1965 a small mine was operated by Aard Copper, Inc. (IV-D) and the crusher and other

equipment are still at the mine. This operation, like all previous ones, failed because of the nature and quantity of the ore, inexperienced operators, and/or poor economic conditions. Total production from all prospects in North Texas has exceeded 5,000 tons of crude ore (Stroud and others, 1970).

The Creta copper mine of Oklahoma (fig. 16) has been the only sustained and profitable copper mining venture in the Permian copper belt. It is located southwest of Altus, Oklahoma, and is operated by Eagle-Picher Industries. The Creta mine was opened in 1965 as a strip-mining operation using electric- and diesel-powered drag lines capable of removing relatively large tonnages of ore in a short period of time. The copper ore is a 6-inch copper-bearing gray shale and mudstone immediately below a 3- to 6-inch-thick gypsum cap rock of the sabkha type in the Flowerpot Formation. The ore-bearing shale bed is laterally continuous and mining has taken place in parts of six land sections (each section is 1 square mile). According to Ham and Johnson (1964), the copper-bearing shale being mined contains 2.65 to 4.45 percent copper. The mine supervisor (Jones, personal communication, 1973) indicated that the average ore grade runs less than the 2.65 percent quoted by Ham and Johnson. Currently, 65 feet of overburden is being stripped to reach the copper-bearing horizon. Below approximately 10 feet, the copper ore is unaffected by recent oxidation and only chalcocite is present. The first step in mining the copper-bearing shale at Creta involves drilling a relatively shallow hole in which a small charge of dynamite is set off to break up the mudstone overburden, which includes a thick gypsum bed. Drag lines are used to remove the overburden down to the thin cap gypsum over the ore bed. A machine with a large drum equipped with spikes is then driven over the cap gypsum to break it up, and a skip loader strips off the broken gypsum and removes it to a waste pile. This process exposes the ore bed so that it can be loaded by a skip loader into a dump truck for transportation to the mill. The mill is designed to process 1,000 tons of crude ore per day. At the mill, the ore is crushed and converted to a slurry, then fed through a grinder to release mineral particles. From the grinding process, the ore is sent to a conditioner where it is prepared for passage to the flotation circuit. In the flotation cells, chalcocite is skimmed off in a froth, which is allowed to settle and thicken before it is

fed into a rotary dryer. Finally, the copper concentrate from the dryer is sent from a nearby railhead to a smelter in El Paso, Texas. Tailings from the beneficiation process are stored in a tailings pond near the mill.

ECONOMIC EVALUATION

The facies control of copper mineralization in the North Texas San Angelo Formation has been described (figs. 8, 10, 12, and 17). These facies include: (1) algal mat, (2) tidal channel-fill, (3) swash-zone (Cedar Mountain tidal-flat system), (4) basal sabkha (Blaine sabkha and tidal-flat system), (5) basal delta front (Old Glory and Copper Breaks fluvial-deltaic systems), and (6) basal tidal channel-fill and sandflat (Buzzard Peak tidal-flat system).

All mining ventures in the area of this report have been economic failures because they concentrated on mining copper from the tidal channel-fill deposits of the Cedar Mountain system, and in one case, the copper at the base of the Buzzard Peak system (III-J). Although these facies (especially the tidal channel-fill deposits) are characterized by pockets of rich ore, the ore bodies are discontinuous and too locally distributed to allow an economic mining operation. Modern economics and the current state of mining and extractive technology make the widespread copper-bearing shales of the Cedar Mountain system potentially economic exploration targets. Copper concentration in the mineralized shale beds of Texas runs as high as 4.4 percent (2-inch interval at location I-6, see appendix III) and up to 14 inches thick (near IV-3). A 7-inch channel sample at locality V-4 averages 2.2 percent copper. Accumulations of mineralized shale of possible ore grade are present at a number of localities (I-6, I-44, III-10, IV-3, V-1, V-4, V-5). Although channel samples were not taken in those localities to determine the average thickness and grade of the potentially economic copper-bearing shales, a range of between 0.5 and 1.5 percent copper may be a reasonable average grade for the total thickness of copper-bearing shale. Appendices III and IV list copper values, along with the location, stratigraphic position, and host facies.

An exploration venture in the area should be preceded by depositional systems analyses of the sequence, including investigation of the lateral

and vertical changes in the various facies, and the manner in which copper mineralization occurs in these facies. An understanding of the genetic significance of the various facies provides a useful tool for predicting host-rock distribution. The absence of faulting in the area and the strata-bound nature of the mineralization serve to make elevation a useful exploration tool, since a mineralized horizon may continue at about the same elevation for a number of miles. Use of elevation is especially helpful in tracing the copper-bearing shale at the top of the Cedar Mountain system and the copper at the base of the San Angelo Formation (Old Glory, Copper Breaks, and Buzzard Peak depositional systems). The zone at the contact between the Blaine and San Angelo Formations (pls. I-V) is a critical interval for prospecting. The presence of organic matter, orange spores such as found at Creta (orange spheres have also been found in the study area and are visible with a hand lens, but their organic origin has not been definitely established), and hematitic or limonitic gossan-like zones may be useful exploration guides indicating that copper may be nearby. In the replacement of 1 cc of pyrite by an equal volume of chalcocite, 1.51 grams of sulfur is lost. Some of the sulfur may be removed from the mineralized zone as the sulfate ion, ultimately forming gypsum; some of it, however, may be mobilized, transported, and then a short distance away reprecipitated with iron as secondary pyrite. At the margin of a mineralized tidal channel-fill (I-H) where it pinches out laterally into surrounding mudstones, an iron oxide zone is present; the copper at this prospect may have been present in the middle of the channel. Dingess (1969) noticed an inverse relationship between copper and iron in the Medicine Mounds area: where copper values are high, iron values are low; where copper values are low, iron values are high. Of course these copper-iron zonal relationships can also be explained by early diagenetic formation of pyrite without any causal connection to replacement, mobilization, or reprecipitation of pyrite.

Stroud and others (1970) divide the copper mineralization in the area of this study into three zones based on elevation and position in the stratigraphic section. Zone A is stratigraphically the highest of the three zones and the copper occurs in shale, mudstone, and dolomite; according to Stroud and others it represents deposition in a "... basinal environment." Zone B copper mineralization occurs in dolomite, mudstone,

shale, and sandstone and represents deposition in both "... basinal environments and channel-scour ..." environments. Zone C is stratigraphically the lowest zone and copper occurs primarily in sandstone with minor amounts in the underlying shale. Zone C represents deposition in "... paleoalluvial fan or deltaic ..." type deposits.

Channel-scour copper deposits (Zone B) are interpreted by the writer to represent tidal channel deposits. The basinal deposits (Zones A and B) are algal-bound shale beds of the Cedar Mountain system. The paleoalluvial-deltaic host rocks (Zone C) are basal tidal channel-fill sandstone lenses, delta front - distributary mouth bar sandstone beds, and tidal sandflat sandstone beds. The writer disagrees with the concept of three zones as proposed by Stroud and others. It is best to discuss mineralization in the San Angelo Formation and the lower part of the Blaine Formation in terms of facies host rocks. Mineralized zones in these stratigraphic units can be set up only on a very local basis. According to Stroud and others, Zone C at the base of the San Angelo Formation is potentially the best stratigraphic horizon for commercial development possibly by in situ leaching; the writer does not agree with this interpretation. The quantity of copper seen on outcrop (taking Holocene ground-water leaching into account), the scarcity of organic matter, and the depositional facies with which the copper is associated make it doubtful that copper is present in large and uniform concentrations sufficient for an economic mining development. Physical and chemical processes associated with the sabkha-diagenetic model would tend to indicate that facies near the contact between the Cedar Mountain and Blaine systems (fig. 17) have the best potential for commercial copper development. Stroud and others (1970) provide a useful analysis of the mining methods, physical plant equipment, and economics (e.g. ore grade, tonnage) that must be considered before establishing a mining operation in the area of this study.

The Creta copper mine of Eagle-Picher Industries in southwestern Oklahoma is currently an economic operation for specific geologic, mining, and technological reasons. The ore bed has a constant stratigraphic position and a relatively uniform thickness and concentration over the area being mined. These factors make it easy to extend the operations. An excellent stratigraphic marker is provided by the cap gypsum over the ore bed. The

presence of the cap gypsum makes it possible for the drag line operator to mine down to the ore bed rapidly without accidentally mining out the ore bed or getting it mixed with overburden. Combination of an ore that is readily separable into chalcocite and shale matrix, and an efficient milling and flotation process that Eagle-Picher personnel have utilized, produces a high-grade copper concentrate (D. E. Gorski, personal communication, 1972).

Exploration for copper in the San Angelo Formation of North Texas will require a thorough understanding of the facies control of the ore deposits and a careful exploration program of outcrop sampling and core drilling in order to delineate an economic ore body. The prime target for exploration would be the widespread copper-bearing shale beds of the Cedar Mountain system. This facies is well developed along outcrop south of Old Glory (V-4, V-5, V-1), around and south of Buzzard Peak (IV-3, III-10), and near Medicine Mounds (I-6). A program designed to evaluate potential copper-bearing shale ore beds will have to consider carefully the amount of overburden and whether there are any stratigraphic marker beds, such as dolomite or gypsum, that would help in locating the ore bed during mining. The ore-bearing shale beds near Medicine Mounds and south of Old Glory both have thicknesses of overburden that probably would not be economically prohibitive to strip, and they also have an overlying gypsum marker bed. The copper will have to be strip-mined with consideration given to state and Federal environmental regulations. A railhead for shipment of ore or concentrate could be established within 4 to 12 miles of any of the potentially economic copper-bearing shale beds. The copper-bearing shale beds in the area of this study have good potential for a relatively small, 1,000 to 4,000 ton per day, mining operation.

The price of copper has been almost constantly rising since 1945 (fig. 20). During the same time span, the average grade of ore mined has constantly decreased and will continue to decrease (fig. 20). Ageton and Greenspoon (1970) estimate that to meet increasing demand and future costs, the price of copper in the year 2000 will have to be 75¢ per pound in constant 1968 dollars. With the price of copper increasing and the economic grade of ore continually decreasing, the copper deposits in the area of this report probably will be economically minable in the near future, if they have not already reached that point.

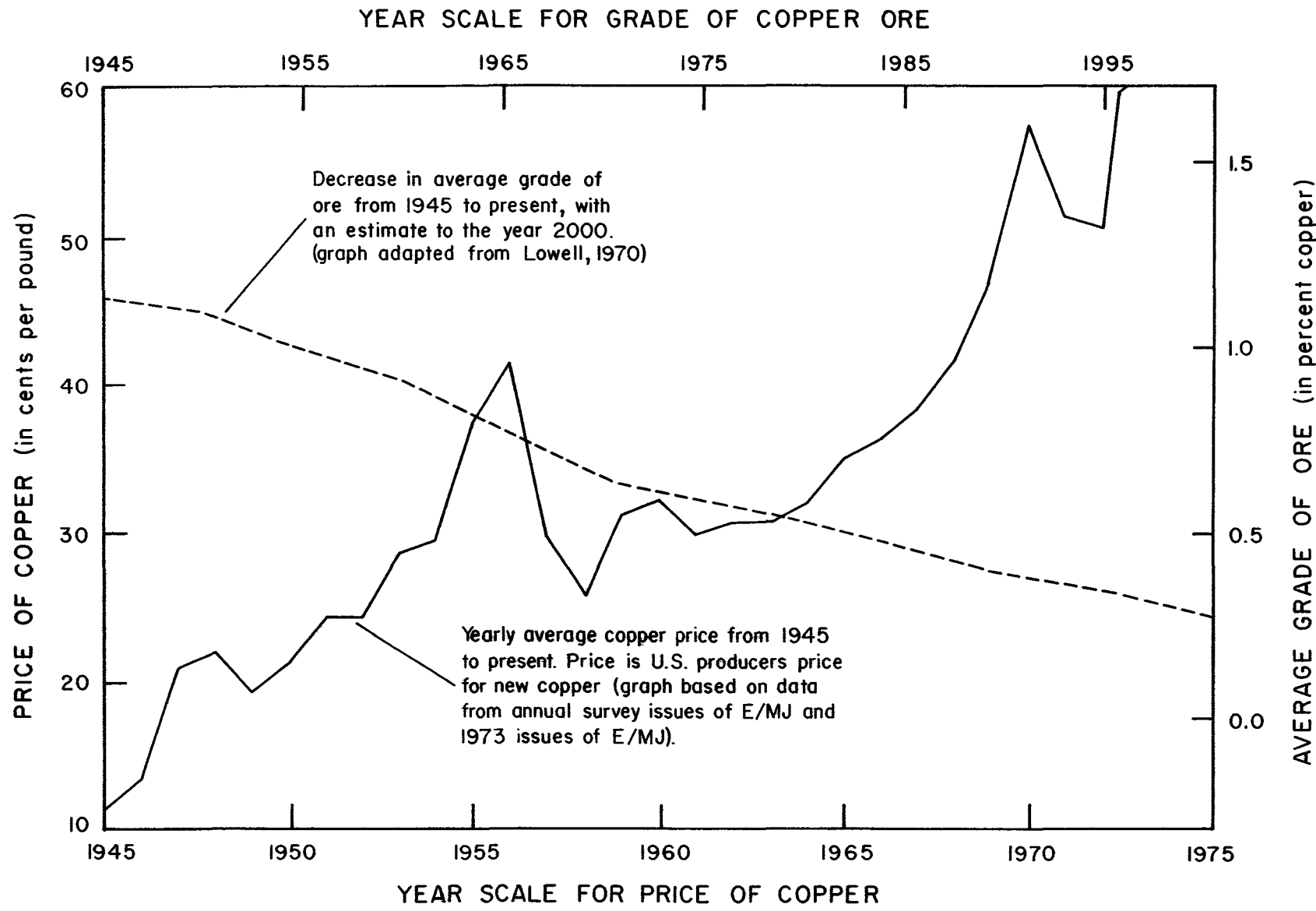


Fig. 20. Price of copper from 1945 to present, and decrease of average grades of ore mined from 1945 to present with a projection to the year 2000.

SUMMARY AND CONCLUSIONS

The San Angelo Formation is a mid-Permian complex of progradational facies composed of terrigenous clastics derived primarily from the Ouachita foldbelt and older Paleozoic rocks. The San Angelo has been divided in Texas into two members: a lower sand-rich Duncan Member, and an upper mud-rich Flowerpot Member (fig. 5).

The Duncan Member is composed of the northern Copper Breaks deltaic system and southern Old Glory fluvial-deltaic system (fig. 6), both of which prograded across the Choza subtidal facies and the submerged tidal-flat and sabkha facies on the eastern side of the Midland Basin. The Copper Breaks and Old Glory systems are composed of a progradational facies tract composed (upward) of prodelta, delta-front, distributary mouth bar, and a complex of distributary channel-fill and associated delta-plain facies. Intermediate between these two fluvial-deltaic systems, and as a thin veneer under them, is the strike-fed Buzzard Peak sand-rich tidal-flat system (fig. 7). The Buzzard Peak system is composed of sandstone beds of the tidal sandflat facies interbedded with sandy mudstone and tidal channel-fill sandstone lenses of the tidal channel facies (fig. 10).

Transitionally above the depositional systems of the Duncan Member is the Cedar Mountain mud-rich tidal-flat system which essentially is stratigraphically equivalent to the Flowerpot Member (fig. 6). With gradual cessation of deltaic outbuilding and subsidence of the deltaic sediments, the shoreline was prograded by the Cedar Mountain system (fig. 6) which was supplied by mud transported along strike from active deltas to the south (fig. 11). The Cedar Mountain system is characterized by sandstone lenses of the tidal channel facies, thin ripple-bedded sandstone beds of the swash-zone facies, and laminated algal-bound shale, dolomitic shale, and dolomite of the algal mat facies (fig. 12). Gypsum and barite nodules are common in the Cedar Mountain system.

Coastal tidal-flat progradation led to a gradual raising of the landward portion of the Cedar Mountain system above mean high tide and to the subsequent offlap of sabkha facies of the Blaine sabkha and tidal-flat system (lower Blaine Formation). The Blaine system is composed of diagenetically formed nodular gypsum beds of the sabkha facies (figs. 12 and 13) interbedded with thin dolomite and mudstone beds of both tidal-flat

and sabkha origin. Halite casts, representing desiccation of shallow ponds on the supratidal flats, are also present.

The principal strata-bound copper deposits are present in relatively widespread mineralized zones in laminated, algal-bound shale beds at the top of the Cedar Mountain system; copper also occurs as discontinuous deposits in sandstone lenses filling tidal channels in the Cedar Mountain system (fig. 17). Minor amounts of copper occur in the basal part of the Duncan Member, at the base of thin ripple-bedded sandstone beds in the Cedar Mountain system, and in thin dolomite and nodular gypsum beds at the top of the Cedar Mountain system and in the lower part of the Blaine system. The most important sulfide mineral is chalcocite, which shows evidence of having replaced pyrite (pl. VII, C). Minor amounts of covellite, primarily present as a replacement of chalcocite, are also present. Where recent oxygen-rich waters containing CO_2 have permeated the mineralized facies, malachite and azurite have formed. Organic matter (wood and algal mats) served as loci for the copper mineralization.

Three theories for the origin of San Angelo copper mineralization are proposed. The sabkha-diagenetic theory (fig. 18) involves evaporative pumping of copper-bearing ground water through the sabkha surface. As ground water passed through algal mats buried beneath the sabkha sediments, copper was stripped out by the H_2S and HS^- that was generated by sulfate-reducing anaerobic bacteria. Some of the copper also replaced pyrite that was formed earlier. Alternate, epigenetic theories involve (1) the ascension of copper chloride solutions along faults and fractures with lateral movement to stratigraphic zones favorable for concentration (fig. 19A), and (2) ascension of copper by intergranular and intra-granular metasomatic diffusion (fig. 19B). The source of the copper in the epigenetic theories would have been primarily from leaching of the thick underlying sedimentary pile in the Midland Basin with deposition occurring upon contact with H_2S or HS^- in organic-rich facies.

The progradation of the Blaine sabkhas and tidal flats over the Cedar Mountain algal mats, the process of evaporative discharge through the sabkha facies, and the length of time inferred for deposition of the Blaine system provide the essential elements for a viable diagenetic theory.

REFERENCES

- Adams, J. E., Cheney, M. G., DeFord, R. K., Dickey, R. I., Dunbar, C. O., Hills, J. M., King, R. E., Lloyd, E. R., Miller, A. K., and Needham, C. E., 1939, Standard Permian section of North America: *Am. Assoc. Petroleum Geologists Bull.*, v. 23, no. 11, p. 1673-1681.
- Ageton, R. W., and Greenspoon, G. N., 1970, Mineral facts and problems, copper: *U. S. Bur. Mines Bull.* 650, p. 535-553.
- Baas Becking, L. G. M., and Moore, D., 1961, Biogenic sulfides: *Econ. Geology*, v. 56, no. 2, p. 259-272.
- Baker, E. T., Jr., Long, A. T., Jr., Reeves, R. D., and Wood, L. A., 1963, Reconnaissance investigation of the ground-water resources of the Red River, Sulphur River, and Cypress Creek Basins, Texas: *Texas Water Comm. Bull.* 6306, 127 p.
- Baker, W. E., 1973, The role of humic acids from Tasmanian podzolic soils in mineral degradation and metal mobilization: *Geochim. et Cosmochim. Acta*, v. 37, no. 2, p. 269-281.
- Barton, P. B., Jr., 1959, The chemical environment of ore deposition and the problem of low-temperature ore transport, *in* Abelson, P. H., ed., *Researches in geochemistry*, vol. 1: New York, John Wiley and Sons, Inc., p. 279-300.
- Bateman, A. M., 1951, *The formation of mineral deposits*: New York, John Wiley and Sons, Inc., 371 p.
- Bates, C. C., 1953, Rational theory of delta formation: *Am. Assoc. Petroleum Geologists Bull.*, v. 37, no. 9, p. 2119-2162.
- Beall, A. O., Jr., 1968, Sedimentary processes operative along the Western Louisiana shoreline: *Jour. Sed. Petrology*, v. 38, no. 3, p. 869-877.
- Bebout, D. G., and Maiklem, W. R., 1973, Ancient anhydrite facies and environments, Middle Devonian Elk Point Basin, Alberta: *Canadian Petroleum Geology Bull.*, v. 21, no. 3, p. 287-343.
- Beede, J. W., and Bentley, W. P., 1918, The geology of Coke County: *Univ. Texas Bull.* 1850, 80 p.
- _____, and Christner, D. D., 1926, The San Angelo Formation; the geology of Foard County: *Univ. Texas Bull.* 2607, 57 p.
- _____, and Waite, V. V., 1918, The geology of Runnels County: *Univ. Texas Bull.* 1816, 64 p.
- Bosellini, Alfonso, and Hardie, L. A., 1973, Depositional theme of a marginal marine evaporite: *Sedimentology*, v. 20, no. 1, p. 5-27.
- Brown, L. F., Jr., and Goodson, J. L., 1972, Abilene sheet, *in* Barnes, V. E., project director, *Geologic atlas of Texas*: Univ. Texas, Austin, *Bur. Econ. Geology*, scale 1:250,000.
- Bruins, H. R., 1929, Coefficient of diffusion in liquids, *in* Washburn, E. W., ed., *International critical tables of numerical data*: New York, McGraw Hill Book Co., Inc., p. 63-76.
- Butler, G. P., 1969, Modern evaporite deposition and geochemistry of coexisting brines, the sabkha, Trucial coast, Arabian Gulf: *Jour. Sed. Petrology*, v. 39, no. 1, p. 70-89.
- _____, 1970, Holocene gypsum and anhydrite of the Abu Dhabi sabkha, Trucial coast: an alternative explanation of origin, *in* Rau, J. L., and Dellwig, L. F., eds., *Third symposium on salt*, vol. 1: Cleveland, Northern Ohio Geol. Soc., p. 120-152.
- Clifton, R. L., 1946, Middle Permian Cephalopoda from Texas and New Mexico: *Jour. Paleontology*, v. 20, no. 6, p. 556-559.
- Coleman, J. M., and Gagliano, S. M., 1964, Cyclic sedimentation in the Mississippi River deltaic plain: *Gulf Coast Assoc. Geol. Socs. Trans.*, v. 14, p. 67-80.
- Collins, B. I., 1973, The concentration control of soluble copper in a mine tailings stream: *Geochim. et Cosmochim. Acta*, v. 37, no. 1, p. 69-75.
- Cragin, F. W., 1896, The Cimarron series of Kansas: *Colorado Coll. Studies*, v. 6, p. 1-4.
- Cronin, J. G., Follett, C. R., Shafer, G. H., and Rettman, P. L., 1963, Reconnaissance investigation of the ground-water resources of the Brazos River Basin, Texas: *Texas Water Comm., Bull.* 6310, 152 p.
- Cummins, W. F., 1890, Permian of Texas and its overlying beds, *in* First annual report, Geological Survey of Texas, 1889: *Geol. Survey Texas*, p. 185-197.
- _____, 1891, Report on the geology of northwestern Texas, part II, economic geology, *in* Dumble, E. T., Second annual

- report, Geological Survey of Texas, 1890: Geol. Survey Texas, p. 436–491.
- Curry, J. R., 1964, Transgressions and regressions, *in* Miller, R. L., ed., *Papers in marine geology*: New York, Macmillan Co., p. 175–203.
- _____, and Moore, D. G., 1964, Holocene regressive littoral sand, Costa de Nayarit, Mexico, *in* Straaten, L. M. J. U. van, ed., *Developments in sedimentology*, vol. 1, deltaic and shallow marine deposits: New York, Elsevier Publishing Co., p. 76–82.
- Dalrymple, D. W., 1965, Calcium carbonate deposition associated with blue-green algal mats, Baffin Bay, Texas: *Univ. Texas, Inst. Marine Sci. Pub.*, v. 10, p. 187–200.
- Dandurand, J. L., Fortune, J. P., Perami, R., Schott, J., and Tollon, F., 1972, On the importance of mechanical action and thermal gradient in the formation of metal-bearing deposits: *Mineralium Deposita*, v. 7, no. 4, p. 339–350.
- Davidson, C. F., 1962, The origin of some strata-bound sulfide ore deposits (discussion): *Econ. Geology*, v. 57, no. 2, p. 265–273.
- _____, 1965, A possible mode of origin of strata-bound copper ores: *Econ. Geology*, v. 60, no. 5, p. 942–954.
- Davies, G. R., 1970, Algal-laminated sediments, Gladstone embayment, Shark Bay, western Australia, *in* Logan, G. W., Davies, G. R., Read, J. F., and Cebulski, D. E., *Carbonate sedimentation and environments, Shark Bay, western Australia*: *Am. Assoc. Petroleum Geologists Mem.* 13, p. 169–205.
- Degens, E. T., and Ross, D. A., eds., 1969, *Hot brines and recent heavy mineral deposits in the Red Sea*: New York, Springer-Verlag, 600 p.
- Dingess, P. R., 1969, Medicine Mound project—Brown ranch: Eagle-Picher Industries intra-company correspondence.
- Donaldson, A. C., Martin, R. H., and Kanies, W. H., 1970, Holocene Guadalupe delta of Texas Gulf Coast, *in* Morgan, J. P., ed., *Deltaic sedimentation, modern and ancient*: *Soc. Econ. Paleontologists and Mineralogists Spec. Pub.*, no. 15, p. 107–137.
- Dozy, J. J., 1970, A geological model for the genesis of the lead-zinc ores of the Mississippi Valley, U. S. A.: *Inst. Mining Metall. Trans., Sec. B Bull.*, no. 765, p. B163–B170.
- Dunham, Kingsley, 1971, Introductory talk: rock association and genesis, *in* *Proceeding of the IMA-IAGOD [Internat. Mineralog. Assoc. and Internat. Assoc. Genesis of Ore Deposits] meetings, 1970, symposium on stratabound sulfide ore deposits*: *Japan Soc. Mining Geologists, Spec. Issue* 3, p. 167–171.
- Engineering and Mining Journal*, 1957–1973, Copper, *in* *Annual survey issues: Eng. Mining Jour.*, v. 159–174.
- Evans, G., 1965, Intertidal flat sediments and their environment of deposition in the Wash: *Geol. Soc. London Quart. Jour.*, v. 121, p. 209–245.
- _____, Schmidt, V., Bush, P., and Nelson, H., 1969, Stratigraphy and geologic history of the sabkha, Abu Dhabi, Persian Gulf: *Sedimentology*, v. 12, no. 1/2, p. 145–159.
- Fay, R. O., 1964, The Blaine and related formations of northwestern Oklahoma and southern Kansas: *Oklahoma Geol. Survey Bull.* 98, 238 p.
- Fisher, W. L., Brown, L. F., Jr., Scott, A. J., and McGowen, J. H., 1969, Delta systems in the exploration for oil and gas—a research colloquium: *Univ. Texas, Austin, Bur. Econ. Geology Spec. Pub.*, 212 p.
- Fisk, H. N., McFarlan, E., Jr., Kolb, C. R., and Wilbert, L. J., Jr., 1954, Sedimentary framework of the modern Mississippi delta: *Jour. Sed. Petrology*, v. 24, no. 2, p. 76–99.
- _____, 1955, Sand facies of recent Mississippi delta deposits: *Rome, World Petroleum Cong.* 4, Proc., sec. 1, p. 377–398.
- _____, 1959, Padre Island and the Laguna Madre flats, coastal South Texas, *in* *Russell, R. J., ed., Second coastal geography conference*: Washington, U. S. Office Naval Research, p. 103–151.
- Flawn, P. T., 1956, Basement rocks of Texas and Southeast New Mexico: *Univ. Texas, Austin, Bur. Econ. Geology Pub.* 5605, 261 p.
- _____, Goldstein, August, Jr., King, P. B., and Weaver, C. E., 1961, The Ouachita system: *Univ. Texas, Austin, Bur. Econ. Geology Pub.* 6120, 401 p.
- Folk, R. L., 1968, *Petrology of sedimentary rocks*: Austin, Texas, Hemphill's, 170 p.
- Frazier, D. E., 1967, Recent deltaic deposits of the Mississippi River: their development and chronology: *Gulf Coast Assoc. Geol. Socs. Trans.*, v. 17, p. 287–315.

- Galloway, W. E., 1970, Preliminary report on Permian red bed copper deposits, North-Central Texas: Univ. Texas, Austin, Bur. Econ. Geology open-file rept., 17 p.
- _____, and Brown, L. F., Jr., 1972, Depositional systems and shelf-slope relationships in Upper Pennsylvanian rocks, North-Central Texas: Univ. Texas, Austin, Bur. Econ. Geology Rept. Inv. 75, 62 p.
- Garrels, R. M., Dreyer, R. M., and Rowland, A. L., 1949, Diffusion of ions through intergranular spaces in water-saturated rocks: *Geol. Soc. America Bull.*, v. 60, no. 12, p. 1809–1828.
- _____, and Christ, C. L., 1965, Solutions, minerals, and equilibria: New York, Harper and Row Publishers, 450 p.
- Goddard, E. M., chm., 1948, Rock-color chart: Washington, D. C., National Research Council.
- Gould, C. N., 1905, Geology and water resources of Oklahoma: U. S. Geol. Survey Water-Supply Paper 148, 178 p.
- _____, 1924, A new classification of the Permian redbeds of southwestern Oklahoma: *Am. Assoc. Petroleum Geologists Bull.*, v. 8, no. 3, p. 322–341.
- Gould, H. R., and McFarlan, E., Jr., 1959, Geologic history of the chenier plain, southwestern Louisiana: *Gulf Coast Assoc. Geol. Soc. Trans.*, v. 9, p. 261–270.
- Green, D. A., 1937, Major divisions of Permian in Oklahoma and southern Kansas: *Am. Assoc. Petroleum Geologists Bull.*, v. 21, no. 12, p. 1515–1533.
- Ham, W. E., and Johnson, K. S., 1964, Copper in the Flowerpot shale (Permian) of the Creta area, Jackson County, Oklahoma: *Oklahoma Geol. Survey Circ.* 64, 32 p.
- Harms, J. C., and Fahnestock, R. K., 1965, Stratification, bed forms, and flow phenomena (with an example from the Rio Grande), in Middleton, G. V., ed., Primary sedimentary structures and their hydrodynamic interpretation: *Soc. Econ. Paleontologists and Mineralogists Spec. Pub.* 12, p. 84–115.
- Helgeson, H. C., 1964, Complexing and hydrothermal ore deposition: New York, Macmillan Co., 128 p.
- Hem, J. D., 1959, Study and interpretation of the chemical characteristics of natural water: U. S. Geol. Survey Water-Supply Paper 1473, 269 p.
- Hills, J. M., 1942, Rhythm of Permian seas—a paleogeographic study: *Am. Assoc. Petroleum Geologists Bull.*, v. 26, no. 2, p. 217–255.
- Hoyt, J. H., 1969, Chenier versus barrier, genetic and stratigraphic distinction: *Am. Assoc. Petroleum Geologists Bull.*, v. 53, no. 2, p. 299–306.
- Hsü, K. J., and Siegenthaler, Christoph, 1969, Preliminary experiments on hydrodynamic movement induced by evaporation and their bearing on the dolomite problem: *Sedimentology*, v. 12, no. 1/2, p. 11–25.
- Illing, L. V., Wells, A. J., and Taylor, J. C. M., 1965, Penecontemporary dolomite in the Persian Gulf, in Pray, L. C., and Murray, R. C., eds., Dolomitization and limestone diagenesis, a symposium: *Soc. Econ. Paleontologists and Mineralogists Spec. Pub.* 13, p. 89–111.
- Kendall, C. G. St. C., and Skipwith, P. A. d'E., 1969, Holocene shallow-water carbonate and evaporite sediments of Khor al Bazam, Abu Dhabi, Southwest Persian Gulf: *Am. Assoc. Petroleum Geologists Bull.*, v. 53, no. 4, p. 841–869.
- Kellerhals, Peter, and Murray, J. W., 1969, Tidal flats at boundary bay, Fraser River delta, British Columbia: *Canadian Petroleum Geology Bull.*, v. 17, no. 1, p. 67–91.
- Kharkar, D. P., Turekian, K. K., and Bertine, K. K., 1968, Stream supply of dissolved silver, molybdenum, antimony, selenium, chromium, cobalt, rubidium and cesium to the oceans: *Geochim. et Cosmochim. Acta*, v. 32, no. 3, p. 285–298.
- Kinsman, D. J. J., 1969, Modes of formation, sedimentary associations, and diagnostic features of shallow-water and supratidal evaporites: *Am. Assoc. Petroleum Geologists Bull.*, v. 53, no. 4, p. 830–840.
- Lerch, Otto, 1891, Remarks on the geology of the Concho country, State of Texas: *Am. Geologist*, v. 7, no. 2, p. 73–77.
- Livingstone, D. A., 1963, Data of geochemistry, chemical composition of rivers and lakes: U. S. Geol. Survey Prof. Paper 440-G, 64 p.
- Lloyd, A. M., and Thompson, W. C., 1929, Correlation of Permian outcrops on eastern side of the West Texas basin: *Am. Assoc. Petroleum Geologists Bull.*, v. 13, no. 8, p. 945–956.
- Lockwood, R. P., 1972, Geochemistry and petrology of some Oklahoma redbed

- copper occurrences: Oklahoma Univ., Ph.D. dissert., 58 p.
- Lougheed, M. S., and Mancuso, J. J., 1973, Hematite framboids in the Negaunee Iron Formation, Michigan: evidence for their biogenic origin: *Econ. Geology*, v. 68, no. 2, p. 202–209.
- Love, L. G., 1962, Biogenic primary sulfide of the Permian Kupferschiefer and marl slate: *Econ. Geology*, v. 57, no. 3, p. 350–366.
- _____, 1971, Early diagenetic polyframboidal pyrite, primary and redeposited, from the Wenlockian Denbigh Grit Group, Conway, North Wales, U. K.: *Jour. Sed. Petrology*, v. 41, no. 4, p. 1038–1044.
- Lowell, J. D., 1970, Copper resources in 1970: *Mining Eng.*, v. 22, no. 4, p. 67–73.
- Lucia, F. C., 1972, Recognition of evaporite-carbonate shoreline sedimentation, *in* Rigby, J. K., and Hamblin, W. K., eds., *Recognition of ancient sedimentary environments: Soc. Econ. Paleontologists and Mineralogists Spec. Pub. 16*, p. 160–191.
- Manheim, F. T., 1970, The diffusion of ions in unconsolidated sediments: *Earth and Planetary Sci. Letters*, v. 9, p. 307–309.
- Marcy, R. B., 1854, Exploration of the Red River of Louisiana in 1852: *Exec. Doc.*, 33rd Cong., 1st sess., p. 391–393.
- Martin, D. F., Doig, M. T., III, and Pierce, R. H., Jr., 1971, Distribution of naturally occurring chelators (humic acids) and selected trace metals in some west coast Florida streams, 1968–1969: Florida Dept. Nat. Resources, Univ. South Florida, Prof. Paper Series 12, 52 p.
- Miller, A. K., and Furnish, W. M., 1940, Permian ammonoids of the Guadalupe Mountain region and adjacent areas: *Geol. Soc. America Spec. Paper 26*, 242 p.
- Morgan, J. P., Van Lopik, J. R., and Nichols, L. G., 1953, Occurrence and development of mudflats along the western Louisiana coast: Baton Rouge, Louisiana State Univ. Coastal Studies Inst. Tech. Rept. 2, 34 p.
- Nobel, E. A., 1963, Formation of ore deposits by water of compaction: *Econ. Geology*, v. 58, no. 7, p. 1145–1156.
- Olson, E. C., 1956, Fauna of the Vale and Choza: part 13, *Diadectes*, *Xenacanthus*, and specimens of uncertain affinities: *Fieldiana Geology*, v. 10, no. 27, p. 329–334.
- _____, 1962, Late Permian terrestrial vertebrates, U. S. A. and U. S. S. R.: *Am. Philos. Soc. Trans., New Series*, v. 52, pt. 2, 224 p.
- _____, and Beerbower, J. R., 1953, The San Angelo Formation, Permian of Texas, and its vertebrates: *Jour. Geology*, v. 61, no. 5, p. 389–423.
- Oriel, S. S., Myers, D. A., and Crosby, E. J., 1967, West Texas Permian basin region, *in* McKee, E. D., Oriel, S. S., and others, *Paleotectonic investigations of the Permian System in the United States: U. S. Geol. Survey Prof. Paper 515*, p. 21–60.
- Phillips, L. C., 1917a(?), The copper beds of Knox County: Univ. Texas, Austin, Bur. Econ. Geology open-file rept., 14 p.
- _____, 1917b(?), Report on the property of the Foard County Copper Company: Univ. Texas, Austin, Bur. Econ. Geology open-file rept., 6 p.
- Purdy, E. G., 1963, Recent calcium carbonate facies of the Great Bahama bank, part 2, sedimentary facies: *Jour. Geology*, v. 71, no. 4, p. 472–497.
- Ramberg, Hans, 1952, The origin of metamorphic and metasomatic rocks: Chicago, Univ. Chicago Press, 317 p.
- Ramdohr, Paul, 1969, The ore minerals and their intergrowths: Oxford, Pergamon Press, 1174 p.
- Rashid, M. A., and Leonard, J. D., 1973, Modifications in the solubility and precipitation behavior of various metals as a result of their interaction with sedimentary humic acid: *Chem. Geology*, v. 11, no. 2, p. 89–97.
- Reineck, H. E., 1967, Layered sediments of tidal flats, beaches, and shelf bottoms of the North Sea, *in* Lauff, G. H., ed., *Estuaries: Am. Assoc. Adv. Sci., Pub. 83*, p. 191–205.
- _____, 1972, Tidal flats, *in* Rigby, J. K., and Hamblin, W. K., eds., *Recognition of ancient sedimentary environments: Soc. Econ. Paleontologists and Mineralogists Spec. Pub. 16*, p. 146–159.
- _____, and Singh, I. B., 1967, Primary sedimentary structures in the recent sediments of the Jade, North Sea: *Marine Geology*, v. 5, p. 227–235.
- Renfro, A. R., 1974, Genesis of evaporite associated stratiform metalliferous deposits—a sabkha process: *Econ. Geology*, v. 69, no. 1, p. 33–45.

- Rickard, D. T., 1970, The chemistry of copper in natural aqueous solutions: *Stockholm Contributions in Geology*, v. 23, no. 1, 64 p.
- Roth, Robert, 1945, Permian Pease River group of Texas: *Geol. Soc. America Bull.*, v. 56, no. 10, p. 893–908.
- Russell, R. J., and McIntire, W. G., 1966, Australian tidal flats: Baton Rouge, Louisiana State Univ. Press, Coastal Studies Series No. 12, 48 p.
- Rust, G. W., 1935, Colloidal primary copper ores at Cornwall mines, southeastern Missouri: *Jour. Geology*, v. 43, no. 4, p. 398–426.
- Scales, B. F., 1959, Copper and gypsum deposits of North-Central Texas, in Hamilton, W. C., Jr., ed., *A guide to the Upper Permian and Quaternary of North Central Texas*: North Texas Geological Soc., Field Guide, p. 35–38.
- Schlanger, S. O., 1965, Dolomite-evaporite relations on Pacific Islands: *Tohoku Univ., Sci. Rept.*, 2d ser., v. 37, no. 1, p. 15–29.
- Schmitz, E. J., 1897, Copper-ores in the Permian of Texas: *Am. Inst. Mining Engineers Trans.*, v. 26, p. 97–108.
- Scruton, P. C., 1960, Delta building and the deltaic sequence, in Shepard, F. P., Phleger, F. B., and van Andel, T. H., eds., *Recent sediments, northwest Gulf of Mexico*: La Jolla, California Univ., Scripps Inst. Oceanography, p. 82–102.
- Sippel, R. F., 1968, Sandstone petrology, evidence from luminescence petrography: *Jour. Sed. Petrology*, v. 38, no. 2, p. 530–554.
- Stricklin, F. L., Jr., 1961, Degradational stream deposits of the Brazos River, Central Texas: *Geol. Soc. America Bull.*, v. 72, no. 1, p. 19–36.
- Stroud, R. B., McMahan, A. B., Stroup, R. K., and Hibpsman, M. H., 1970, Production potential of copper deposits associated with Permian red bed formations in Texas, Oklahoma, and Kansas: *U. S. Bur. Mines Rept. Inv. 7422*, 103 p.
- Swanson, V. E., Love, A. H., and Frost, I. C., 1972, Geochemistry and diagenesis of tidal-marsh sediment, northeastern Gulf of Mexico: *U. S. Geol. Survey Bull.* 1360, 83 p.
- Tarling, D. H., 1973, Metallic ore deposits and continental drift: *Nature*, v. 243, no. 5404, p. 193–196.
- Temple, K. L., and LeRoux, N. W., 1964, Syngeneses of sulfide ores: sulfate-reducing bacteria and copper toxicity: *Econ. Geology*, v. 59, no. 2, p. 271–278.
- Trudinger, P. A., Lambert, I. B., and Skyring, G. W., 1972, Biogenic sulfide ores: a feasibility study: *Econ. Geol.*, v. 67, no. 8, p. 1114–1127.
- van Straaten, L. M. J. U., 1954, Composition and structure of recent marine sediments in the Netherlands: *Leiden, Holland, Leidse Geol. Meded.*, v. 19, p. 1–110.
- , 1961, Sedimentation in tidal flat areas: *Alberta Soc. Petroleum Geologists Jour.*, v. 9, no. 7, p. 203–226.
- , and Kuenen, P. M., 1957, Accumulation of fine grained sediments in the Dutch Wadden Sea: *Geologie en Mijnbouw*, v. 19, no. 7, p. 328–354.
- Vol'fson, F. I., and Arkhangel'skaya, V. V., 1971, The conditions of formation of cupriferous sandstone deposits: *Lithology and Mineral Resources*, v. 7, no. 3, p. 268–279.
- Walper, J. L., and Rowett, C. L., 1972, Plate tectonics and the origin of the Caribbean Sea and the Gulf of Mexico: *Gulf Coast Assoc. Geol. Soc. Trans.*, v. 22, p. 105–116.
- Weast, R. C., 1971, *Handbook of chemistry and physics*: Cleveland, Chem. Rubber Co., 1144 p.
- White, D. E., 1968, Environments of generation of some base-metal ore deposits: *Econ. Geology*, v. 63, no. 4, p. 301–335.
- , Hem, J. D., and Waring, G. A., 1963, Data of geochemistry, chemical composition of subsurface waters: *U. S. Geol. Survey Prof. Paper 440-F*, 67 p.
- Wrather, W. E., 1917, Notes on the Texas Permian: *Southwestern Assoc. Petroleum Geologists Bull.*, v. 1, p. 93–106.

APPENDIX I PETROGRAPHIC DATA

Name of rock specimens examined in thin section including, when applicable, general comments concerning petrographic properties. Letters and numbers in parentheses refer to the identification mark that is scribed on this section.¹ Roman numerals and numbers refer to geologic maps (pls. I-V) and specific locations on the individual maps, respectively.

V-6 (SA-3)	Fine sandstone: calcitic and slightly siliceous, supermature, intraclast-bearing sublitharenite. Reworked overgrowths suggest that the quartz grains were supplied by erosion of previously deposited sedimentary rocks. Rock fragments comprise 19.3% of the framework grains and are equally divided between a phyllite grain metamorphic component and a micaceous siltstone grain sedimentary component. Carbonate intraclasts suggest that shallow ponds or basins with carbonate precipitating in them were present on the deltaic plain.	I-14 (SA-6)	Fine sandstone: siliceous and slightly calcareous, supermature, mud-chip-bearing sublitharenite. Thin section is almost a quartzarenite. This thin section and the previous seven came from the distributary channel-fill facies.
V-10 (SA-4)	Slightly conglomeratic fine sandstone: calcitic and siliceous, submature, intraclast-bearing sublitharenite.	III-12 (SA-2)	Very fine sandstone: slightly siliceous, supermature quartzarenite. Three illitic clay laminae less than one-half millimeter thick are present in the field of the thin section. Sandstone is almost fine sized.
V-17 (ST-2)	Fine sandstone: calcareous and hematitic, supermature, intraclast-bearing quartzarenite.	III-11 (Kn-60.1)	Fine sandstone: slightly siliceous, supermature, mud-clast-bearing quartzarenite. Mud clasts suggest breakup of clay laminae by tidal currents, and entrapment of the clasts before they could be eroded.
IV-8 (ST-33.4)	Fine sandstone: calcareous and hematitic, supermature, intraclast-bearing sublitharenite. In contrast to sample V-6 which was almost a litharenite, this sample is almost a quartzarenite. Clasts are very hematitic, and some may be mud chips whereas others are carbonate intraclasts.	III-11 (Kn-60.2)	Very fine sandstone: slightly siliceous, supermature quartzarenite. Sample Kn-60.2 was collected from the top 1 foot of an approximately 7-foot-thick sequence of thin- to medium-bedded sandstone, whereas Kn-60.1 was collected from the bottom half of the sandstone interval. This thin section and the previous two came from the tidal sandflat facies of the Buzzard Peak system.
IV-10 (ST-35.5)	Very fine sandstone: calcareous, supermature, mud-chip-bearing quartzarenite. Mud chips are highly saturated with hematite.	IV-1 (SA-1)	Fine sandstone: gypsiferous, supermature quartzarenite. Thin section exhibits gypsum seams and segregations of zircon grains along individual laminae. Sandstone is almost fine sized.
I-2 (SA-5)	Fine sandstone: calcitic, supermature, mud-chip-bearing sublitharenite.	III-4 (Kn-46F)	Fine sandstone: slightly siliceous, supermature quartzarenite.
I-12 (Hr-1)	Fine sandstone: calcitic and siliceous, supermature, mud-chip-bearing quartzarenite. Thin section contains 2% siltstone sedimentary rock fragments and 1% feldspar.	III-7 (Kn-6F)	Fine sandstone: calcareous, supermature, intraclast-bearing quartzarenite. Thin section consists of interbedded layers of sand grains with carbonate clasts, and layers of micrite mud containing carbonate clasts.
¹ Thin sections used in this report are on file at the Bureau of Economic Geology, except for five (designated by asterisk) polished thin sections that are on file in The University of Texas at Austin, Department of Geological Sciences ore microscopy collection.		III-7 (Kn-6L)	Very fine sandstone: siliceous and calcitic, supermature, mud-clast-bearing quartzarenite. Thin section contains clay laminae and mud clasts derived from the clay laminae.

I-9 (Fo-5)	Very fine sandstone: gypsiferous, supermature, mud-clast-bearing quartzarenite.	I-6 (St-55)	Calcitic, illitic, slightly silty, malachite- and chalcocite-bearing, algally laminated clay-shale. Thin section contains framboid and polyframboidal mineralized spherules.
IV-1 (Ki-10)	Very fine sandstone: siliceous, supermature, mud-clast- and malachite-bearing quartzarenite. Sandstone exhibits alternating laminae of fine and very fine sand grain sizes, with the very fine size predominating. Individual flaser clay laminae are present in the thin section, and copper mineralization is predominantly confined to the clay flasers and the area surrounding the clay flasers.	Creta mine ore (EP-10)	Weakly siliceous, illitic, chalcocite-bearing claystone.
Unknown (Ki-16)	Very fine sandstone: gypsiferous, supermature, mud-clast-bearing quartzarenite. Individual flaser clay laminae and mud clasts derived from them are present in the section. This section and the previous six came from the tidal channel-fill facies. The gypsiferous-cemented thin sections came from tidal channel-fill facies in the Cedar Mountain system and at the base of the Buzzard Peak system, and the siliceous-cemented thin sections came from tidal channel-fill facies that were continuous with tidal sandflat facies.	I-8 (Hr-33c)	Dolomitic, algally bound, malachite-bearing biolithite. Mahogany-colored organic staining is present as a coating associated with many of the algal crenulations.
V-12 (St-53.3)	Fine sandstone: calcitic, supermature, intraclast-bearing quartzarenite.	III-10 (Ki-16)	Dolomitic, intraclast-bearing, algal biolithite (bottom quarter of slide); and dolomitic, poorly washed, malachite-bearing intrasparite (remainder of slide). Copper mineralization was precipitated in the pore space between intraclasts. Some malachite was present in the algally bound portion of the slide. Part of the intrasparite portion of the thin section exhibits evidence of being algally bound.
I-19 (Hr-56A)	Fine sandstone: calcareous and slightly siliceous, submature, mud-clast-bearing sublitharenite. Thin section contains 13% phyllite rock fragments and 3% siltstone rock fragments. This thin section and the previous one came from the delta-front facies of the Old Glory and Copper Breaks systems, respectively.	IV-C (K-11)	Dolomitic, chalcocite-bearing pelmicrite. Thin section is extremely rich in organic matter.
I-22 (Hr-73)	Siltstone: calcareous, immature quartzarenite. Rock sample is mottled red and gray.	III-5 (Kn-20)	Dolomitic, intraclast- and malachite-bearing, algal biolithite; and dolomitic intramicrite. Thin section contains less than 10% silt-size quartz grains.
IV-10 (St-35.3)	Fine sandstone: calcareous, immature, mud-clast-bearing, silty quartzarenite. Rock sample is primarily moderately reddish brown with minor gray mottling.	I-6 (Hr-10)*	Dolomitic, chalcocite-bearing, algal biolithite; dolomicrite; and dolomitic, chalcocite-bearing oosparite. Some of the oolites have organic nuclei.
I-5 (Hr-25s)	Siliceous, illitic, quartzarenite, very silty mudstone. This section and the previous two came from the delta-plain facies of the Old Glory and Copper Breaks systems.	I-6 (Hr-7a)*	Dolomitic, chalcocite-bearing oosparite; and dolomitic, chalcocite- and intraclast-bearing, algal biolithite. Many of the oolites contain organic nuclei with chalcocite replacing the organic matter.
I-3 (Hr-36a)	Calcitic, illitic, slightly silty claystone. Thin section contains about 5% silt-size quartz grains, and is a red claystone from the bottom part of the prodelta facies which becomes sandier vertically.	II-8 (Fo-TM)	Dolomitic, intraclast-bearing pelmicrite; dolomitic, pellet-bearing, algal biolithite; and gypsum being replaced by medium crystalline dolomite. Malachite and chalcocite is present at the contact between the algal biolithite and the replaced gypsum. The gypsum appears to have formed after the algal biolithite, and individual laths of superposed gypsum crystalized into the biolithite. Later, most of the gypsum was replaced by dolomite. This section and the previous nine (excluding Creta ore sample) came from algal mat facies of the Cedar Mountain system.

II-8
(Fo-33.1)

Clayey gypsum.

the abandoned Goldberg mine at III-F.

III-15
(FP-A)*

Copper nodule containing chalcocite, malachite, covellite, pyrite, quartz grains, and carbonaceous matter.

Nodule was collected from a pile of nodules near the intersection of the fence line and dirt road near III-15. It may have come from

III-15
(FP-B)*

Copper nodule containing chalcocite and minor covellite.

Collected from same location as previous nodule.

III-7
(FP-C)*

Chalcocite- and malachite-impregnated sandstone.

Petrographic properties of fluvial-deltaic and tidal-flat facies. Numbers indicate the percentage of the total number of samples in each facies (column) that exhibit the particular property (row). Because some samples may exhibit several properties (e.g. both calcareous and siliceous cement), column totals may not equal 100 percent.

PETROGRAPHIC PROPERTIES		Fluvial-deltaic systems: Facies					Tidal-flat systems: Facies		
		Copper Breaks distributary	Old Glory distributary	Delta plain	Delta front	Prodelta	Tidal sandflat	Tidal channel	Algal mat
Color	10-R (reddish values)	100	100	67	50	100			
	N8-N6 (gray values)			100	50			83	100
	10YR-N9 (white, very pale orange)						100	17	
Cement	Calcareous	100	80	67	100	100		17	
	Gypsum							50	
	Siliceous	75	60	33	50		100	50	
Grain size	Clay			33		100			14
	Silt			100					
	Very fine sand		20	33			67	67	
	Fine sand	100	60	33	100		33	33	
	Gravel and sand		20						
Sorting	Well	67	80		50		100	100	
	Moderate	33			50				
	Poor, very poor		20	100		100			
Mineralogy	Quartzarenite	33	40	33	50		100	100	
	Sublitharenite	67	60		50				
	Siltstone			33					
	Mudstone and shale			33		100			14
	Dolomitic algal biolithite								67
	Intraclast- and oolite-bearing dolomite								50
Total number of samples		3	5	3	2	1	3	6	6

APPENDIX II
SIGNIFICANT COPPER MINES AND PROSPECTS IN THE SAN ANGELO FORMATION

LOCATION	NAME	PRESENT CONDITION*
III-A	Pyron (Craig Ranch)	Partially filled adit at stock tank.
V-B	Copper Queen	Adits collapsed, abandoned cables.
IV-C	Brazos-Wichita	Scattered pieces of copper-impregnated organic matter and nodules present.
IV-D	Aard Copper, Inc. (Farris Prospect)	Partially filled adit, copper-bearing sandstone common. Crusher nearby.
IV-E	Hugh-Rogers (Smelter Canyon or Kiowa Peak)	Mine not visited (approximate location).
III-F	Smelter Mine (Pyron Prospect)	Mine car rails, smelter, and other equipment present. Adit collapsed.
I-G	McClellan	Numerous pieces of organic matter replaced by copper. Mill and smelter equipment present.
I-H	Gibbs	Scattered pieces of copper-impregnated organic matter.
IV-I	Buzzard Peak	Mine not visited (approximate location).
III-J	McFaddin	Mine not visited (approximate location).

* Additional information on periods of operation and copper production can be found in Stroud and others (1970, p. 37).

APPENDIX III
OUTCROP COPPER SAMPLES: U. S. BUREAU OF MINES AND THIS REPORT *

MAP LOCATION	USBM NO.	THICKNESS (INCHES)	COPPER (%)	LITHOLOGY	STRATIGRAPHIC LOCATION AND/OR FACIES
I-6	—	1.25	.5	Gray shale	Top of Cedar Mountain system,
I-6	—	.do.	4.4	.do.	algal mat facies. First 13
I-6	—	.do.	.62	.do.	samples from location I-6
I-6	—	1.75	.50	.do.	represent a channel sample
I-6	—	.do.	.55	.do.	from top to bottom of channel
I-6	—	1.50	.30	.do.	sample. Samples 2 through 5
I-6	—	2.50	.3	.do.	determined colorimetrically.
I-6	—	3.75	.3	.do.	Other samples determined
I-6	—	.do.	.1	.do.	spectrographically.
I-6	—	.do.	.05	.do.	
I-6	—	2.50	.004	Gray & red shale	
I-6	—	3.75	.009	.do.	
I-6	—	7.5	.005	Red shale	
I-7	—	4.0	.003	Gray shale	Cedar Mountain system.
I-8	—	2.0	.2	.do.	Top of Cedar Mountain system.
I-8	—	.do.	.06	.do.	From under previous sample.
I-9	—	7.0	.14	Shale & sandstone	Cedar Mountain system, tidal
					channel-fill facies.
I-17	—	9.0	.4	Muddy sandstone	.do.
I-17	—	.do.	.3	.do.	.do.
I-20	—	6.0	.14	Sandy mudstone	Base of Copper Breaks system.
I-6	—	.do.	.03	Gray shale	Base of Blaine system, above
I-6	—	12.0	.02	.do.	basal gypsum bed. Bottom of
					upper copper zone.
I-13	—	2.0	.2	Muddy sandstone	Base of Buzzard Peak system.
I-30	RAF-87	8.0	.09	Shale & dolomite	Top of Cedar Mountain system,
					algal mat facies.
I-30	RAF-88	6.0	.05	Shale	.do.
I-31	RAF-90	.do.	.33	Shale & mudstone	.do.
I-32	RAF-91	5.0	.04	.do.	.do.
I-33	RAF-92	8.0	.13	Limestone & mudstone	.do.
I-34	RAF-62	.do.	3.65	Shale	.do.
I-35	RAF-59	7.0	.80	.do.	.do.
I-36	RAF-60	6.0	2.75	.do.	.do.
I-37	RAF-58	18.0	.50	.do.	.do.
I-38	RAF-48	10.0	.17	.do.	.do.
I-39	RAF-55	8.0	1.25	.do.	.do.
I-40	RAF-56	22.0	.80	.do.	.do.
I-41	RAF-5	10.0	.18	.do.	.do.
I-42	RAF-1	6.0	.90	.do.	.do.
I-43	—	2.0	.01	Gray shale	Blaine system, 4 to 6 inches
					above basal gypsum. Upper copper
					zone.
I-43	—	3.75	.70	.do.	Top of Cedar Mountain system,
					algal mat facies.

* Bureau of Mines data from Stroud and others (1970).

I-51	—	1.0	.20	Gray shale	Top of Cedar Mountain system, algal mat facies.
III-5	RAF-37	4.0	1.60	Dolomite	.do.
III-7	—	.do.	.25	Gray shale	Base of Buzzard Peak system.
III-10	—	2.5	3.3	.do.	Base of Blaine system, algal mat facies. Poorly developed basal gypsum with a well-developed algal dolomite at this location.
III-10	—	.do.	3.7	.do.	Interfingering of Cedar Mountain and Blaine systems. Colorimetric data.
III-10	—	.do.	3.8	.do.	
III-A	—	1.0	.004	Sandy mudstone	Base of Blaine system
III-14	—	2.0	3.0	Sandstone	Base of Buzzard Peak system.
III-29	RAF-68	8.0	.55	Shale	Top of Cedar Mountain system algal mat facies.
III-30	RAF-24	10.0	.33	.do.	.do.
IV-2	—	—	.10	Gray shale	Near top of Cedar Mountain system.
IV-9	—	—	.16	Woody material	Cedar Mountain system, tidal channel-fill facies.
V-1	—	5.0	.48	Gray shale	Top of Cedar Mountain system, algal mat facies.
V-3	—	—	1.7	Sandstone	Cedar Mountain system, tidal channel-fill facies.
V-4	—	—	2.2	Gray shale	Top of Cedar Mountain system, algal mat facies.
V-4	—	1.5	2.8	.do.	Top of Cedar Mountain system, algal mat facies. The last five samples are from a channel sample taken in the algal mat facies and are listed from the top of the channel sample to the bottom. Copper was determined colorimetrically.
V-4	—	.do.	3.8	.do.	
V-4	—	.do.	1.3	.do.	
V-4	—	.do.	2.6	.do.	
V-4	—	1.5	.55	.do.	

APPENDIX IV TRACE ELEMENT ANALYSES

MAP LOCATION	TRACE ELEMENT		THICKNESS (INCHES)	LITHOLOGY	STRATIGRAPHIC LOCATION AND/OR FACIES
	AG	NI			
V-4	5.0 ppm	50 ppm	1.5	Gray shale	Top of Cedar Mountain system, algal mat facies. These five samples are from a channel sample, top to bottom.
V-4	4.6 ppm	55 ppm	.do.	.do.	
V-4	3.6 ppm	55 ppm	.do.	.do.	
V-4	1.6 ppm	55 ppm	.do.	.do.	
V-4	1.0 ppm	40 ppm	.do.	.do.	

Forty-one samples were analyzed semiquantitatively for Ti, Ga, Al, As, Mn, Cr, Zn, Pb, Au, Nb, La, Y, U, and B. Trace amounts of Al, Ti, B, Cr, Mn, Co, Ga, and Ag were noted in most samples although no exact figures were obtained. Iron averaged about 0.7% in all of the samples analyzed by semiquantitative spectrographic analysis, with a range of from .3 to 2% iron.

APPENDIX V
SUMMARY OF U. S. BUREAU OF MINES DRILL HOLE DATA¹

MAP LOCATION	USBM NO.	DEPTH (FEET)	ANALYSIS (COPPER %) ²	STRATIGRAPHIC LOCATION AND/OR FACIES
I-23	E-1	42.9 - 43.5	.42 (avg)	Top of Cedar Mountain system, algal mat facies.
		43.5 - 43.8	1.50	
		43.8 - 44.1	.27	
		49.3 - 49.8	.04	
I-24	E-2	—	No copper	—
I-25	E-3	58.8 - 59.7	.03 (avg)	Top of Cedar Mountain system, algal mat facies.
I-26	E-4	64.6 - 64.8	.16	.do.
		64.8 - 65.1	.65	
		65.1 - 65.4	.40	
		65.4 - 65.7	.16	
I-27	E-5	43.4 - 43.7	.82	.do.
		43.7 - 44.1	.07	
		49.5 - 49.8	.20	
I-28	E-6	38.0 - 38.3	.14	.do.
		38.3 - 38.6	1.25	
		38.6 - 38.9	.65	
I-29	E-7	47.3 - 47.9	.11 (avg)	.do.
		47.9 - 48.2	.36	
III-2	D-1	—	No copper	—
III-3	D-2	—	.do.	—
III-23	A-5	—	.do.	—
III-24	A-8	54.0 - 54.6	.09 (avg)	Top of Cedar Mountain system, algal mat facies.
		54.6 - 55.7	< .01	
III-25	A-9	140.0 - 140.9	7.01	Base of Buzzard Peak system.
III-26	C-10	32.8 - 33.8	.08 (avg)	.do.
		33.8 - 34.1	.50	
		34.1 - 34.4	.04	
III-27	C-7	—	No copper	—
III-28	C-11	—	.do.	—
IV-13	C-9	59.9 - 60.5	.24 (avg)	Base of Buzzard Peak system.
IV-14	C-6	44.7 - 45.0	.03	.do.
		45.3 - 45.6	.23	
		45.6 - 45.9	.04	

¹Modified from Stroud and others (1970).

²Copper values deviating less than .10% were averaged together and are indicated as: (avg).

IV-15	C-8	24.5 - 25.0 25.0 - 25.3 25.3 - 25.6	.16 .58	Base of Buzzard Peak system.
IV-16	A-6	40.3 - 40.6 40.6 - 40.9 70.0 - 72.6 170.5 - 171.0 171.0 - 171.5	.15 < .01 < .01 (avg) .16 .05	40.3-72.6; Cedar Mountain system, facies unknown. 170.5-171.5; base of Buzzard Peak system.
IV-17	A-7	97.0 - 99.0	< .01	Cedar Mountain system, facies unknown (tidal channel-fill ?).
IV-18	A-3	97.0 - 97.6	.02	Top of Cedar Mountain system, algal mat facies.
IV-19	A-4	55.0 - 58.0	.02	.do.
IV-20	A-4A	55.0 - 55.5 55.5 - 56.0 56.0 - 56.5 56.5 - 57.0 57.0 - 57.5 57.5 - 58.0 58.0 - 60.0 60.0 - 60.3 77.0 - 78.4 164.6 - 164.9 164.9 - 165.0	.74 .98 .48 .84 .55 .42 .48 (avg) .09 < .01 (avg) < .01 .21	55.0-60.3; top of Cedar Mountain system, algal mat facies (coring may have spread out the zone). 77.0-78.4; Cedar Mountain system, swash-zone facies (?). 164.6-165.0; base of Buzzard Peak system.
IV-21	C-4	62.4 - 63.0	.05 (avg)	Base of Buzzard Peak system.
IV-22	C-14	23.5 - 24.3 24.3 - 24.6 24.6 - 24.9	.08 (avg) .40 .04	.do.
IV-23	B-3	39.8 - 40.9 163.9 - 164.4 164.4 - 164.7	.09 .06 (avg) .70	39.8-40.9; top of Cedar Mountain system, unknown facies. 163.9-174.7; base of Buzzard Peak system.
IV-24	C-3	74.4 - 74.7 74.7 - 75.0	.59 .05	Base of Buzzard Peak system.
IV-25	B-2	—	No copper	—
IV-26	B-1	26.8 - 30.1 30.1 - 30.6 30.6 - 33.6	.03 (avg) .22 .11 (avg)	Top of Cedar Mountain system, algal mat facies.
IV-27	A-1	—	No copper	—
IV-28	C-15	48.5 - 49.7 49.7 - 50.0	.10 (avg) .28	Base of Buzzard Peak system.
IV-34	C-12B	—	No copper	—
IV-35	C-5	—	.do.	—
IV-36	A-2	—	.do.	—

APPENDIX VI SYNOPSIS OF MEASURED SECTIONS

<p>I-2 Section begins in Choza Formation and continues into the Duncan Member of the San Angelo Formation. A thin veneer (4.3 feet) of Buzzard Peak system facies is overlain by a progradational facies tract of deltaic facies (41 feet) of the Copper Breaks system. Prodelta, delta front - distributary mouth bar, and distributary channel facies are well exposed. Sedimentary load structures are common at the top of the section.</p>	<p>53.0 feet</p>	<p>I-46 Composite section of the total San Angelo Formation. Section begins at base of Buzzard Peak system and continues upwards through Copper Breaks and Cedar Mountain systems. Section is capped by a 4.2-foot-thick gypsum bed at the base of the Blaine system. Distributary channel sandstone lenses are well exposed along the section. <i>Ophiomorpha</i>-like burrows are present towards the top of the Copper Breaks system. Malachite-bearing algal mat facies are exposed at the base of the gypsum bed.</p>	<p>114.6 feet</p>
<p>I-9 Section begins in the Flowerpot Member of the San Angelo Formation and extends upwards to the first nodular gypsum bed (1.8 feet thick) of the sabkha and tidal-flat system of the Blaine Formation. Flakes of malachite that have weathered from algal mat facies shale are present near the base of the section.</p>	<p>49.9 feet</p>	<p>I-47 Section comprised of top of Cedar Mountain system and basal part of Blaine system.</p>	<p>63.0 feet</p>
<p>I-15 Section begins in tidal channel facies of the Buzzard Peak system and continues upward into thick deltaic facies sandstone and siltstone.</p>	<p>53.2 feet</p>	<p>I-48 Measured section of Choza Formation and Buzzard Peak and Copper Breaks systems of the San Angelo Formation. Isolated gypsum nodules and thin layers of gypsum nodules are found in the Choza.</p>	<p>72.0 feet</p>
<p>I-16 Exposure of Cedar Mountain mud-rich tidal-flat system (Flowerpot Member) mudflat facies. Section is capped by a 4-foot-thick sandstone of the tidal channel facies.</p>	<p>23.5 feet</p>	<p>I-49 Exposure of Cedar Mountain system facies with malachite weathering from the base of swash-zone facies sandstone.</p>	<p>35.3 feet</p>
<p>I-18 Section begins in the Choza Formation and continues upwards through facies of the Buzzard Peak and Copper Breaks systems. Copper mineralization is present at the base of flaser-bedded tidal channel facies of the Buzzard Peak system.</p>	<p>66.6 feet</p>	<p>II-1 Upper part of the Choza Formation overlain conformably by 56 feet of interbedded sandstone and mudstone layers. Section is capped by red mudstone of the Cedar Mountain system.</p>	<p>102.3 feet</p>
<p>I-19 Exposure of Copper Breaks deltaic system underlain by thin Buzzard Peak system facies.</p>	<p>68.1 feet</p>	<p>II-2 Section of upper part of Buzzard Peak system and lower part of Cedar Mountain system.</p>	<p>63.1 feet</p>
<p>I-20 Section begins in Choza Formation and continues upward through facies of the Buzzard Peak and Copper Breaks systems with traces of malachite at the base of tidal channel and delta-front sandstone facies. Sedimentary load features and burrowing are present in the distributary channel and delta-plain facies.</p>	<p>64.8 feet</p>	<p>II-3 Exposure of Cedar Mountain system with barite nodules weathering from the outcrop.</p>	<p>31.4 feet</p>
<p>I-21 Measured section starts in mudstone of the Flowerpot Member (Cedar Mountain mud-rich tidal-flat system) and includes 94 feet of the Blaine system. Numerous nodular gypsum layers and thin dolomite layers are present.</p>	<p>129.6 feet</p>	<p>II-5 Measured section of Choza Formation capped by 8 feet of Buzzard Peak system tidal sandflat facies. Sandstone of the sandflat facies is horizontal and flaser bedded and changes laterally into trough-bedded tidal channel facies. Malachite is present at the base of the sandstone bed. The Choza exhibits selenite seams, gray-green reduction spots, gypsum nodules, and ripple-bedded siltstone.</p>	<p>52.5 feet</p>
<p>I-45 Exposure of delta front - distributary mouth bar facies overlain and dissected by distributary mouth bar facies of the Copper Breaks system.</p>	<p>30.0 feet</p>	<p>II-7 Measured section in Buzzard Peak system facies.</p>	<p>27.8 feet</p>
		<p>II-9 Section begins in the Choza and grades transitionally into Buzzard Peak system facies. Flaser-bedded gray sandstone of the tidal channel facies at the base of the Buzzard Peak sequence is followed upward by sandy mudstone and sandstone of the sandflat facies.</p>	<p>66.6 feet</p>

- II-10 50.6 feet
Measured section of Choza capped by Buzzard Peak system facies.
- II-11 17.4 feet
Section begins at base of Buzzard Peak system. Interbedded sandstone and sandy mudstone layers are well exposed in this section with flaser bedding the predominant bedding type; nearby, low-angle trough bedding, representing tidal channel-fill facies, predominates.
- II-12 69.1 feet
Section begins in the Choza which is overlain conformably by Buzzard Peak system sandflat facies. Horizontal bedding, alternating with burrowed silty sandstone, is exhibited at this locality.
- II-13 50.2 feet
Section begins in Choza and is capped by Buzzard Peak system facies.
- III-1 206.2 feet
Measured section includes the upper part of the Choza Formation, Buzzard Peak and Cedar Mountain systems, and the basal part of the Blaine system. At the top of the section, a 3-inch dolomite bed contains traces of malachite.
- III-4 56.9 feet
Section of upper Choza Formation capped by 10.5 feet of trough-bedded sandstone of the Buzzard Peak system.
- III-6 167.0 feet
Measured section starts in the Choza and includes a complete San Angelo Formation section (96.4 feet of Buzzard Peak and Cedar Mountain system deposits). Malachite was found in sandy mudstone at the base of the Buzzard Peak system, at the base of Cedar Mountain system tidal channel facies, and in Blaine system dolomite at the top of the section.
- III-8 134.6 feet
Section from top of Choza Formation to lower part of Blaine Formation.
- III-9 170.5 feet
Section from top of Choza to base of Blaine system. Middle tidal channel-fill segment at the base of the Buzzard Peak system is 8 feet thick.
- III-12 103.0 feet
Composite section begins in red mudstone and siltstone of the Choza Formation and is capped by 21.5 feet of sandstone of the Buzzard Peak system with a trace of malachite at the base of the section.
- III-17 77.6 feet
Section from top of Choza Formation through the lower half of the Buzzard Peak system.
- III-18 51.0 feet
Section from top of Choza Formation to near the top of the Buzzard Peak system. Malachite is present at the base of the Buzzard Peak system in tidal channel-fill facies.
- III-19 87.9 feet
Section includes Cedar Mountain and Blaine system facies. Malachite staining is found on sandstone fragments weathering from swash-zone facies.
- III-21 36.8 feet
Section starts at top of Cedar Mountain system and includes the lower part of the Blaine system. Malachite-bearing dolomite at the top of the Cedar Mountain system is a foot thick at this locality.
- III-22 53.7 feet
Section from top of Choza through Buzzard Peak system. Sandstone of the tidal sandflat facies is horizontally bedded with current lineations on bedding-plain surfaces.
- III-31 91.0 feet
Section from upper part of Choza Formation, through the Buzzard Peak system, and into the lower part of the Cedar Mountain system.
- IV-1 59.5 feet
Top of Choza Formation and base of Buzzard Peak system included in measured section. Malachite is disseminated in sandstone of tidal channel-fill facies at the base of the Buzzard Peak system.
- IV-2 59.3 feet
Section from near top of Cedar Mountain system through basal part of Blaine system. Malachite was found weathering from shale at base of section.
- IV-3 59.8 feet
Measured section of upper part of Cedar Mountain system and lower part of Blaine system. 14-inch-thick malachite-bearing zone is present approximately 23 feet from base of section.
- IV-6 80.9 feet
Section of Cedar Mountain and Blaine system facies. Malachite associated with flaser-bedded tidal channel-fill facies.
- IV-7 51.6 feet
Section of Old Glory fluvial-deltaic system sandstone and siltstone.
- IV-8 132.4 feet
Section from base of Old Glory system, through Cedar Mountain system, and into lower part of Blaine system.
- IV-10 102.0 feet
Measured section includes a complete Duncan Member sequence with copper at its base. Well-developed delta-plain facies sandy mudstone of Old Glory system is exhibited.

- IV-11 49.2 feet
Section of upper part of Cedar Mountain system with minor amount of malachite associated with tidal channel facies. Top 20 feet of the section is in the Blaine system.
- IV-12 51.4 feet
Upper part of Choza system and lower 29 feet of Buzzard Peak system. Tidal channel-fill and tidal sandflat facies of Buzzard Peak system are well developed.
- IV-37 50.6 feet
Mudstone and siltstone beds of Cedar Mountain system are present in this section.
- IV-38 51.3 feet
Section of upper Choza Formation and Buzzard Peak system.
- IV-39 56.0 feet
Section starts at top of Choza and includes most of Buzzard Peak system. Malachite is noted in sandstone at the base of Buzzard Peak system.
- IV-40 83.2 feet
Section begins in Choza and includes a complete Buzzard Peak system section consisting of interbedded mudstone and sandstone beds. Malachite is present at the base of the Buzzard Peak system associated with tidal channel-fill facies.
- IV-41 103.5 feet
Old Glory system distributary channel facies, consisting predominantly of trough-bedded sandstone, and delta-plain siltstone and mudstone exhibited in this section. Upper part of section includes facies of Cedar Mountain system.
- V-2 44.3 feet
Section includes sandy mudstone and lenticular channel-fill sandstone bodies of Cedar Mountain system capped by 12 feet of Blaine system.
- V-3 52.6 feet
Measured section of upper part of Cedar Mountain system and lower part of Blaine system. Copper is present as malachite in the base of an 8-foot-thick tidal channel-fill and as chalcocite and malachite in a 2-inch-thick dolomite.
- V-5 36.0 feet
Eight inches of malachite-bearing algal mat facies shale in upper part of the Cedar Mountain system exhibited in measured section.
- V-6 79.8 feet
Upper part of Choza Formation and lower 12.5 feet of the Old Glory system exhibited in section. Quartz pebbles are present in the sandstone. Merkle Dolomite is 8 feet below base of San Angelo Formation at this locality.
- V-7 52.2 feet
Section of upper Choza and the lower part of Old Glory system with sandstone lying on top of the Merkle Dolomite.
- V-8 108.2 feet
Measured section consists of upper part of Choza Formation; Merkle Dolomite is 3 feet thick and caps the section.
- V-9 28.2 feet
Section with upper part of Choza Formation and lower 17 feet of Old Glory system sandstone.
- V-10 45.3 feet
Sandstone with large-scale trough bedding and scattered quartz pebbles exhibited in section. Sandstone of the Old Glory fluvial-deltaic system lies directly on top of the Merkle Dolomite at this locality.
- V-11 63.6 feet
Measured section of total Old Glory system sequence of predominantly trough-bedded sandstone.
- V-17 74.4 feet
Section begins in Choza Formation and continues upward through fluvial-deltaic facies of Old Glory system.

APPENDIX VII LOCALITIES

Each outcrop locality includes representative exposures of facies and other features described in the text. Localities are shown on geologic map (pls. I-V).

I-2

Exposure of Copper Breaks system progradational facies tract. Choza at base followed by gypsum-cemented tidal channel-fill of Buzzard Peak system and a vertical deltaic sequence of prodelta facies, delta-front and distributary mouth bar facies, and distributary channel-fill facies. Exposed up side of canyon at Pease River overlook in Copper Breaks State Park.

I-3

Excellent exposure of distributary channel-fill facies of Copper Breaks system. Low-angle trough bedding in channel-fill overlies 6 feet of prodelta mudstone. Tidal channel-fill facies of Buzzard Peak system is exposed in the creek bottom. Location in drainage of Devils Creek in Copper Breaks State Park. Road leads down close to the exposure. Dams that have been proposed for Devils Creek by the park service may flood this outcrop.

I-4

Exposure of Copper Breaks system distributary channel-fill facies. Exhibits reoccupation of channel-fill by later channel-fill deposit, large-scale trough cross-stratification, horizontal bedding, burrowing, and gypsum nodules imbedded in sandstone. Exposed in drainage of Cottonwood Creek on the Brown ranch. A dirt road leads to the exposure.

I-6

Nodular gypsum, about 4 feet thick, of the Blaine sabkha facies is being undercut by erosion. Immediately under the gypsum is 2 inches of dolomite and approximately 3 inches of gray shale interpreted to represent algal mat facies at the top of the Cedar Mountain system. Malachite and chalcocite are present in the shale and dolomite and in the base of the gypsum. Exposure located at headward limit of erosion of Cottonwood Creek near an old windmill. Copper content exposed on outcrop in this area is variable.

I-8

Thin dolomite of the algal mat facies of the Cedar Mountain system is exposed alongside Highway 283 on the north side of the Pease River. Nodular gypsum capping the dolomite has been removed by dissolution. With careful examination of the dolomite, crenulations caused by algal mat growth can be found. Chalcocite and malachite are exhibited on fresh surfaces of the dolomite.

I-17

A recent prospect pit in a tidal channel fill of the Cedar Mountain system has exposed good copper mineralization on the Johnson-Eckert ranch near the abandoned McClellan mine.

I-18

Mineralization at the base of the San Angelo Formation, in primarily the tidal channel-fill facies of the Buzzard Peak system, is exhibited on the east side of Highway 283 north of the Pease River.

II-4

Excellent exposure of gypsiferous tidal channel-fill facies at the base of the Buzzard Peak system. A number of tidal channel fills are exposed as lenticular bodies characterized by flaser bedding in a 10- to 15-foot interval along the canyon wall. This locality is best viewed from the top of the other side of the canyon in order to see the lenticular shape of the channel fills.

II-11

Buzzard Peak system facies are well exposed in road-cut. Facies include interbedded sandy mudstone and horizontal- and ripple-bedded sandstone of the tidal channel-fill facies which laterally grade into the tidal sandflat facies.

III-11

Excellent exposure of horizontally bedded Buzzard Peak system tidal sandflat facies on the McFarlin ranch.

III-13

Exhumed upper segment of tidal channel-fill facies east of Snake Den Tank near Buzzard Peak.

III-15

Erosion of the surrounding mudflat facies has exhumed sandstone deposits of the upper segment of the tidal channel-fill facies in the Cedar Mountain system. The meandering deposits of the individual channel fill can be walked on for a few hundred feet. Numerous nodules of copper minerals are present near the intersection of the fence line and the dirt road. A load of nodules may have dropped off of an ore wagon coming from the Goldberg mine at III-F. Location is near the Lyles ranch on the McFarlin estate.

III-20

Horizontal-bedded sandstone of the sandflat facies is well exposed north of Highway 82 at this location.

IV-3

Ripple-bedded sandstone of the swash-zone facies and scattered pieces of weathered sandstone containing malachite derived from this facies can be found near this location.

IV-9

Recent copper prospect has exposed lower and middle segments of the tidal channel-fill facies. Copper and woody material are common in the sandy mudstone and muddy sandstone of the lower segment. Prospect is about 50 feet west of the road near Kiowa Peak.

IV-12

Outcrop of Buzzard Peak system facies, including tidal channel-fill and tidal sandflat facies. Copper mineralization is present at the base of the first sandstone bed. Oscillation ripples were present in the talus of the hillslope to the southeast of this location.

IV-5

Exposed at this location is a basal tidal channel fill of the Buzzard Peak system with copper in the sandy shale at the base of the channel fill. Also at this location is a cliff above the Salt Fork of the Brazos River on which is an excellent exposure of over 50 feet of Old Glory system facies.

V-4

Outcrop of calcareous shale and well-laminated shale of the algal mat facies with both lithologies bearing copper mineralization. Copper-bearing shale is exposed at the drainage duct under the dirt road on the Swenson ranch and can be traced throughout the area. A few hundred feet down the stream gully is an excellent exposure of the upper segment of the tidal channel-fill facies. Flaser bedding is the primary bedding type, with about 6 inches of bimodal bedding at the base of the channel fill. Interesting depositional features in the area include polygonal mud cracks with gypsum squeezed between the cracks, thin dolomite layers containing vesicles, and malachite-bearing woody

fragments inferred to have been associated with tidal channel facies.

V-14

Outcrop of calcareous shale, well-laminated shale, and poorly laminated shale of the algal mat facies. A minor amount of malachite was noted, and syneresis cracks were found on the calcareous shale. Erosion has exposed a large surface area of this shale and its white to very light-gray color provides a striking contrast to the surrounding facies. The location is northwest of Old Glory on land owned by G. F. Spitzer of Old Glory.

V-15

Pseudomorphs of copper after pyrite (?) embedded in gypsum are exposed in drainage emptying into the Salt Fork of the Brazos River.

V-16

Excellent exposure of a succession of nodular gypsum beds of the Blaine sabkha facies is dissected by the road leading to the Farris mine north of the Salt Fork of the Brazos River.

V-18

Exposure of a thin dolomite bed inferred to be laterally equivalent to calcareous shale at localities V-14 and V-4. The dolomite exhibits a birdseye (vesicular) texture, with traces of copper present in some of the pore spaces.

V-19

Gypsum of the sabkha facies rests directly on calcareous copper-bearing shale of the algal mat facies at the top of the Cedar Mountain system.

APPENDIX VIII METHODS

Calculations for table 1: Approximate time required to concentrate the required amount of copper from ground water containing .06 ppm copper.

$$.06 \text{ ppm of Cu} = \frac{.06 \text{ mg Cu}}{1000 \text{ g of H}_2\text{O}}$$

$$\frac{6 \times 10^{-2} \text{ mg Cu}}{1 \times 10^3 \text{ ml of H}_2\text{O}} \quad 1 \text{ ml} = 1 \text{ cc}$$

$$\frac{6 \times 10^{-2} \text{ mg Cu}}{1 \times 10^3 \text{ cc}} \quad \frac{6 \times 10^{-5} \text{ mg Cu}}{\text{cm}^3 \text{ H}_2\text{O}}$$

In one year the evaporation is $100 \text{ cm}^3/\text{cm}^2$.

$$(1 \times 10^2 \text{ cm}^3/\text{cm}^2) \frac{(6 \times 10^{-5} \text{ mg Cu})}{\text{cm}^3}$$

In one year = $6 \times 10^{-3} \text{ mg Cu}$, or in one year $6 \times 10^{-6} \text{ g Cu}$.

Therefore, in one year $6 \times 10^{-3} \text{ mg}$ of Cu will be brought up.

$8.93 \times 10^3 \text{ g/cm}^3$ density of Cu.

$2.5 \times 10^3 \text{ g/cm}^3$ for shale (approximate)

$2.5 \times 10^3 \text{ g shale/cm}^3$

We have a 25 cc (cm^3) volume.

$$\frac{2.5 \times 10^3 \text{ g shale} \times 25 \text{ cm}^3}{1000 \text{ cm}^3} = \frac{2.5 \times 10^3 \text{ g shale}}{4 \times 10^1} = 6.25 \times 10^1 \text{ g shale in prism } 25 \text{ cm deep}$$

We assume that the $6.25 \times 10^1 \text{ g}$ includes all trace elements; therefore, addition of copper is taken into account and does not contribute appreciably to weight of shale.

Therefore, 1% copper in shale would equal a weight of $6.25 \times 10^1 \text{ g} \times 1 \times 10^{-2} = 6.25 \times 10^{-1} \text{ g}$ of copper.

Therefore, we need to know how long it would take to deposit $6.25 \times 10^{-1} \text{ g}$ of copper.

$$\frac{6.25 \times 10^{-1} \text{ g of Cu for } 25 \text{ cm}^3 \text{ prism}}{6 \times 10^{-6} \text{ g Cu/yr}} = 1.04 \times 10^5 \text{ years (or 100,000) to deposit enough copper to make a } 25 \text{ cm}^3 \text{ of shale } 1\% \text{ Cu.}$$

This is assuming that the evaporation rate on the surface equals the amount that can be drawn from the shale.

25 cm of shale was chosen since this is the approximate average thickness of the copper-bearing shale in the area of this report.

Formula, data, and method for calculating the time for diffusion to concentrate 1% copper in a 10-inch-thick shale.

$$t = \frac{m \cdot h}{\Delta \cdot A (d_2 - d_1)} \quad (\text{Weast, 1971})$$

t = time for diffusion to concentrate the copper.

m = mass of substance which diffuses through a specific cross section in a specific time (t).

A = cross sectional area which is diffused through.

Δ = diffusion coefficient.

h = distance through which diffusion occurs.

$d_2 - d_1$ = initial concentration of copper.

Data used:

$$\Delta = 0.50 \times 10^{-5} \text{ cm}^2/\text{sec} \text{ (Bruins, 1929)}$$

$$h = 4,500 \text{ feet } (1.37 \times 10^5 \text{ cm})$$

$$A = 1 \text{ cm}^2$$

$$m = .265 \text{ grams (1\% of 26.5 g of shale)}$$

$$d_2 - d_1 = 100 \text{ ppm (0.1 mg/cc or } 1 \times 10^{-4} \text{ g/cm}^3\text{)}$$

Additional data: $\text{sec/year} = 3 \times 10^7$; 10 inches of shale @ 2.65 specific gravity = 26.5 grams of shale.

$$t = \frac{.265 \text{ g} \cdot 1.37 \times 10^5 \text{ cm}}{0.5 \times 10^{-5} \text{ cm}^2/\text{sec} \cdot 1 \text{ cm}^2 \cdot 1 \times 10^{-4} \text{ g/cm}^3} = \frac{7.2 \times 10^{13}}{3.0 \times 10^7} =$$

$$= 2.4 \times 10^6 \text{ years} = 2,400,000 \text{ years}$$

Preparation of sandstone isolith map of the San Angelo Formation: Total sandstone thickness was calculated from electric logs using the S.P. profile, and in some cases, the resistivity profile. No rigorous geometric technique was used to arrive at net sandstone values; rather, visual estimation proved sufficiently accurate and consistent. Electric log patterns of the San Angelo in south-central Stonewall County and northeastern Fisher County were very poor; net sandstone values in those areas were estimated by comparing the electric logs with additional control obtained from sample logs and drill hole cuttings.

APPENDIX IX LEGEND FOR FIGURES 5 AND 6

Legend for figure 5 (strike section of Duncan and Flowerpot Members) and figure 6 (strike section of inferred depositional environments).

	Red and grey mudstone and sandy mudstone
	Sandstone (with trough cross stratification; ripples represent ripple or flaser bedding)
	Nodular gypsum bed
	Gypsum nodules
	Dolomite
	Burrows
	Gray shale and calcareous shale
	Siltstone

Measured section number (from figures)	Corresponding measured section (from appendix VI)
17	I-46 (top 12 feet from Eagle-Picher core log)
16	I-19 (0-59 feet), I-47 (59-122 feet)
15	I-2 (0-46 feet), I-16 (62-86 feet), I-15 (46-53 feet)
14	I-9
13	II-11
12	II-1
11	II-5
10	III-9
9	III-6
8	III-22 (0-32 feet), III-25 (32-67 feet), III-24 (67-93 feet)
7	IV-40 (0-64.5 feet), IV-37 (64.5-111 feet)
6	IV-10, IV-11
5	IV-41 (0-9.4 feet), IV-7 (9.4-61 feet), IV-6 (61 feet to top of section)
4	V-17
3	V-11, V-5
2	V-2
1	V-9

PLATES

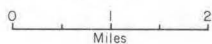
GEOLOGIC MAP - SAN ANGELO FORMATION
MEDICINE MOUND AREA

PLATE I

EXPLANATION

- Quaternary
- Recent stream alluvium, sand & gravel
 - Alluvium
 - Undifferentiated
- Permian
- Interbedded gypsum, gray & light-red mudstones, & dolomite
 - Dark-red & gray sandstone, siltstone, & mudstone
 - Red & gray mudstone with satin spar stringers & gray reduction spots
- H x Abandoned copper mines
 - 29o Bureau of Mines drill hole location
 - 3• Location for copper sample, thin-section sample, facies outcrop (representative)
 - 36Δ Bureau of Mines copper sample location
 - 20// Measured section
 - Boundary of Copper Breaks State Park

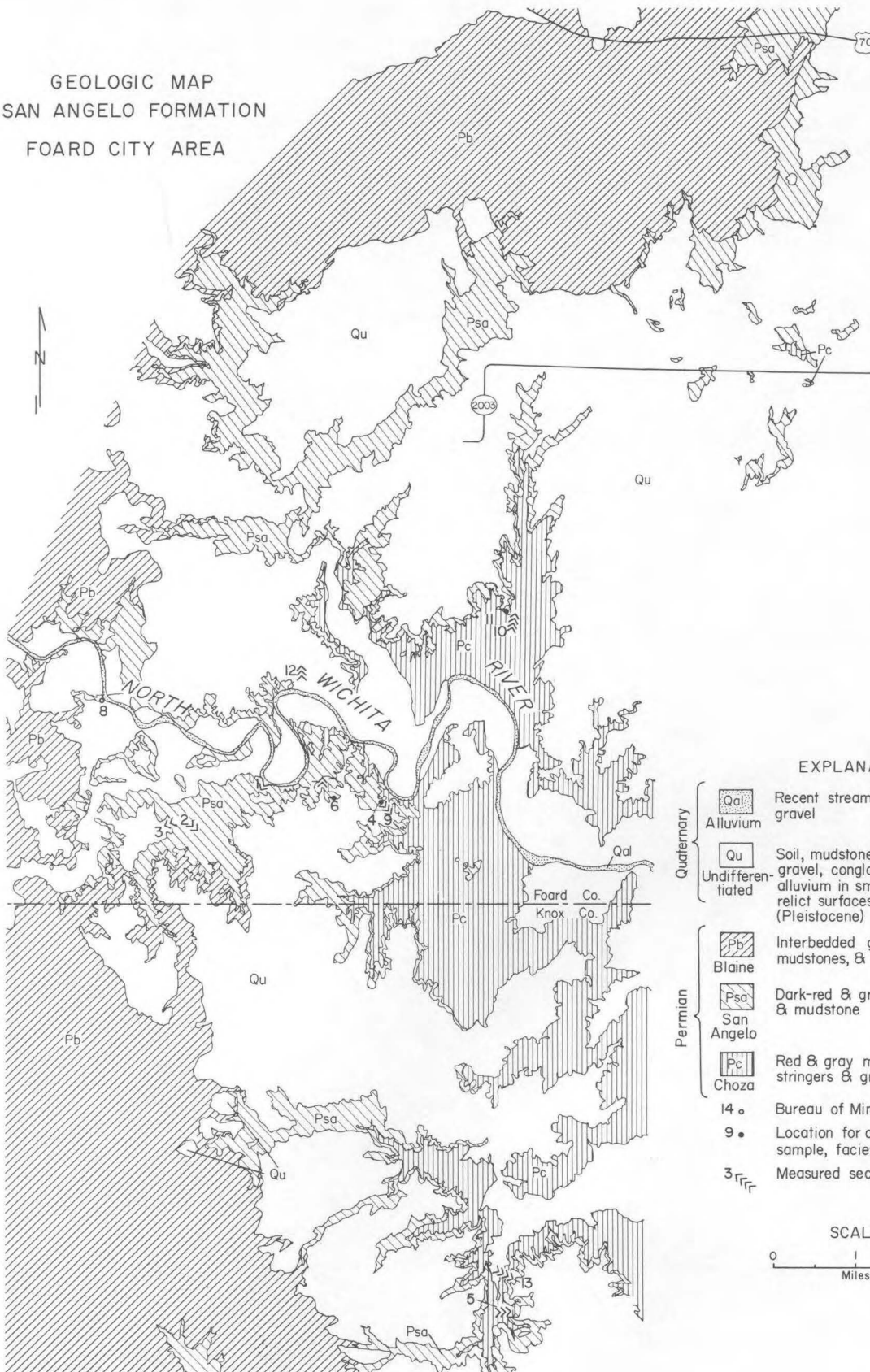
SCALE



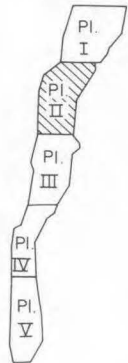
INDEX MAP



GEOLOGIC MAP
SAN ANGELO FORMATION
FOARD CITY AREA



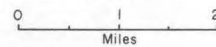
INDEX MAP



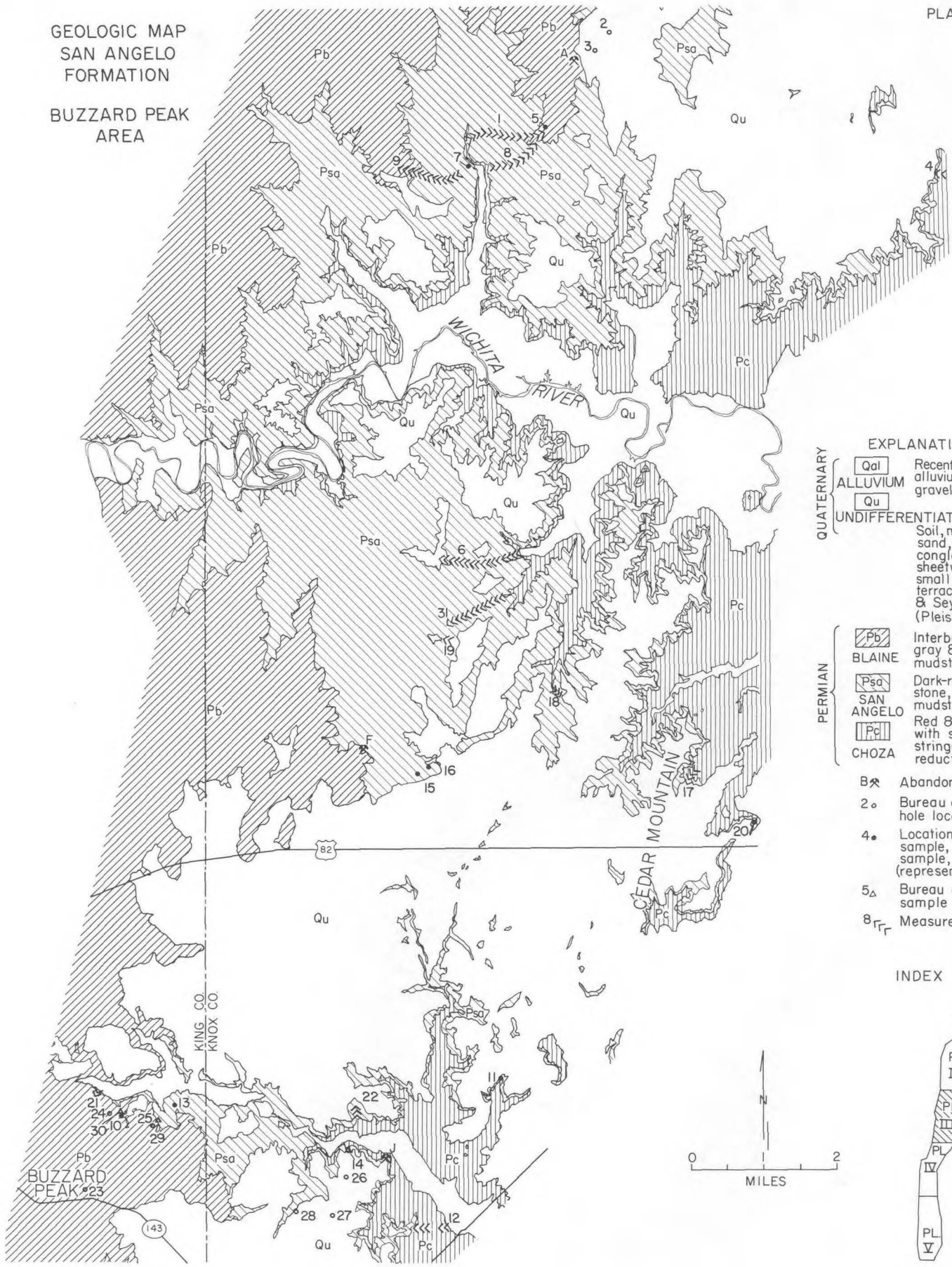
EXPLANATION

- | | | |
|------------|------|--|
| Quaternary | Qal | Recent stream alluvium; sand and gravel |
| | Qu | Alluvium |
| Permian | Pb | Soil, mudstone, loose sand, sandstone, gravel, conglomerate; includes sheetwash, alluvium in small streams, older terraces, relict surfaces, & Seymour Formation (Pleistocene) |
| | Psa | Blaine |
| | Pc | Interbedded gypsum, gray & light-red mudstones, & dolomite |
| | Psa | San Angelo |
| | Pc | Dark-red & gray sandstone, siltstone, & mudstone |
| | Pc | Choza |
| | 14 • | Red & gray mudstone with satin spar stringers & gray reduction spots |
| | 9 • | Bureau of Mines drill hole location |
| | 3 | Location for copper sample, thin-section sample, facies outcrop (representative) |
| | 3 | Measured section |

SCALE

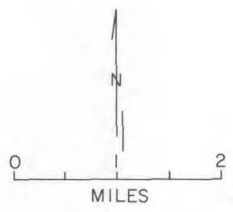
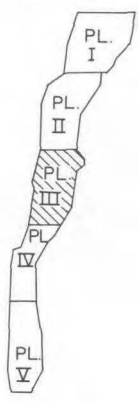


GEOLOGIC MAP
SAN ANGELO
FORMATION
BUZZARD PEAK
AREA

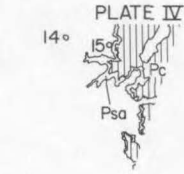
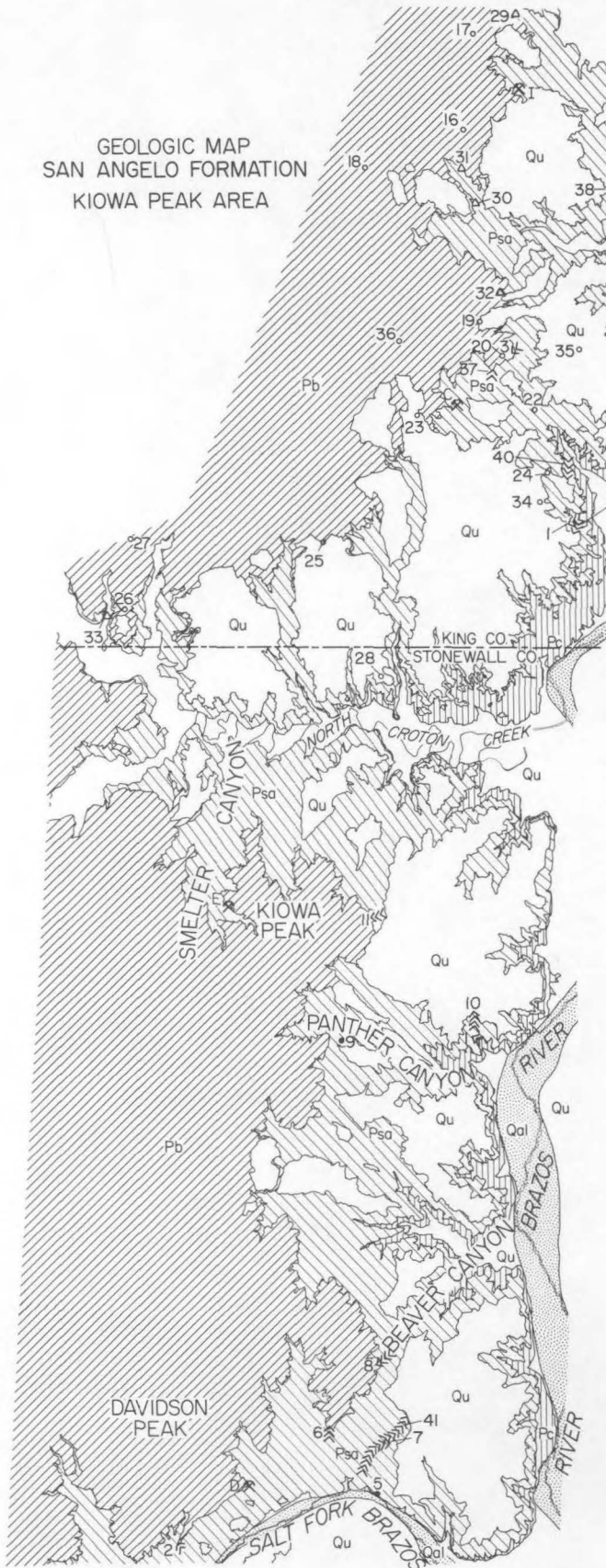


- EXPLANATION**
- QUATERNARY**
- Qal Recent stream alluvium; sand & gravel.
 - Qu **UNDIFFERENTIATED**
Soil, mudstone, loose sand, sandstone, gravel, conglomerate; includes sheetwash, alluvium in small streams, older terraces, relict surfaces, & Seymour Formation (Pleistocene).
- PERMIAN**
- Pb **BLAINE**
Interbedded gypsum, gray & light-red mudstones, & dolomite
 - Psa **SAN ANGELO**
Dark-red & gray sandstone, siltstone, & mudstone
 - Pc **CHOZA**
Red & gray mudstone with satin spar stringers & gray reduction spots
- Bx Abandoned copper mine
 - 2o Bureau of Mines drill hole location
 - 4o Location for copper sample, thin-section sample, facies outcrop (representative)
 - 5Δ Bureau of Mines copper sample location
 - 8TT Measured section

INDEX MAP



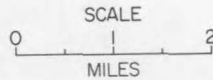
GEOLOGIC MAP
SAN ANGELO FORMATION
KIOWA PEAK AREA



INDEX MAP

EXPLANATION

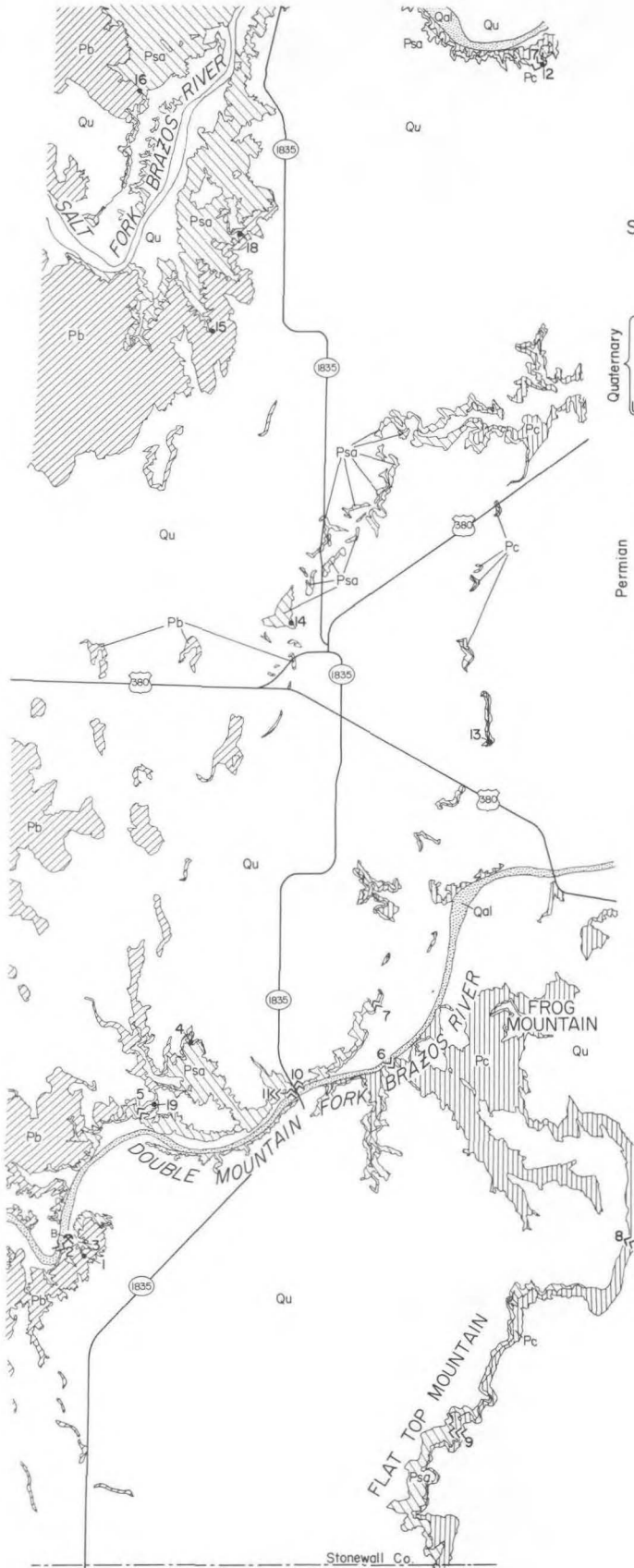
- | | | |
|------------|--|---|
| QUATERNARY | | Recent stream alluvium;
sand & gravel |
| | | Soil, mudstone, loose
sand, sandstone, gravel,
conglomerate; includes
sheetwash, alluvium in
small streams, older ter-
races, relict surfaces, &
Seymour Formation
(Pleistocene) |
| PERMIAN | | Interbedded gypsum, gray
& light-red mudstones, &
dolomite |
| | | Dark-red & gray sand-
stone, siltstone, & mud-
stone |
| | | Red & gray mudstone
with satin spar stringers
& gray reduction spots |
| | | Abandoned copper mine |
| | | Bureau of Mines drill hole
location |
| | | Location for copper sample,
thin-section sample, facies
outcrop (representative) |
| | | Bureau of Mines copper
sample location |
| | | Measured section |



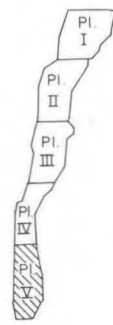
GEOLOGIC MAP
SAN ANGELO FORMATION
OLD GLORY AREA

EXPLANATION

- | | | |
|------------|--|--|
| Quaternary | | Recent stream alluvium; sand and gravel |
| | | Alluvium |
| Permian | | Interbedded gypsum, gray and light-red mudstones, and dolomite |
| | | Dark-red and gray sandstone, siltstone, and mudstone |
| | | Red and gray mudstone with satin spar stringers and gray reduction spots |
| | | Chaza |
| | | Abandoned copper mine |
| | | Location for copper sample, thin-section sample, facies outcrop (representative) |
| | | Measured section |



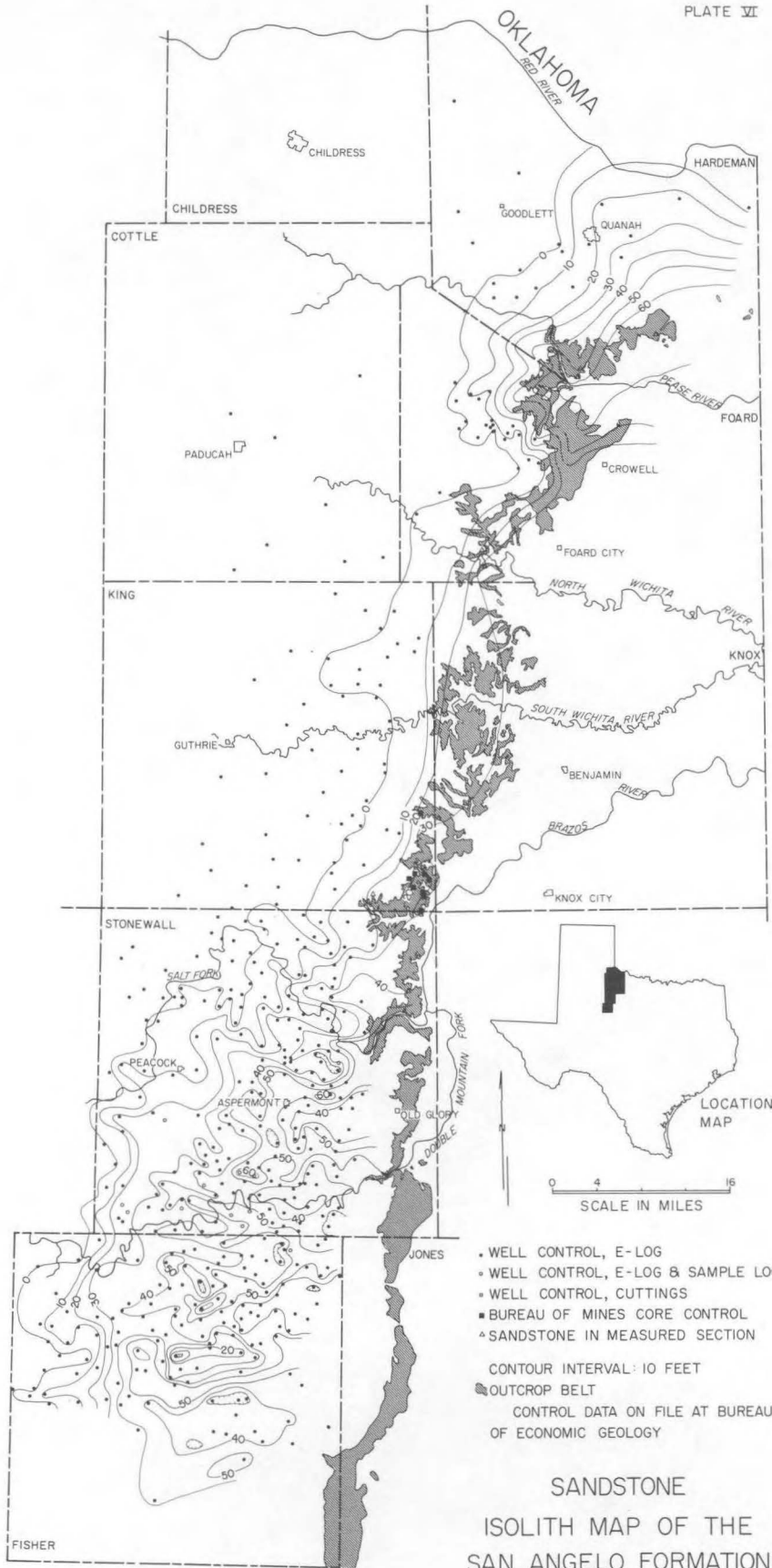
INDEX MAP



SCALE

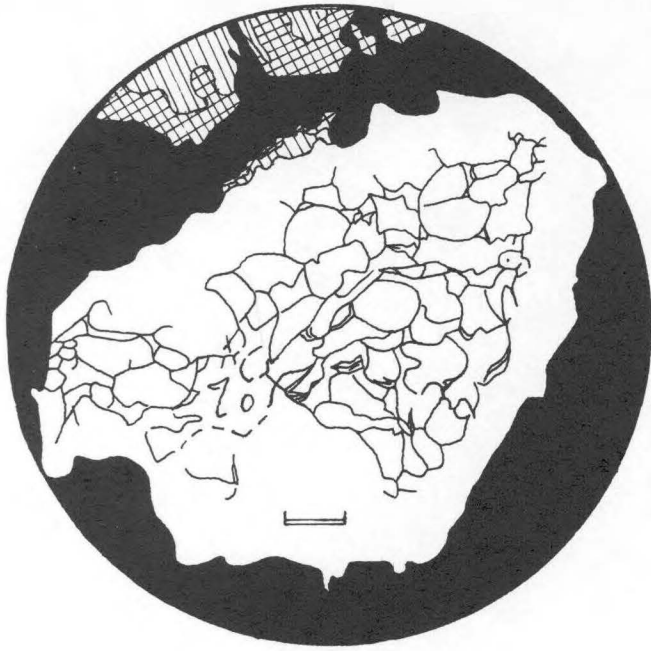


Stonewall Co.



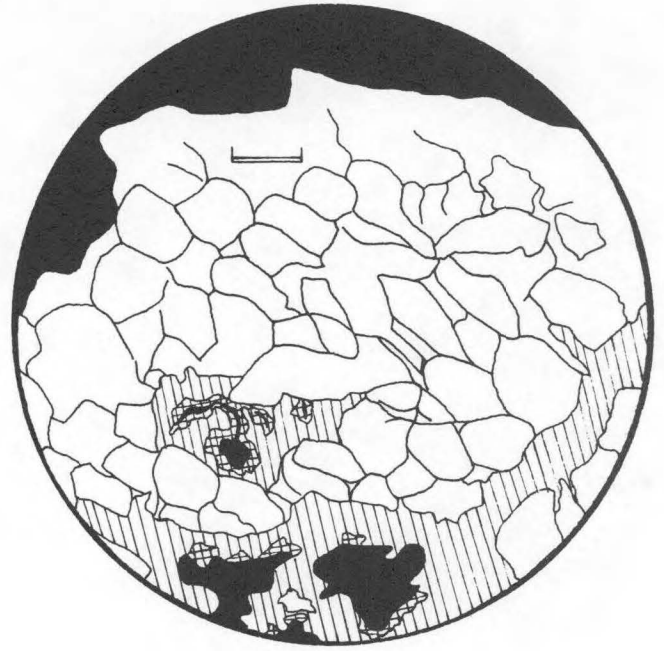
SANDSTONE
ISOLITH MAP OF THE
SAN ANGELO FORMATION

PLATE VII



A

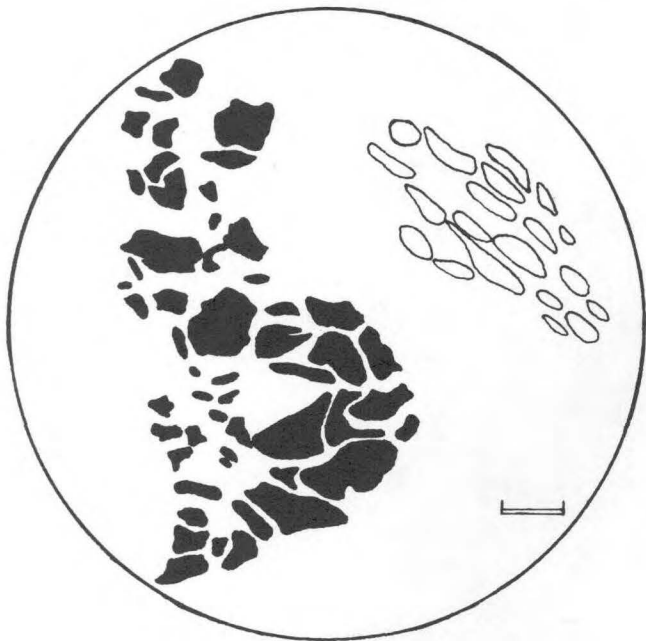
Pyrite with relict wood structure and "clear" rim.



B

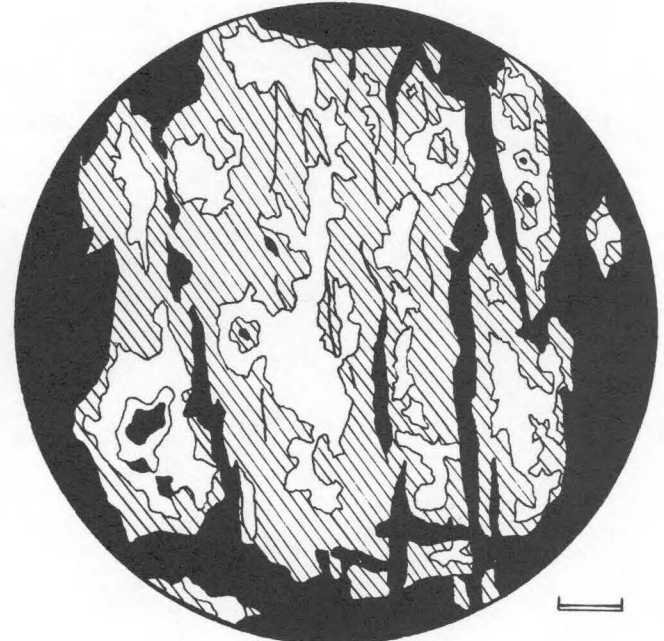
Pyrite with relict wood structure.

Pl. VII A,B: White = pyrite, black = woody matter, cross hatch = covellite, parallel lines = chalcocite.



C

Chalcocite (white) replacing pyrite (black) with relict wood structure preferentially along cell walls; ghosts of wood structure in upper right.

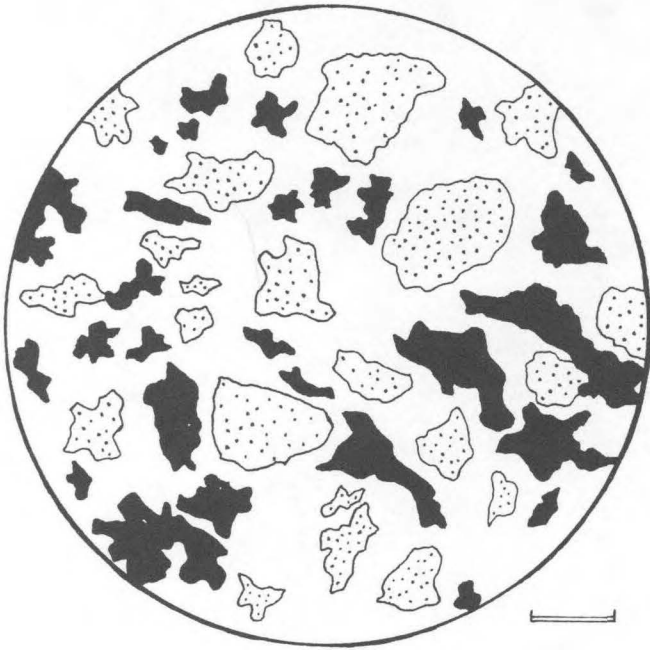


D

Covellite replacing chalcocite; white = chalcocite, parallel lines = covellite, black = woody matter.

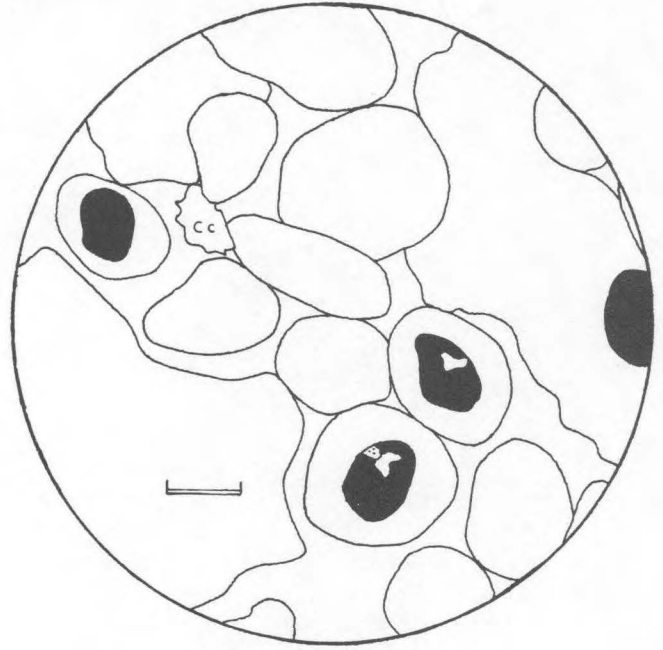
Camera lucida sketches (Pl. VII, A-D) of polished thin section, copper nodule FP-A (III-15). Bar scales are .1 mm long.

PLATE VIII



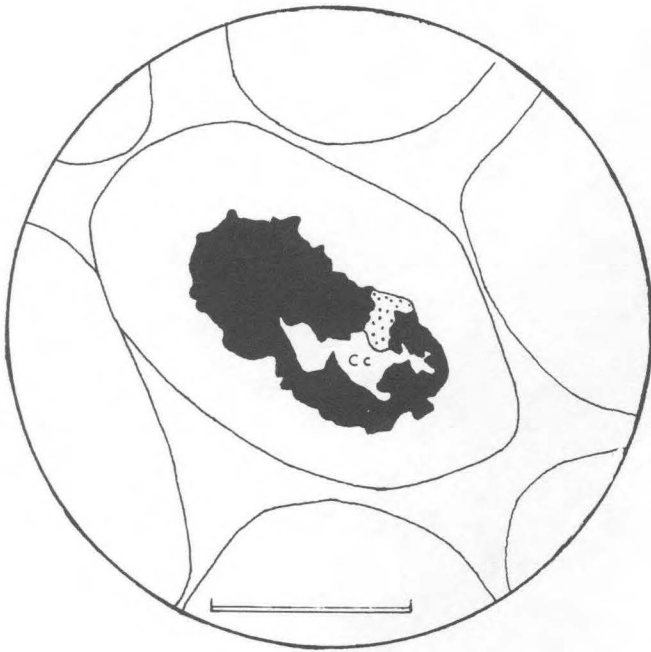
A

Solution and mechanical disintegration of quartz (dot pattern); white = chalcocite, black = pyrite.



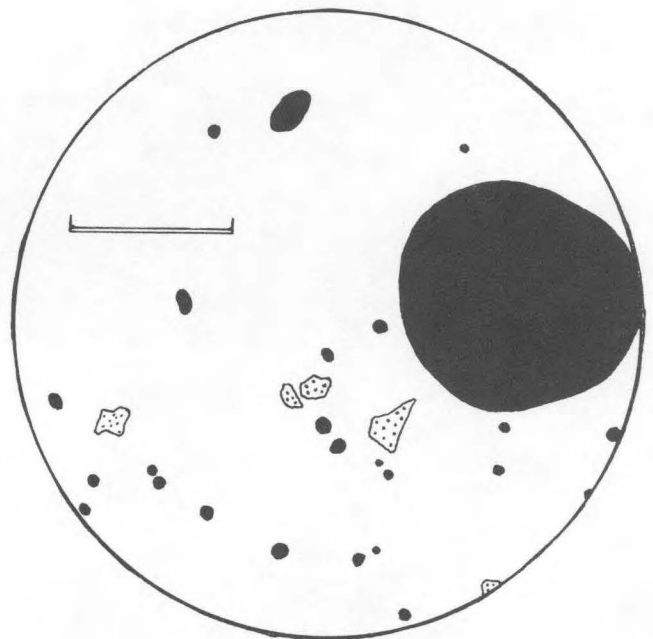
B

Precipitation of chalcocite in pore space between oolites in dolomite; Cc = chalcocite, white = dolomite, black = organic matter.



C

Chalcocite replacing organic matter in the nucleus of an oolite; Cc = chalcocite, dots = quartz, white = dolomite, black = organic matter.

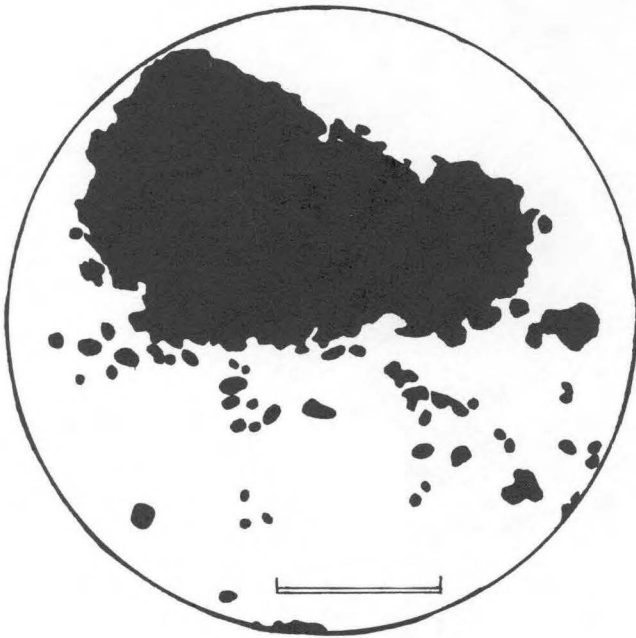


D

Mineralized spore (.15mm sphere) and framboidal spherules (4-10 micron spheres) in copper-bearing claystone, Creta mine; black = chalcocite, white = claystone.

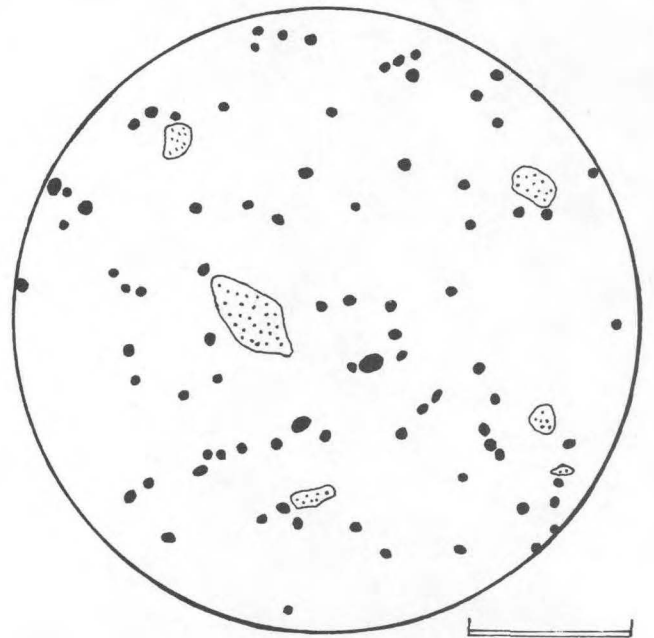
Camera lucida sketch of (A) polished thin section, copper nodule (FP-A); (B,C) tracings of photomicrographs, polished thin section of copper-bearing dolomite (Hr-7a, loc. I-6); and (D) tracing of photomicrograph, thin section of Creta copper-bearing claystone (EP-10). Bar scales are .1 mm long.

PLATE IX



A

Mineralized polyframboidal structure (black) in dolomite (white).



B

Mineralized framboidal spherules (black) in copper-bearing claystone (white), Creta mine; black = chalcocite, dots = quartz.

Tracing of photomicrograph of (A) thin section Hr-10 (I-6); (B) thin section of Creta copper-bearing claystone. Bar scales are .1 mm long.